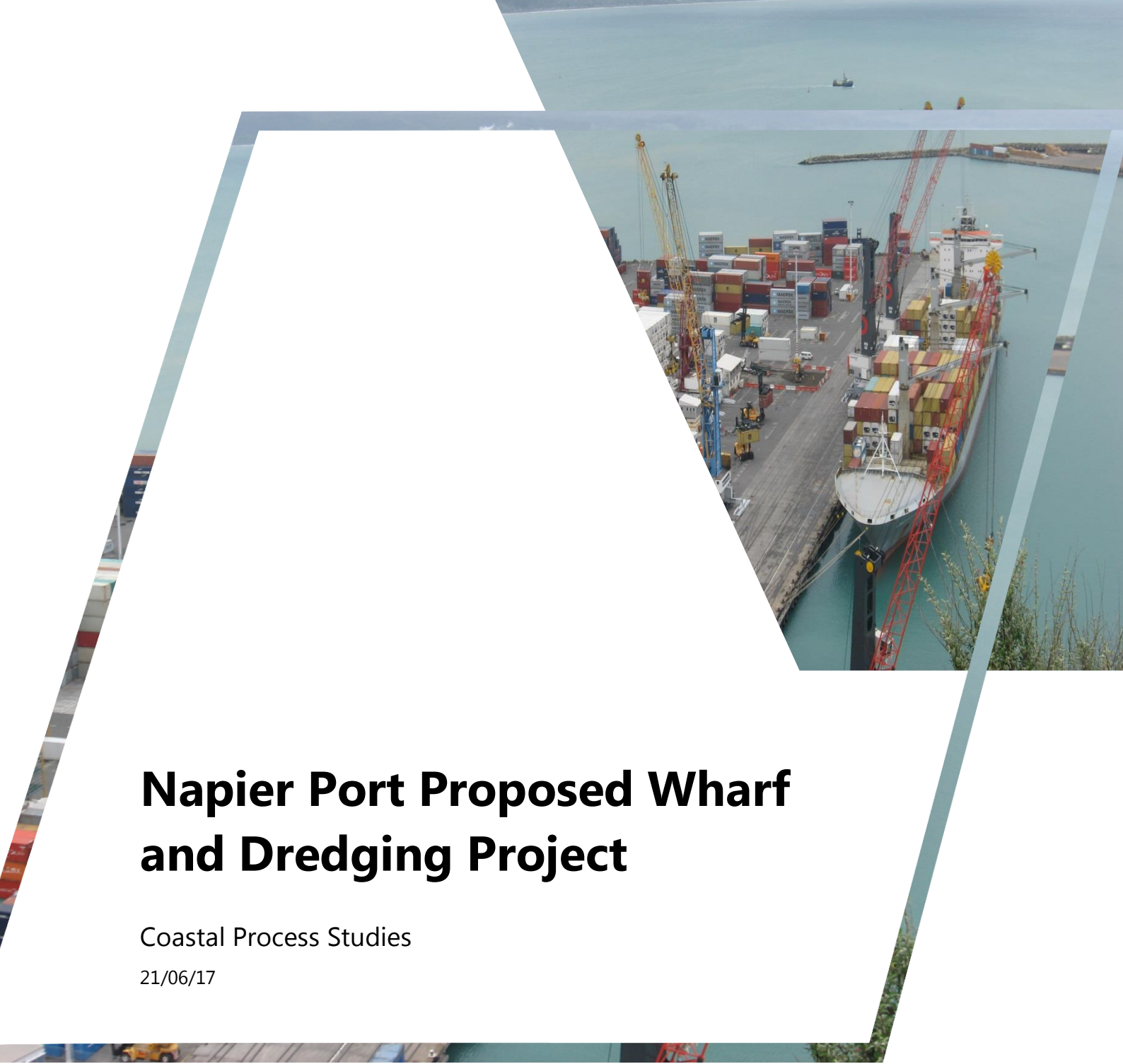


APPENDIX D

**NAPIER PORT PROPOSED
WHARF AND DREDGING
PROJECT – COASTAL
PROCESS STUDIES**

NAPIER
PORT





Napier Port Proposed Wharf and Dredging Project

Coastal Process Studies

21/06/17

Level 17, 141 Walker St
North Sydney NSW 2060
Australia

301015-03651-Rep-CS-002-E

www.advisian.com



Advisian

WorleyParsons Group



Disclaimer

This report has been prepared on behalf of and for the exclusive use of Napier Port Ltd, and is subject to and issued in accordance with the agreement between Napier Port Ltd and Advisian.

Advisian accepts no liability or responsibility whatsoever for it in respect of any use of or reliance upon this report by any third party.

Copying this report without the permission of Napier Port Ltd and Advisian is not permitted.

Project No: -301015-03651-Rep-CS-0002 – Napier Port Proposed Wharf and Dredging Project: Coastal Process Studies

Rev	Description	Author	Review	Advisian Approval	Date
A	Draft for Internal Review	<u>BGW</u>	<u>LN</u>	<u>BGW</u>	16/11/2016
B	Draft for Client Review	<u>BGW</u>	<u>LN</u>	<u>BGW</u>	16/11/2016
C	Draft for Client Review including surfing assessment	<u>BGW/CA</u>	<u>LN</u>	<u>CA</u>	23/03/2017
D	Draft Following Comments	<u>BGW</u>	<u>CA</u>	<u>LN</u>	05/06/2017
E	Draft Following Comments	<u></u> B. Williams	<u></u> C. Adamantidis	<u></u> L. Nielsen	21/06/2017



Table of Contents

Executive Summary.....	vii
1 Introduction	1
1.1 Background	1
1.2 Dredge Case.....	1
1.3 Conceptual Paradigm	1
2 Physiography	4
2.1 Geological and Tectonic Setting.....	4
2.2 Oceanography.....	5
2.2.1 Wave Climate.....	5
2.2.2 Wind.....	6
2.2.3 Currents	8
2.2.4 Water Levels.....	9
2.3 Coastal Geomorphology	9
2.3.1 Littoral Cells.....	9
2.3.2 Beach Composition and Morphology.....	10
2.3.3 Sediment Sources	11
2.3.4 Impact of 1931 Earthquake	12
2.4 Littoral Transport and Sediment Pathways.....	12
2.4.1 Sediment Budget.....	12
2.4.2 Sources of Uncertainties in Sediment Budget.....	14
2.4.3 Sources and Sinks of Sediment around Napier Port	14
3 Available Field Data.....	18
3.1 Bathymetry and Topography.....	18
3.2 Marine Sediments	19



3.3	Beach Sediments	21
3.4	Waves	24
3.5	Wind.....	26
3.6	Currents	26
4	Numerical Model Systems.....	28
4.1	Model Descriptions	28
4.1.1	Delft3D	28
4.1.2	MIKE21 BW	30
4.2	Wave Model Calibration and Validation.....	30
4.2.1	Calibration.....	30
4.2.2	Validation	37
5	Wave Refraction	40
5.1	Introduction	40
5.2	Method of Assessment	40
5.3	Optimisation of Channel Footprint.....	41
5.4	Impact of 'Final' Dredge Channel Design.....	44
5.4.1	Wave refraction patterns.....	44
5.4.2	Changes to Energy Weighted Mean Wave Height and Direction....	45
6	Impact of Channel on Surf Breaks	47
6.1	Analysis	47
6.2	Results.....	47
6.2.1	Significant Wave Height.....	47
6.2.2	Maximum Wave Height.....	49
6.2.3	Wave Crest Patterns.....	51
6.3	Detailed Assessment of Surfing Amenity	52



6.4	Quantification of surfing amenity	53
6.4.1	Wave Peel Angle.....	53
6.4.2	Breaking Intensity	54
6.4.3	Methods for describing surfing amenity.....	56
6.5	City Reef	59
6.5.1	Surfing Amenity – take-off location.....	61
6.5.2	City Reef – Left-hand break.....	63
6.5.3	City Reef – Right-hand break.....	66
6.6	Hardinge Road	68
6.6.1	Surfing Amenity Assessment	69
6.7	Summary	73
7	Impact of Channel on Shoreline Change	74
7.1	Introduction	74
7.2	Analysis	74
7.3	Relative Change in Wave Height and Incidence Angle	74
8	Wave-driven Sub-Littoral Sediment Transport	78
8.1	Spatial Distribution of Marine Sands around Napier	78
8.2	Selection of ‘Morphological Waves’	78
8.3	Results	81
8.4	Interpretation of Numerical Model Results	84
8.4.1	Conceptual Model of Sand Movement at Napier.....	85
9	Conclusions and Recommendations.....	90
9.1	Wave Refraction.....	90
9.2	Surf Breaks.....	90
9.3	Sediment Movement and Shoreline Change	91



9.4	Recommendations.....	91
10	References	93

Table List

Table 3-1: Locations of wave gauges.....	25
Table 4-1: Skill Score qualifications (after Sutherland et al, 2004)	31
Table 4-2: Summary of calibration error statistics for calibrated wave model.....	31
Table 6-1: Range of wave directions, periods and significant wave heights run through SWAN model.....	53
Table 6-2: Description of regions in nomogram in Figure 6-8 (Hutt <i>et al.</i> 2001).....	58
Table 6-3: Existing and post-dredging breaker types, City Reef left-hand break.....	63
Table 6-4: Existing and post-dredging breaker types, City Reef right-hand break.....	66
Table 6-5: Existing and post-dredging breaker types, Hardinge Road break.....	70
Table 7-1: Changes in energy weighted mean wave height and direction at the 2m C.D. contour for various discrete locations between Napier Port and Westshore.	76

Appendix List

Appendix A:	Glossary
-------------	----------



Executive Summary

Napier Port Ltd (NPL) is proposing capital dredging of the central fairway, outer swing basin, and inner swing basin at the Port of Napier.

This report presents an assessment of the potential effects of the dredging works on the wave climate and coastal processes along the shoreline west of the port. The study area extends from the Port to the Esk River in the north, including Hardinge Road Foreshore, Westshore Beach and Bay View Beach.

Wave modelling of pre and post-dredging bathymetries was undertaken. Due to the orientation of the navigation channel, the channel deepening will only affect waves from the east to south. Waves from the northeast sector will not be refracted by the navigation channel (and hence, would not be affected by the change in channel bathymetry). The modelling indicates that the proposed dredging will have the following very minor impacts on the wave climate of the beaches to the west of the Port:

- Reduction in mean wave energy at Port Beach and a change in the mean wave direction of approximately 2° clockwise;
- A slight reduction in mean wave energy along Hardinge Road and a change in the mean wave direction of approximately 2° clockwise;
- A slight increase in mean wave energy at Ahuriri Inlet entrance and a change in the mean wave direction of approximately 1° clockwise;
- No more than a minor change in mean wave energy at Westshore and a change in the mean wave direction of less than 1° clockwise.
- No change in the mean wave climate at Bay View.

Comparative wave refraction calculations based on the wave modelling results and the review of previous studies have been used to evaluate the impact of the proposed dredging on the shoreline at Westshore and have found:

- Wave angles at Westshore are predicted to rotate clockwise by less than one degree. The greatest change occurs at the southern end of Westshore. The change in wave angle suggests a slight increase in northerly littoral drift.
- Wave angles at Ahuriri Inlet are predicted to rotate clockwise by less than 1 degree, suggesting that East Pier Beach will rotate slightly in response to become more easterly facing. This rotation can only be realised if there is sufficient wave energy on the beach to drive morphological change.
- Along Hardinge Road littoral drift potential will become more westerly. At the western boundary of Hardinge Road this will increase sediment transport potential towards East Pier Beach. At the east boundary of Hardinge Road this will reduce the tendency for sediment to be transported eastward towards Port Beach.



- The change in wave climate at Port Beach will cause the beach to rotate clockwise by approximately 2 degrees, becoming more northerly in its orientation. The predicted decrease in wave energy suggests that there is little potential for beach erosion due to changes in wave climate. Rotation of the beach will manifest as erosion on the eastern boundary by the Port, and accretion on the western boundary by the rock groyne.

The impact of the proposed dredging on surfing amenity in the vicinity of Napier Port has been assessed in terms of peel angle, wave height and wave breaker type. It was found that there would be minimal change to the surfing amenity at City Reef as a result of the proposed dredging, with very little change in peel angle and only a slight increase in the proportion of plunging breakers when compared with spilling breakers. At Hardinge Road, there would be a slight increase in the peel angle, caused by a clockwise rotation in the approach direction of the waves. This slight increase would result in very little change in surfing amenity, with a slightly higher proportion of waves being assessed as surfable following the dredging, due to the predicted increase in peel angle.

The predicted increase in littoral drift inferred from changes in wave incidence angles at the shore is likely well within the range of natural variability known to occur through fluctuations in wave climate and sediment supply.

Finally, assessment of sand transport patterns and magnitudes in the subtidal zone around Napier port suggests that any fine sand disposed of at Westshore will, over time, be transported eastward by a persistent shore-parallel current driven by overlying wind activity. Coarse sediment may be moved onshore to nourish the beach, but would be rapidly transported northward by littoral drift, and not remain as useful beach material.

Overall, the predicted impacts of the proposed dredging on the beaches west of the Port are small or negligible.

Studies have been undertaken to understand any potential impacts on the existing surf breaks at Hardinge Road and at City Reef (west of Ahuriri Inlet). This has found that the modified swinging basin and channel will have slight beneficial effects on the Hardinge Road surf break and no noticeable effect on the wave corridor or surf break at City Reef.



1 Introduction

1.1 Background

Napier Port Ltd (NPL) is proposing capital dredging of the central fairway, outer swing basin, and inner swing basin at the Port of Napier. This report presents an assessment of the potential effects of the dredging works on the wave climate and coastal processes along the shoreline west of the port. The study area extends from the Port to the Esk River in the north, including Hardinge Road, Westshore Beach and Bay View Beach, as shown in Figure 1-1. The footprint of proposed dredging works in connection of the basin development is shown in .

Advisian, previously branded as WorleyParsons, earlier completed a shoreline impact assessment and wave effects studies based on reclamation works for Napier Port Ltd (WorleyParsons, 2002, 2005, 2010). The analysis presented in this report relates to a new proposed wharf and dredging project and represents an advance from previous work by Advisian, with the collection of a substantial dataset (wind, wave, currents, particle size distribution at surface and depth) that is targeted to address previous information gaps. These datasets are used to aid conceptual models of coastal processes for interpretation of numerical modelling results, as well as providing data to calibrate and validate the numerical models.

1.2 Dredge Case

The proposed dredging for the Port of Napier is shown in . A staged approach is proposed by the Port to achieve the final design depth. Initially the fairway and swing basin will be excavated to a depth of -12.5m C.D. Subsequent campaigns over a number of years will then lower the depth in 0.5m increments until the final design depth is achieved.

Spoil material, which borehole data has indicated will predominantly be sand and silty material, with some stiff clays, was anticipated to be disposed of in the existing nearshore disposal site with the aim of being worked onshore by wave action and increasing the average width of the recreational beach at Westshore. However, preliminary investigations have shown that the sediment sizes in the area to be dredged are too fine to provide effective beach replenishment, and therefore an offshore disposal site has been chosen.

The modelling reported here considers the final design dredge depth of the channel. This is the most conservative case for assessing the impact on coastal processes and represents the ultimate state to which the shore will be evolving. Due to the orientation of the channel, the channel deepening would only affect wave directions from east to south. Waves from the northeast sector will not be refracted by the navigation channel (and hence, would not be affected by the change in channel bathymetry).

1.3 Conceptual Paradigm

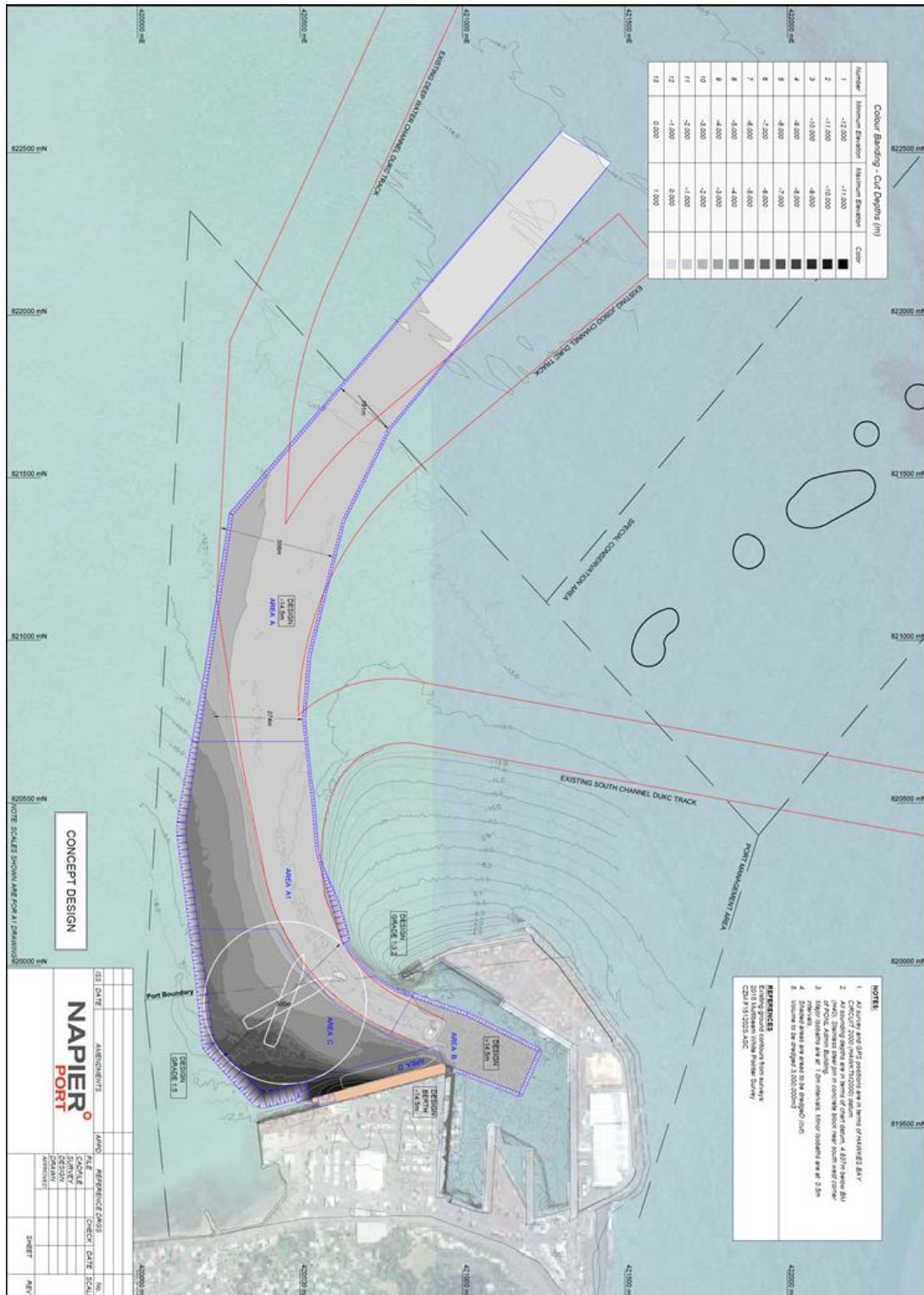
This report is written within the general context of Hawke Bay coastal processes developed by Komar (2005). The wide-ranging and detailed review and interpretation developed by Komar



(2005) is elucidated further in Komar (2010), referenced by scientific journal papers on coastal processes at Hawke Bay (e.g. Dickson et al., 2011), and is used by Hawke Bay Regional Council as the basis for providing coastal management guidance (e.g. Komar & Harris, 2014).



Figure 1-1: Port of Napier and surrounding environs within Hawke Bay, New Zealand. Satellite imagery courtesy of Google Earth. Study areas are highlighted.



2 Physiography

2.1 Geological and Tectonic Setting

Geological processes and, hence, geomorphology, of the Hawke Bay region are dominated by collisions of the Pacific and Australian tectonic plates. The movement of each plate relative to each other is oblique, resulting in both vertical and horizontal movement at a rate of about 50mm/y. The movement manifests as a slip-strike transform fault that intersects New Zealand via the Puysegur Trench, crosses the South Island via the Alpine Fault, and continues past the North Island via the Hikurangi Trough and Tonga-Kermadec Trench (Figure 2-1). This combination of collision and horizontal movement in the Hikurangi Trough is transferred to the land mass of Hawke's Bay, with resultant complex patterns of deformation and thrust-faulting (Komar, 2010).

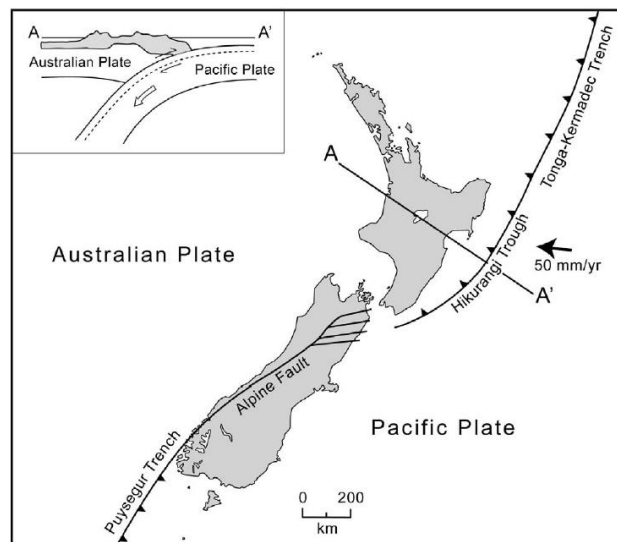


Figure 2-1: The tectonics of Hawke Bay, showing the collision between the Australian and Pacific Plates, with plat subduction along the Hikurangi Trough. From Komar (2010).

Of the earthquakes caused by this plate movement, the most destructive for the North Island and Napier in particular was the Hawke Bay earthquake in 1931 (magnitude 7.8), generated by movement on a fault some 15km to 30km north of Napier. Nearly all buildings in the central areas of Napier and Hastings were levelled.

The earthquake resulted in the abrupt uplift of the Ahuriri Lagoon, which drained rapidly in to the sea, reducing its area by some 12.8km² (Komar, 2005). A reconnaissance investigation by Marshall (1933) reported that the Port of Napier's tide gauge had been raised by 1.8 m. The uplift increased progressively to the north from Napier, reaching 2.0 m at Tangoio, achieving a maximum uplift of 2.7 m along the rocky shore at Moeangiangi, 30 km north of Napier; still further to the north, the extent of uplift rapidly decreased. Today, the exposed former lagoon is now used as farmland and the Hawkes Bay Regional Airport.



2.2 Oceanography

2.2.1 Wave Climate

The deepwater wave climate of the North Island's East Coast is governed by storm activity induced by strong westerlies in the Southern Ocean. The land mass of New Zealand blocks most of the wave energy propagating eastward, causing wave directions to rotate via diffraction and strong refraction so that ocean waves are incident from the south by the time swell waves reach the east coasts of the North Island (Gorman, 2003). Therefore the storm wave activity offshore of Hawke Bay is dominated by swell generated distantly and punctuated by strong local events (Coggins et al., 2015).

Hourly measurements of swell waves in Hawke Bay have been collected by Port of Napier via Triaxis wave-ride buoy. Installed in 2004 and operated to the present day, the buoy provides directional swell wave information in roughly 15m water depth, seaward of the breakwater at Napier Port.

Continuing analysis of the wave data by WorleyParsons (e.g. WorleyParsons, 2006; WorleyParsons, 2011) show that highest wave conditions occur generally during the austral winter (July and August), when the average significant wave height (H_s) is in the order of 1.5m. Highest waves generated by the stronger storms can occur from June through September, typically achieving significant wave heights in the order of 2.5 to 3.5m. The mean peak-energy wave period is approximately 12 seconds, but storm waves with $H_{m0} \geq 4\text{m}$ can occur with periods between 10 and 16 seconds.

The wave climate at the Triaxis wave buoy is highly directional, which is to be expected given that storms in the Southern Ocean are the primary source of wave energy. The largest and most frequent waves are incident from 90° to 120° relative to true north (i.e. from east-southeast), representing some 72% of the measured waves (Worley, 2006). A relatively small portion of the waves, less than about 5%, arrive from north-easterly directions from 0° to 90° . However some sections of the shoreline, particularly around Bay View and Westshore will be relatively exposed to these waves.

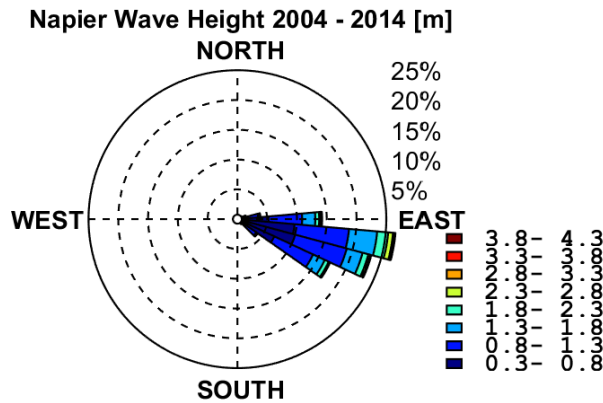


Figure 2-2: Wave statistics recorded at Triaxys wave-rider buoy NE of Napier breakwater.

2.2.2 Wind

Anemometer data has been collected by Napier Port Ltd since 2004 at a level of 10.3m above Napier Mean High Water Springs.

Analysis of 1-minute average wind speeds (Figure 2-3) shows the dominant directions to be South-West and West. Strongest winds occur from the West and North-West. The median wind speed is in the order of 8 m/s.

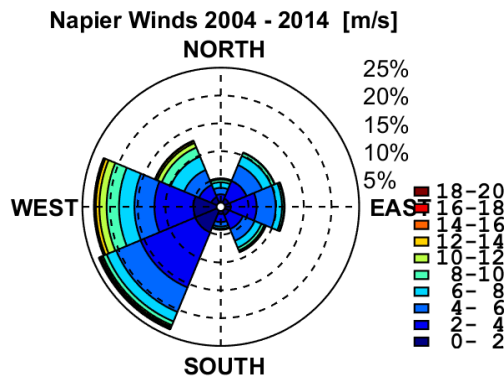


Figure 2-3: Rose plots of 1-minute average wind speed measured at Napier Port. Directions given as 'coming from'.

A simple statistical analysis of the wind climate suggests that monthly average and median wind speeds are reasonably consistent across the year. A seasonal trend does exist, with winds being calmest during March to May, and strongest during September to November (Figure 2-4).

There is also a seasonal component to the wind direction (Figure 2-5). During September to March (Austral summer) winds approach from both NE to SE and SW to NE sectors. During May to



August (Austral winter) the predominant direction is westerly and south-westerly, reflecting storm activity in the 'roaring forties' in the southern ocean.

Previous comparisons with historical wind data measured at Napier Airport (WorleyParsons, 2005) suggests that potential orographic effects due to Bluff Hill in the lee of the Port are likely to be limited and that wind speeds recorded at the Port are representative of the Napier area.

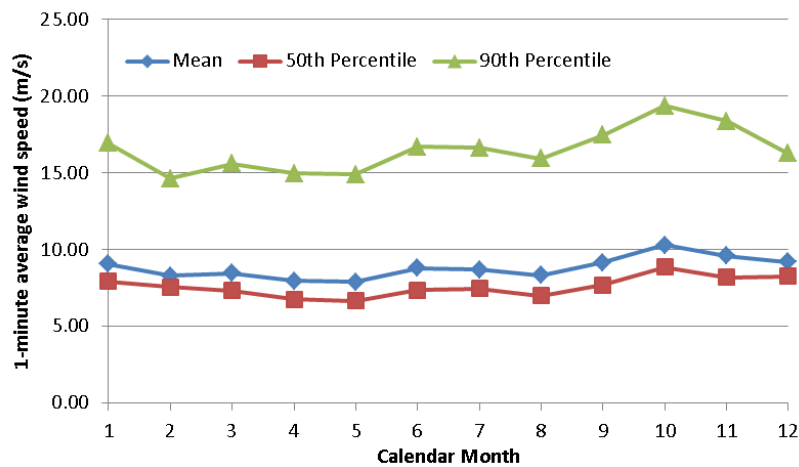


Figure 2-4: Monthly statistics of 1-minute average wind speeds at Napier Port anemometer.

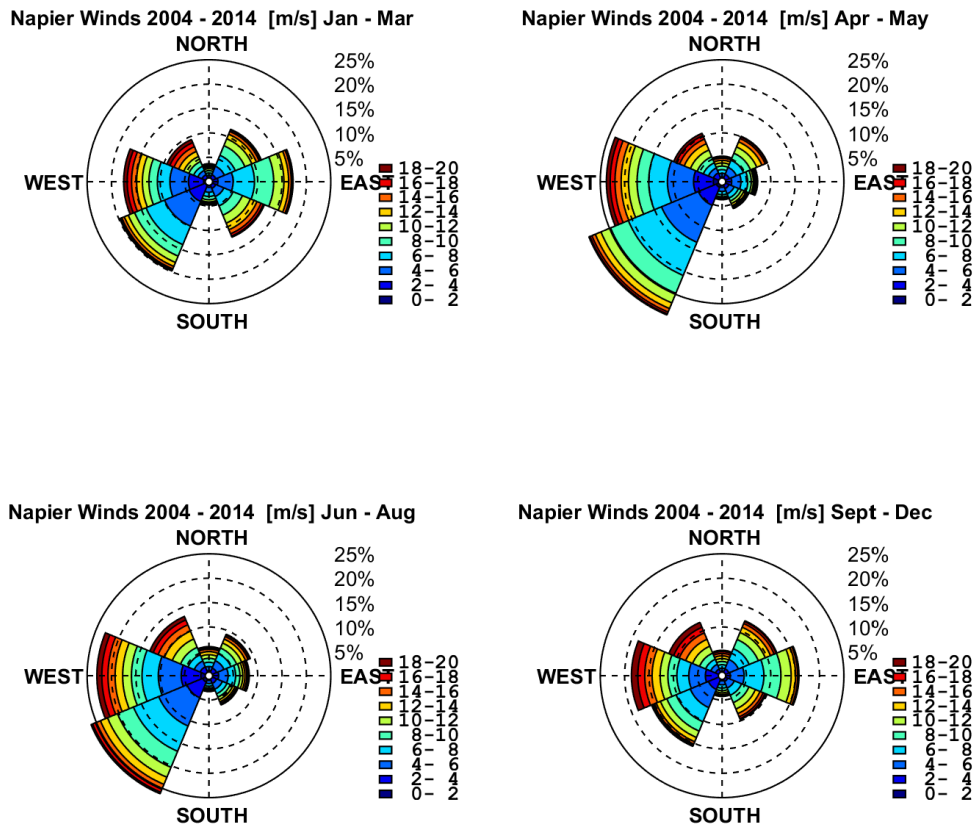


Figure 2-5: Seasonal wind roses of 1-minute average wind speed and directions at Napier Port anemometer. Directions given as 'coming from'.

2.2.3 Currents

Previous investigations of currents at Napier have found current speeds are predominantly controlled by wind, and are typically in the range of 0.05 – 0.1 m/s (Water Quality Center, 1989; Mead et al, 2001; WorleyParsons, 2005). The currents have a tendency to follow bathymetric contours. It is worth noting that the above studies only record currents around Westshore for a period of 14 days to 8 weeks, and only during the Austral summer. These short deployments are unlikely to be sufficiently long or of the right season to define adequately the full range of current speed present at Napier, particularly under strong wind conditions. However, probably they are sufficient to determine the magnitude and direction of mean currents.

Previous numerical modelling (WorleyParsons, 2005) strongly suggests the presence of a persistent anticyclonic gyre immediately north-west of the Port breakwater under strong winds from the South-West. During Westerly and North-Westerly winds currents are directed south-easterly along the coast. These current structures are also reproduced in Advisian’s calibrated 3D model of Hawke Bay (Advisian, 2015), and are consistent with previous analysis of currents at Westshore presented in Water Quality Center (1989), Mead (2001) and WorleyParsons (2005). Generally a net



current of around 0.02 – 0.04 m/s is described for current meter sites between Westshore and the Port. Currents tend to flow parallel to the bathymetric contours, with a net NW to SE flow offshore of Westshore, and a net Easterly flow immediately adjacent to the Port.

Previous analysis of current data within Hawke Bay (e.g. Francis, 1985; Water Quality Center, 1989; Mead et al, 2001; WorleyParsons, 2005) concluded that astronomical tidal currents account for up to 34% of the variance in the current speeds. The tidal component of current speeds is generally accepted at around 0.04 – 0.05 m/s, with little or no contribution to residual currents.

The magnitude of the currents are very low and in themselves are unlikely to contribute much to sediment transport (except in the presence of waves), or to be a hindrance to navigation. The implication of these low but persistent currents in combination with wave activity to suspend and transport sediment is discussed later in this report.

2.2.4 Water Levels

The maximum tidal range at Napier is less than 2.0m, which is generally classified as ‘microtidal’ (Davies, 1964). Spring and neap tidal ranges are 1.9m and 1.2m, respectively. Analysis of monthly-mean water levels from tide gauge data spanning 1999 – 2010 (Komar & Harris, 2014) shows that the highest water levels occur during the winter months of roughly March to June, with a marked decline in summer, reaching a low in September. The maximum difference between the seasonal mean water levels is 0.1m.

Komar (2014) suggests that the most likely explanation for the discrepancy between the seasons is the occurrence of storm surges – that is, the component of water level variations not explainable by the tide – in the winter months. According to de Lange (1996), on average 50% of storm surge elevations experienced along the New Zealand coast are generated by the lowered atmospheric pressures along a storm’s centre, the other 50% being caused by the strong winds of the storm.

2.3 Coastal Geomorphology

2.3.1 Littoral Cells

The coast of Hawke Bay extends along the east coast of New Zealand’s North Island, from the Mahia Peninsula in the north to beyond Cape Kidnappers in the south. The alternating stretches of rocky shores and embayments which contain the main beaches, allow the Bay to be divided in to three largely self-contained littoral cells, each divided by either rock cliffs or bluff headlands. To the west of the Bay the coast is contained by the ‘Bay View’ and ‘Haumoana’ cells, with Napier Port forming the boundary between these north and south compartments (Figure 2-6).

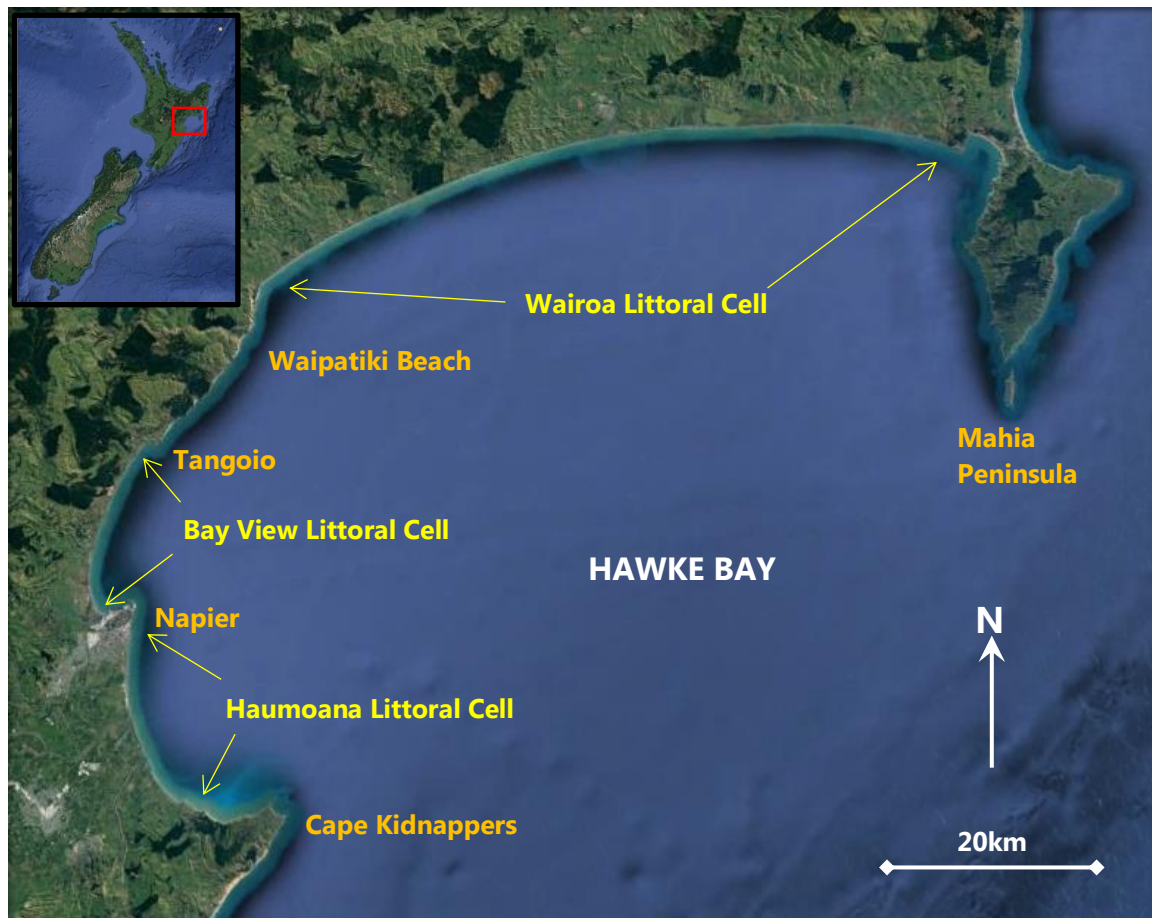


Figure 2-6: Location of Napier in relation to Hawke Bay and its three littoral cells, separated by rocky headlands. Satellite imagery courtesy of Google Earth. Adapted from HBRC (2014).

2.3.2 Beach Composition and Morphology

The beaches immediately north and south of Napier are predominantly comprised of mixed sand and gravel. Jennings and Shulmeister (2002) define mixed sand-gravel beaches as those consisting of a high proportion of both coarse particles and sand, with there being an intimate mixing of the two size fractions in the beach deposit. This composition is relatively rare across the world's coastlines and therefore is comparatively unstudied in comparison with purely coarse-grained (shingle) or fine-grained (sandy) coastlines.

Much uncertainty remains therefore in the behaviour of such beaches and the movement of mixed-sand-and-gravel material. Previous studies of littoral transport on gravel beaches (e.g. Mason and Coates, 2001) found that the sand component could be significant in the dynamic responses of otherwise coarse-grained beaches, even if the percentage of sand was relatively small.



At the surface the beaches appear to be composite, with the berm composed of coarse gravel and cobbles, whereas the lower beach face is composed of a relatively thin sand lens overlying thicker gravel beach deposits. Finer material is percolated downward through the shingle to form a sandy layer of low permeability at the level of the beach water table. Below Low Tide the sediments are purely sand. At Napier the typical beach state is reflective, although during storm conditions waves can be observed breaking offshore, in contrast to breaking on the beach step as is often reported from mixed sand and gravel beaches (Kirk, 1980).



Figure 2-7: Mixed sand and gravel beach material at Westshore. Left panel: Facing onshore. Right panel: Facing offshore.

2.3.3 Sediment Sources

The beaches of Hawke Bay are locally supplied with sand and gravel from erosion of the Cape Kidnappers cliffs and three rivers that drain the Frontal Range of the Ruahine Mountains, composed of Mesozoic greywacke. Previous experiments have shown that abrasion of the greywacke cobbles yields gravel and coarse sand, which further breaks down into finer sediments that are lost from the beach system (Marshall, 1928).

Smith (1968) analysed the sphericity and size of gravels at 19 sites across the Haumoana and Bay View littoral cells. He concluded that on average the gravel size in the Haumoana cell is coarser and has an overall greater range of sizes than found in the Bay View cell, in agreement with Marshall's (1927) observations.



Smith (1968) also analysed the grain sphericity and roundness on pebbles in the 1.5- to 3.0-cm size fraction. In both littoral cells, the more-spherical particles were found in the south, whereas toward the north, the stones became flatter.

Smith's (1968) overall conclusion was that the differences in the sediments between the Haumoana and Bay View littoral cells demonstrated that the cells are separate entities and that, because the input of fresh greywacke gravel to the beach of the Bay View cell is minimal, the pebbles there must have nearly reached their optimum degrees of roundness, noting that they are both uniformly smaller and more polished than the gravel of the Haumoana cell. His conclusion was that the Bay View gravel must represent an "old" deposit, in contrast with the Haumoana cell, where gravel is being actively contributed by the sources, the Tukituki River and the erosion of Cape Kidnappers.

2.3.4 Impact of 1931 Earthquake

The change in land elevations that the 1931 earthquake exerted, and continues to exert, is significant control on geomorphology and coastal processes of the shoreline at and around Napier (Single, 1985; Kirk and Single, 1999; Komar, 2005; 2010). Prior to the 1931 earthquake, a substantial portion of the land had very low elevations, and the beach consisted of a low gravel ridge that was frequently overtopped by storms; the city of Napier was commonly inundated by floods from this overtopping by the sea, and by floods in the rivers (Campbell, 1975).

Although variable, the typical beach slope at Napier above Low Water is roughly 1V:9H, meaning that the uplift following the 1931 earthquake widened the beach profile by some 18m. The uplifted seafloor also created a sand beach fronting the gravel ridge at Westshore. Today this beach is the community's principal recreation beach, although Komar (2010), referencing Smith (1968), suggested that much of the sand has been lost over the decades, being essentially gone by the later 1950's or 1960's.

2.4 Littoral Transport and Sediment Pathways

There have been many estimates of littoral transport around the south Hawke Bay coast, and several previous attempts at generating a sediment budget for the shoreline around Napier (e.g. Gibb, 2002; Tonkin and Taylor, 2005, amongst others). This study utilises the sediment budget constructed by Komar (2010) and the references therein.

2.4.1 Sediment Budget

The principal source of sediment in the Haumoana cell is gravel delivered by the Tukituki River and by erosion of Cape Kidnappers. The angle of the shoreline suggests that longshore sediment transport is at a maximum adjacent to Cape Kidnappers. Analysis of impoundment rates at Haumoana Groyne (Tonkin & Taylor, 2005) indicate that some 46,000 m³/yr are transported northward at the Tukituki River. To the north the coastline gradually becomes aligned closer to the incident swell, with commensurate reduction in northward littoral transport. Immediately south of



Napier Port the transport rate is some 5,000 m³/yr and gravel is unable to travel further north to reach the breakwater and navigation channel. Instead, fine sands and silts abraded from the gravel are transported offshore and around the breakwater by waves and currents.

The Bay View littoral cell is largely closed with no significant source of sediment. The only principal source of gravel is the Westshore nourishment scheme, which is in the order of 12,000 m³/yr, and is removed from the beach by wave action. Abrasion losses are estimated at 27,000 m³/yr (Komar, 2005).

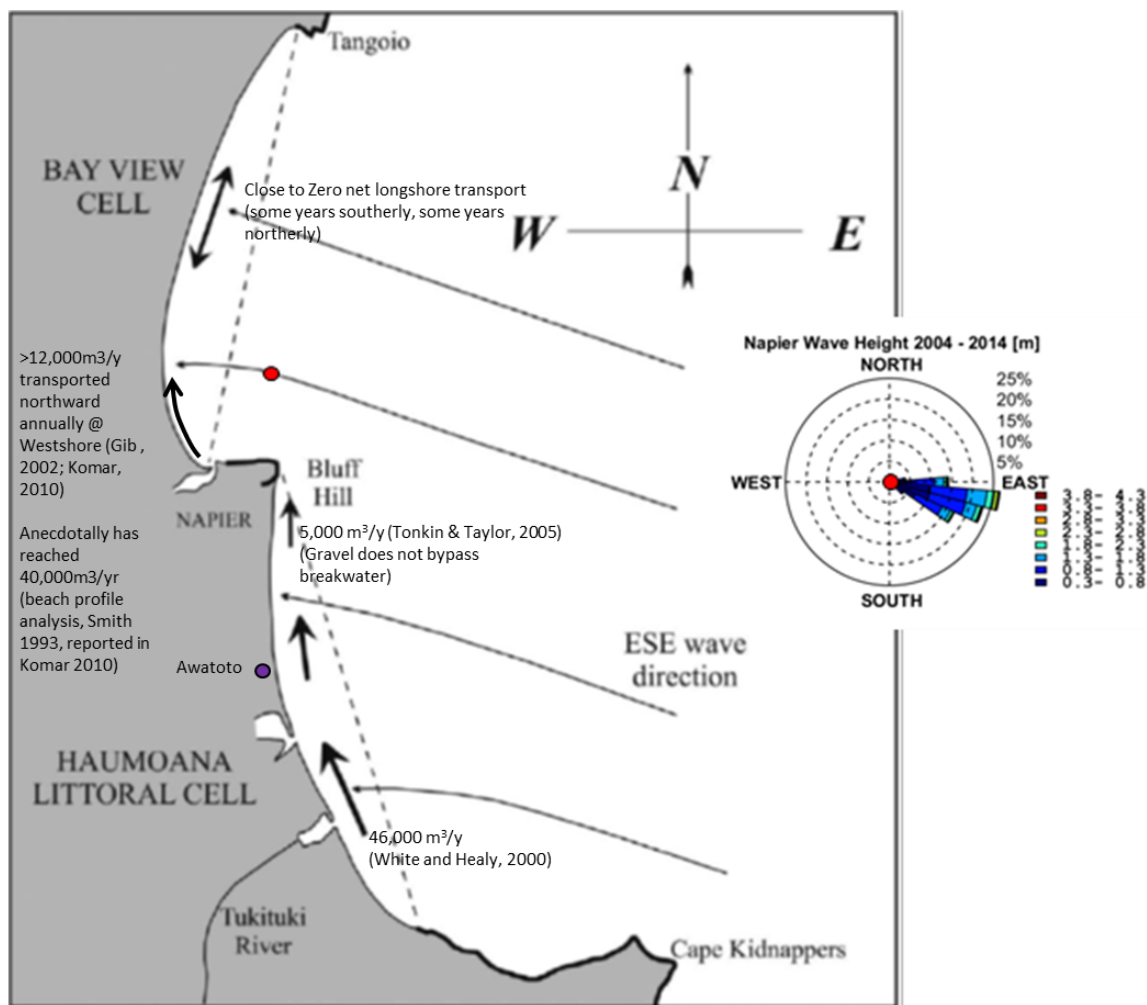


Figure 2-8: Interpretation of sediment transport pathways for gravel, on the basis of sediment budget closure analysis and orientations of the shores of the Bay View and Haumoana littoral cells, compared with the directions (wave rays) of the prevailing waves. The arrows denote the patterns of longshore sediment transport. Modified from Komar (2010) and Smith (1968).



2.4.2 Sources of Uncertainties in Sediment Budget

It should be noted that the above net transport volumes are *estimates*, with various levels of uncertainty attached to longshore drift rates. Setting aside knowledge gaps in present understanding of sediment transport and morphological processes occurring on mixed sand and gravel beaches, the remaining source of uncertainty for understanding sediment pathways around Napier is inferring losses due to abrasion.

Tumbling experiments on greywacke cobbles from beaches in Wellington and Christchurch New Zealand indicate percentage loss rates of 0.6% (Marshall, 1928) and 5.9% (Hemmingson, 2004) of the background sediment transport. A more recent field experiment on the southern Hawke Bay shoreline (Dickson, 2011) implies loss rates of 1.2–3.1%. Komar (2005, 2010) used the sediment budget closure method to derive an aggregate figure of 30,000m³/yr lost from the beach via abrasion within the Haumaona cell, giving an abrasion loss of slightly less than 1m³ per metre length of beach per year. The same rate per length of beach is assumed for the Bay View cell to give a best-estimate of 27,000 m³/yr.

The majority of authors (e.g. Hemmingson, 2004; Komar, 2005) find that the gravel and cobbles fracture to smaller grains, which are then further abraded to fine sand and silt particles from which the greywacke rocks were originally formed.

The movements of fine sediments in the sub-littoral zone are an additional source of uncertainty and will be dependent upon relative exposure to wave and current activity during calm and storm periods, the presence and strength of coastal currents under various wind conditions, and the existence of any net current.

2.4.3 Sources and Sinks of Sediment around Napier Port

2.4.3.1 Westshore Beach Nourishment Scheme

The Westshore beach is a site of active nourishment by Napier City Council (e.g. Gibb, 2002). The sediment used is usually of a slightly coarser size than is naturally present at Westshore.

Gibb (2002) reports that an average of some 12,000 to 15,000 m³/yr is placed on the beach above Mean Sea Level. That the sediment required annual (or near annual) recharge shows that the minimum annual littoral transport rate is in the order of 12,000 m³/yr and will be moved to the north by wave action. It is worth noting that the coarser sediment used for beach nourishment means the *realisable rate*¹ for natural sediment would be higher, and higher still for fine sandy material.

¹ The 'realisable rate' of sediment transport is that which is achieved in nature.



2.4.3.2 Port of Napier Maintenance Dredging

Analysis of dredging records by Single (2017) suggests between 1999 and 2015, on average approximately 37,000 m³/yr was dredged from the channel, fairway and berth areas. Only material dredged from the fairway or in capital dredging of the approaches, and described in dredging records as 'fine sand and silt' was placed at the inshore disposal area adjacent to Westshore ('R' in Figure 2-9), where the coarser fractions of sand sized particles (medium and coarse sand) would be available and suitable to move onshore. Gibb (2002) suggests that the fine sandy material was accumulated on the eastern side of the channel. However the level of aggregation in dredging records is such that a source direction (e.g. onshore/offshore) cannot be ascribed to material infilling the channel. Mud, clay and mixtures of sediment finer than sand were deposited at site 'Ia'.

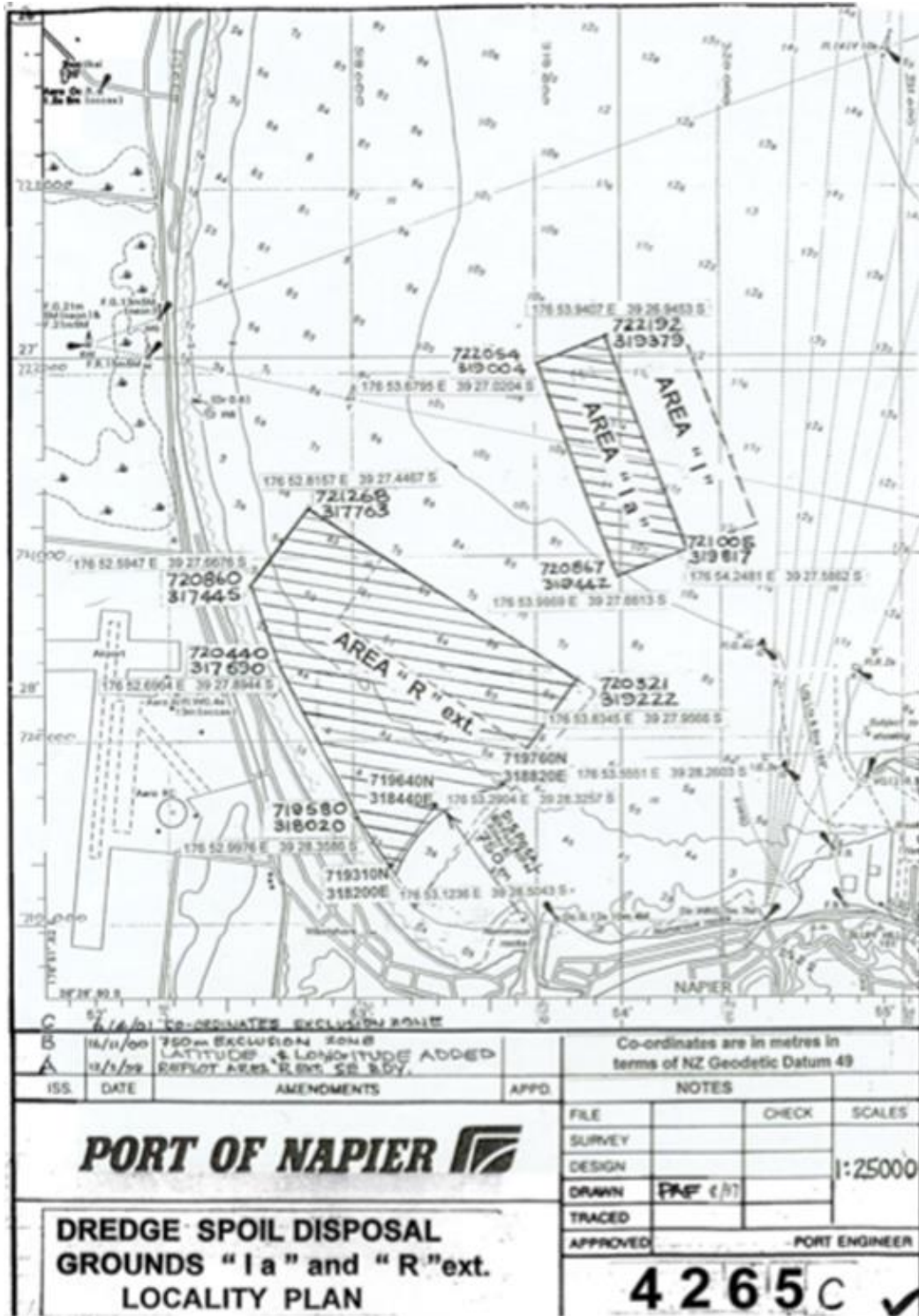


Figure 2-9: Dredge spoil disposal grounds "I a" and "R" ext. from Schedule 1 of Consent CL970159D. Adapted from Single (2017).



2.4.3.3 Ahuriri Entrance

Historically the entrance of Ahuriri Inlet (Ahuriri Inner Harbour) was a sediment sink but with the raising of land levels the sand bars immediately offshore of the entrance transitioned to bypassing types. Remaining sand and gravel deposits at Ahuriri were historically mined and placed on the beach at Westshore. Between 1987 and 2000 this occurred at a rate of approximately 4,000 m³/yr but this practice has since ceased.

Kirk and Single (1999) demonstrate that the presence of small amounts of gravel and sand at East Pier beach, Hardinge Road and Port Beach are the remnants of a sub-tidal bar that existed at Ahuriri in pre-European times. Prior to the 1931 earthquake, the Tutaekuri River flowed into Ahuriri Lagoon (Single 2017). The 1931 earthquake substantially reduced the tidal prism of Ahuriri Lagoon, allowing gradual onshore migration and reworking of whatever marine bars were formerly present at the entrance to the inlet.



3 Available Field Data

Napier Port Ltd have invested considerable resources in collecting field data for the purposes of constructing, calibrating and verifying numerical models of coastal processes at Napier.

3.1 Bathymetry and Topography

Beach profile data has been obtained from Hawkes Bay Regional Council for Standard Profiles HB13, HB14, HB15, HB16, HB17, HB18 and HB19 along Westshore and North Beach. The profiles were measured between December 2015 and January 2016.

Additional topographic survey data was collected by Port of Napier at Port Beach and along Hardinge Road in March 2016, extending seaward from the crest of the revetment to a level of 0m Chart Datum.

High resolution single-beam survey data has been collected and supplied by Napier Port Ltd for the Port entrance area, for survey years 2011, 2013, 2014 and 2015. Additional survey data was collected by Napier Port Ltd for the sea floor fronting Hardinge Road and Ahuriri Inlet in February 2016. Single-beam survey data was obtained by Port of Napier for the inshore disposal area adjacent to Westshore beach, in 2015.

Bathymetric information for the wider area of Hawke Bay is taken from New Zealand hydrographic survey charts NZ 5512, NZ 561, and NZ 56.

All of these data have been incorporated in the construction of the numerical model systems. Figure 3-1 shows spot depths and sounding intervals for the coast around Napier Port, Westshore and Bay View. The data are reduced to depths relative to Chart Datum. Horizontal positions are given to NZGD2000, HawkesBay2000 circuit.

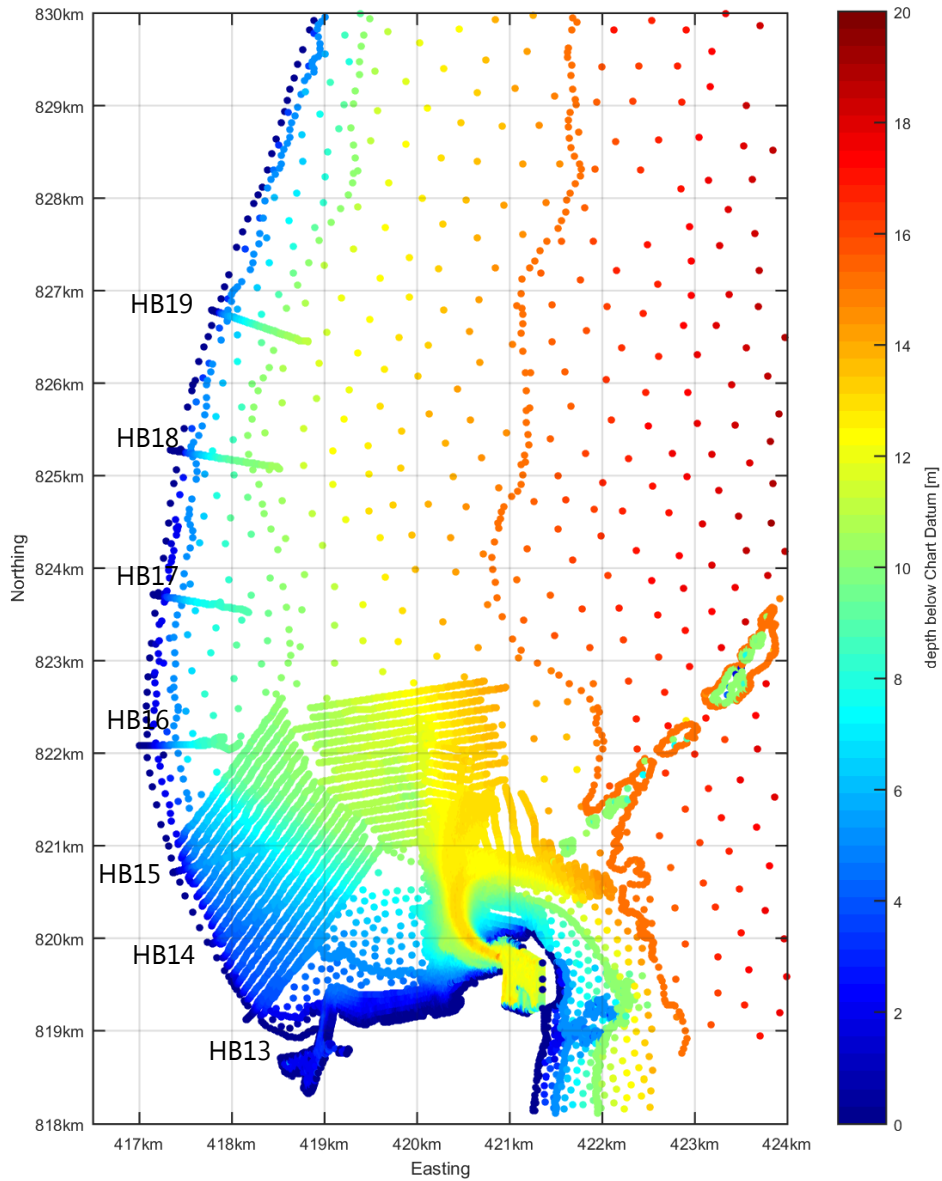


Figure 3-1: Spot depths (relative to Chart Datum) for the sea floor surrounding Napier Port. Locations of beach profiles are also shown.

3.2 Marine Sediments

Sediment data was collated for this project from previous studies including Mead et al. (2001) and Water Quality Center (1989). The data was collected and analysed for the project by NPL and Ocel (2004) at sites along Westshore and around the port.



Sub-tidal sea floor ('Marine') sediments at Napier are characterised by medium to fine sand. Some spatial variation in particle size distribution is evident in the 'sand fillet' area between the Port and North Beach, as described in Mead et al. (2001) and Water Quality Center (1989).

For a composite sediment sample, Water Quality Center (1989) report that the mud fraction (<0.0625 mm) is limited to deep water areas greater than 5 m and generally comprised 10 to 20% of the sample. The sand fraction (0.0625 to 2 mm) generally comprises up to 80 to 100% of the sample, of which the bulk of the sand fraction is fine (0.125-0.25 mm) to very fine sands (0.0625-0.125 mm). Sediment sampling and grading analysis by NPL and Cawthron (2005) further suggest that sands within the Port area have a median size (D_{50}) of 0.10 to 0.12 mm and a 90th percentile diameter (D_{90}) of approximately 0.90 mm. The surface sediments are underlain by a stiff silt/siltstone of variable depth and basement rock at depth. The stiff silt is described as a stiff, cohesive silt rather than clay with stiffness increasing with depth (Ocel, 2004).

Figure 3-2 shows the statistical distribution of the median (D_{50}) grain size for sandy sediments at Napier, based on some 100 grab samples reported in Mead et. al (2001). The median grain size of sandy sediments varies in the range of 0.11 to 0.31mm, with the average being 0.15mm. In general marine sediments are coarser to the northern end of Westshore and finer towards the Port, most likely reflecting the relative wave exposure.

Additional grab samples of surface sediments collected by Port of Napier around Westshore between 2m and 5m below Chart Datum corroborate these previous sediment descriptions. Geotechnical and particle size distributions of sub-tidal and sediments at and below the sea surface within and around the footprint of the proposed navigation channel are described in BECA (2016), and generally correspond to fine to medium sand with some silt fractions in deeper water or with burial depth.

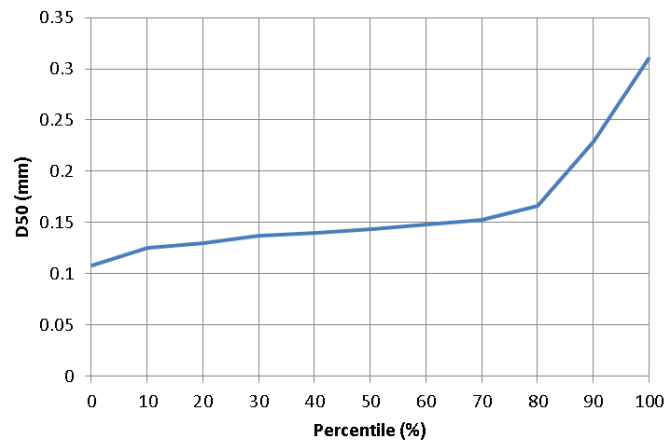


Figure 3-2: Percentile values of sandy marine sediments at Napier, on the basis of multiple sediment grab samples collected within the sub-littoral zone.



3.3 Beach Sediments

Napier Port Ltd has collected and analysed some 45 sediment samples of the gravel beaches at 15 locations between the Port Beach and Esk Estuary entrance (Figure 3-3). Samples were collected in January 2016 within the swash zone, between Low Tide, MHWS and just above MHWS.

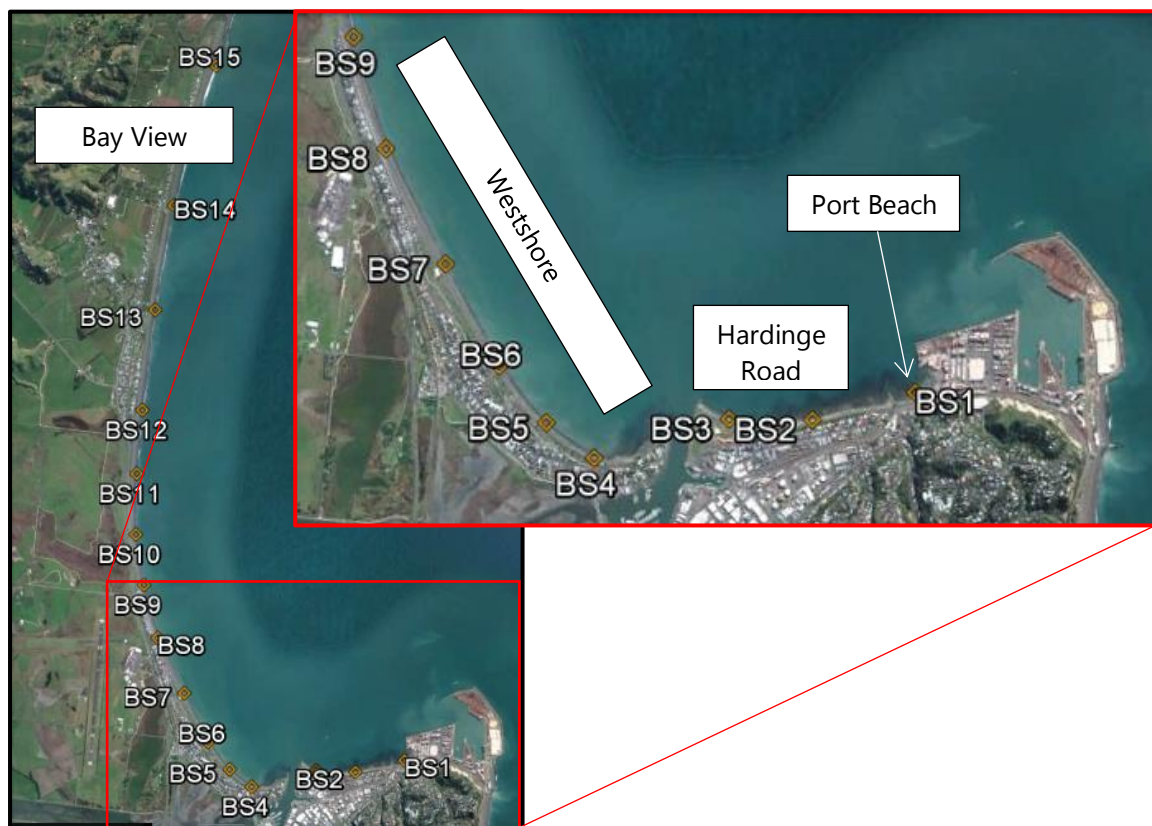


Figure 3-3: Locations of beach sediment samples between Port Beach (BS1) and Esk River entrance (BS15). Satellite imagery courtesy of Google Earth.

The sediments at each site were very widely graded between different sieve fractions (Figure 3-4, Figure 3-5), making it difficult to draw conclusions over a representative grain size for sediment transport estimates. In general, the mixed sediments at Low Tide and MHWS may be classified as fine gravel, with grain sizes in the range from fine to medium sand at the 10th percentile to coarse gravel at the 90th percentile. The particle size distribution of sediments collected at Low Tide generally are consistent between sites. The particle size distribution of sediments collected at MHWS elevation show a great deal of variability between sample locations along Hardinge Road and Westshore, while those collected at North Beach showed an overall trend of increasing grain size with distance northward.

Plotting the median grain size at each site as a function of chainage distance westward and northward from the Port (Figure 3-6) suggests that the beach sediments may be broadly characterised as fine to medium gravel below the elevation of MHWS. At levels corresponding to



Low Tide (i.e. the level at which sediments are always under active transport) the average sediment size is 1.8mm, that at MHWS is 2.5mm and that at just above MWHS is 4.5mm.

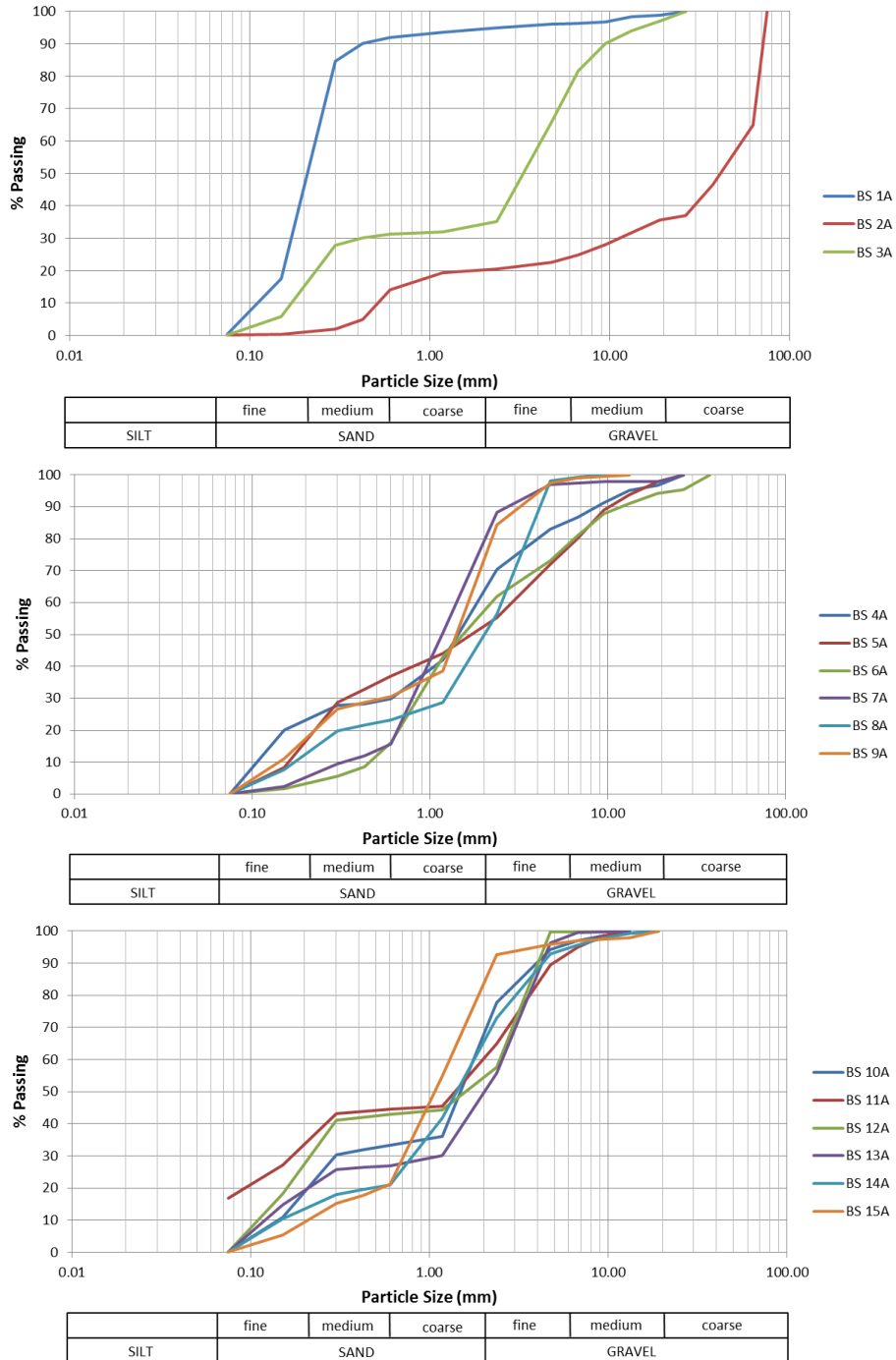


Figure 3-4: Particle size distributions of mixed sand and gravel beach sediments at Low Tide level between Napier Port and Esk River entrance. Upper Panel: Port Beach and Hardinge Road. Middle Panel: Westshore, between Ahuriri Inlet and the Beacons. Lower Panel: North Beach, between the Beacons and Esk River entrance.

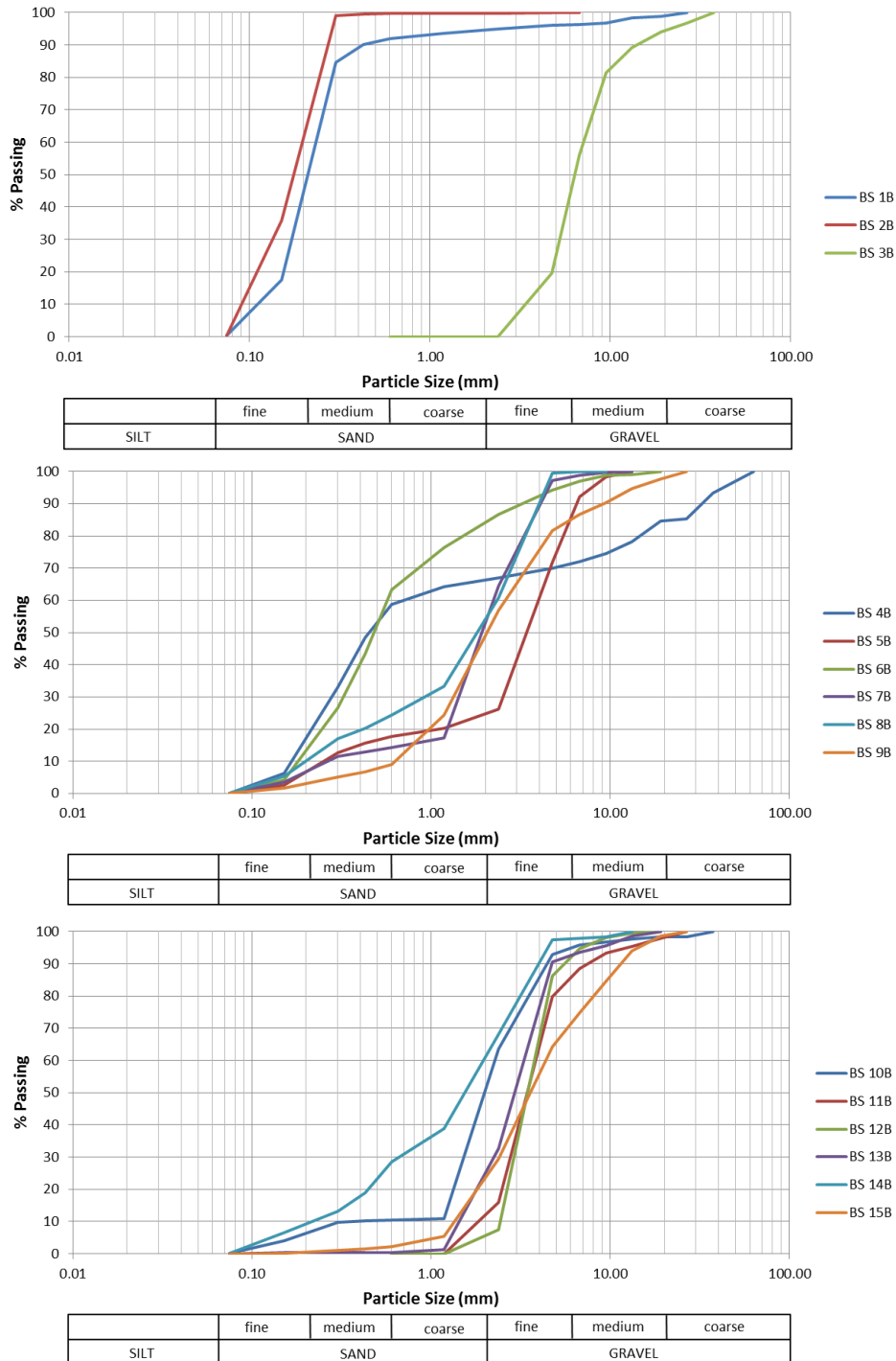


Figure 3-5: Particle size distributions of mixed sand and gravel beach sediments at MHWs level between Napier Port and Esk River entrance. Upper Panel: Port Beach and Hardinge Road. Middle Panel: Westshore, between Ahuriri Inlet and the Beacons. Lower Panel: North Beach, between the Beacons and Esk River entrance.

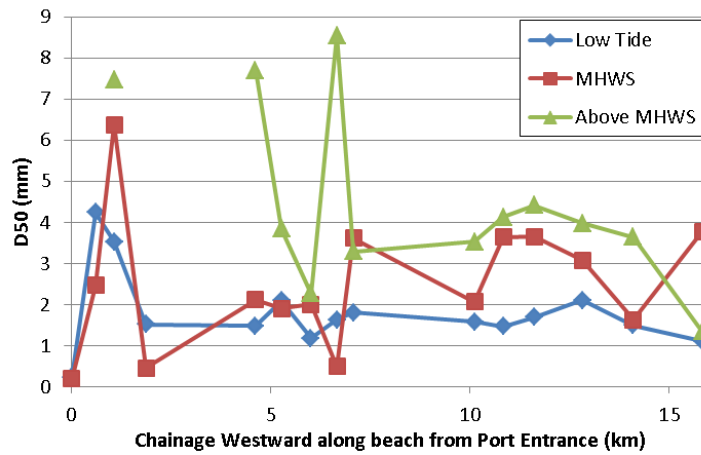


Figure 3-6: Median grain size of beach sediments at three tidal planes as a function of distance from Napier Port.

3.4 Waves

Napier Port Ltd has operated a series of Triaxis wave buoys measuring swell waves incident to the navigation channel adjacent to Pania Reef since 2004. Additional wave data has been collected by Napier Port since April 2016 for the purposes of verifying the performance of wave models. Figure 3-7 shows the location of each of the instruments. Table 3-1 summarises the instrument type, wave parameters measured and data coverage period.

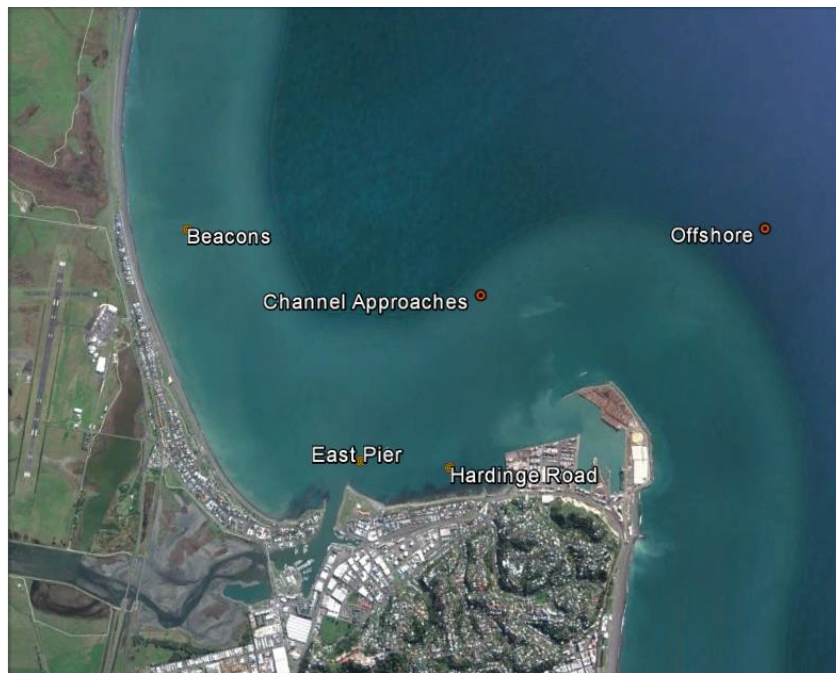


Figure 3-7: Locations of wave gauge instruments in relation to Napier Port

Table 3-1: Locations of wave gauges

Location	Instrument type	Position	Parameters	Period
Offshore	Triaxis buoy	39.457690° S, 176.934442° E	Swell wave height, period, direction	2004 to Present
Channel Approaches	Triaxis buoy	39.463400° S, 176.907713° E	Swell wave height, period, direction	May – September 2016
Beacons	RBR Solo (pressure transducer)	39.459333° S, 176.879575° E	Swell wave height, period	April – September 2016
East Pier	RBR Solo (pressure transducer)	39.475750° S, 176.897098° E	Swell wave height, period	April – September 2016
Hardinge Road	RBR Solo (pressure transducer)	39.476017° S, 176.905400° E	Swell wave height, period	April – September 2016



3.5 Wind

Anemometer data has been collected by Napier Port Ltd since 2004 at a level of 10.3m above Napier Mean High Water Springs.

Analysis of 1-minute average wind speeds (Figure 2-3) show the dominant directions to be South-West and West. Strongest winds occur from the West and North-West. The median 1-minute average wind speed is in the order of 9 m/s but with a seasonal component that varies between about 8 and 10m/s.

Further description of the wind climate is given in Section 2.2.2.

3.6 Currents

Rose plots of depth-averaged ADCP current measurements are shown in Figure 3-8. The deployment period was May to September 2016. The ADCP units were sited in approximately 6m ('Beacons' ADCP) and 10m ('Channel Approaches ADCP'), respectively.

The observed current speeds are in the range of 5 – 10cm per second, occasionally exceeding 20cm/s during storms. Both ADCP sites have a residual current of approximately 2cm per second. The current speeds at both sites are strongly correlated with wind speed. The currents appear to persistently follow bathymetric contours, which is consistent with previous analysis of currents at Westshore presented in Mead (2001) and WorleyParsons (2005). At the 'Beacons' ADCP site the current runs parallel to the coast in a SE direction, whilst at the 'Channel Approaches' ADCP site the current is persistently eastward. Some reversals in currents are observed but a clear predominant flow direction is apparent at each site.

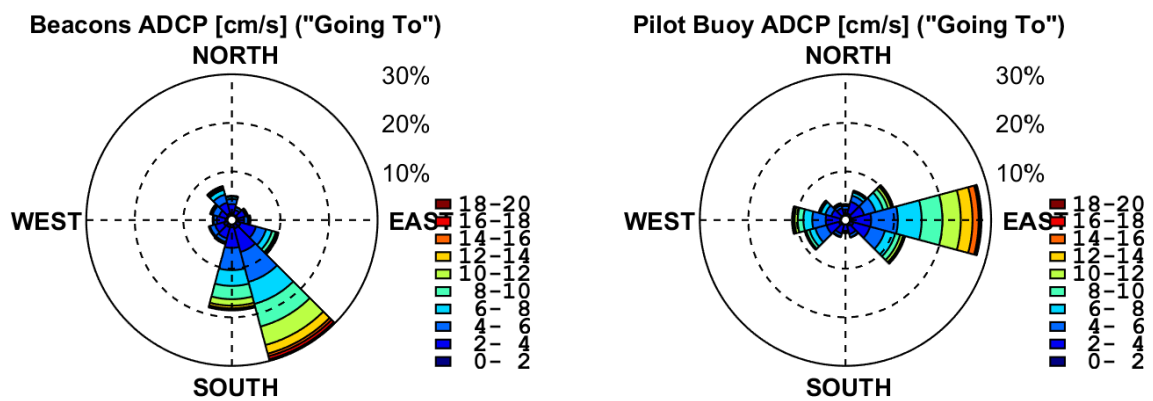
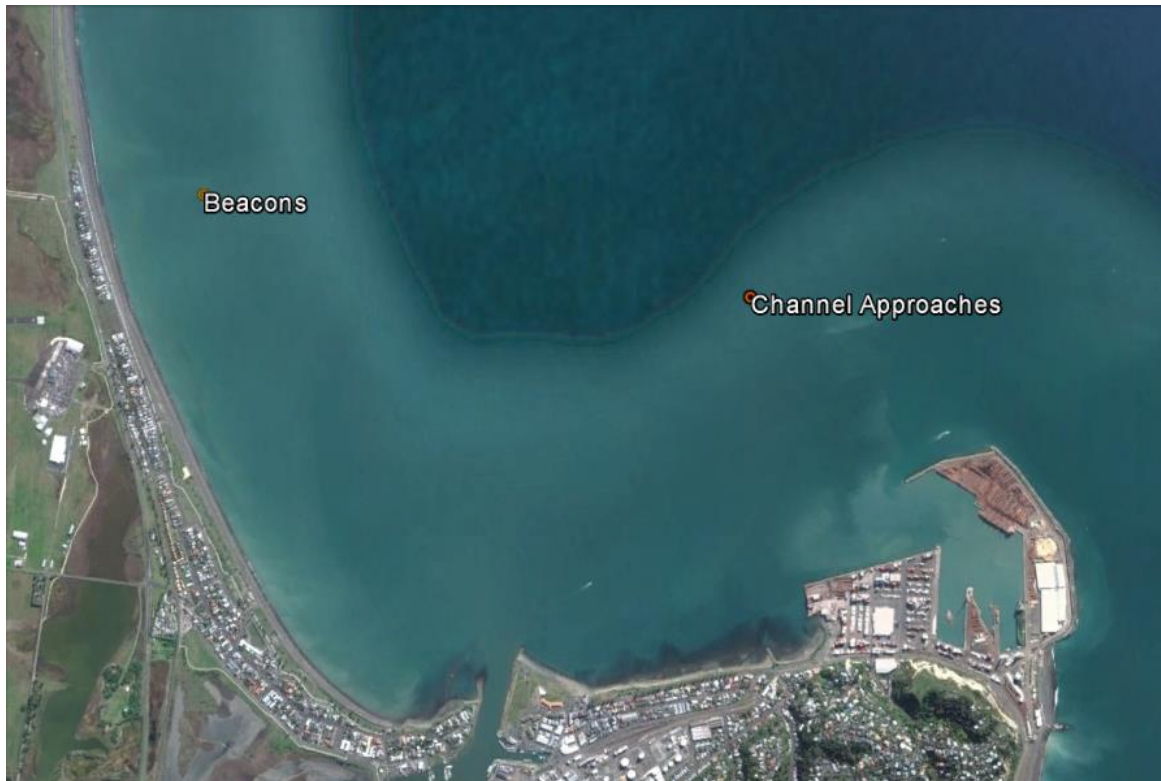


Figure 3-8: ADCP measurements of depth-averaged current speed measured at Napier. Upper Panel: Location of ADCP units. Lower panel: Rose plots of current speed and direction, based on data recorded between May and August 2016.



4 Numerical Model Systems

4.1 Model Descriptions

A series of numerical model systems have been constructed for simulating coastal processes at Napier. Each target the processes to which they are most suited. Wave, current and sandy sediment transport processes are simulated using the Delft3D suite of numerical models. Wave simulations for assessments of impacts to surf breaks are simulated using a Boussinesq model, MIKE21BW. These model systems are described below.

4.1.1 Delft3D

The DELFT3D-FLOW module, which is used to simulate wind-driven and wave-driven currents, is a multi-dimensional (2D or 3D) hydrodynamic (and transport) simulation program that calculates non-steady flow and transport phenomena that result from tidal and meteorological forcing on a curvilinear, boundary fitted grid. For the 3D simulations considered in this study, the vertical grid is defined following the σ co-ordinate approach¹. That is, the model is split in to a number of layers that are defined as a constant percentage of water depth.

Wave processes are simulated by the Delft-3D Wave model, SWAN. SWAN is a 3rd Generation phase-averaged spectral wave model, incorporating most of the key physical processes occurring in the coastal zone. Including generation by wind, refraction and shoaling over a bottom of variable depth and/or a spatially varying ambient current; dissipation by whitecapping, bottom friction and depth-induced breaking; and (to some extent) nonlinear wave-wave interactions.

Wave-induced currents are calculated by coupling Delft3D WAVE with Delft3D FLOW to calculate wave setup and set-down, undertow, near bed current velocities, and near bed shear-stresses induced by the combination of wave dissipation and wave-induced currents. These quantities in turn are used by the sediment transport module and hence the potential for dredged sediments to be re-suspended or remain in suspension

The FLOW and WAVE model grids are operated using dynamic coupling between a 'regional' scale grid encompassing the Bay View littoral cell at 180m, a 'medium' scale grid at 60m resolution encompassing the region from Esk River to Napier Port, and a 'local' scale grid at 20m resolution encompassing Napier Port, to the northern boundary of Westshore. Bathymetric survey data used to construct the model is shown in Figure 3-1. Detail of the wave model bathymetry around Port of Napier and Westshore is shown in Figure 4-1. This bathymetry is also used for the Boussinesq model.

Wave height, period and direction time-series measured at the Triaxis buoy maintained by Port of Napier are used as boundary conditions. The resultant wave heights and periods simulated by the WAVE model are then used by the FLOW model to calculate near bed current velocities and near bed shear-stresses induced by the waves, and hence the potential for sediments to be transported.



Transport of non-cohesive sediments are simulated in the model using the TRANSPOR2004 sediment transport algorithm (Van Rijn, 2007), which represents the state-of-the-art in sediment transport algorithms and knowledge of sediment transport processes for sandy sediments.

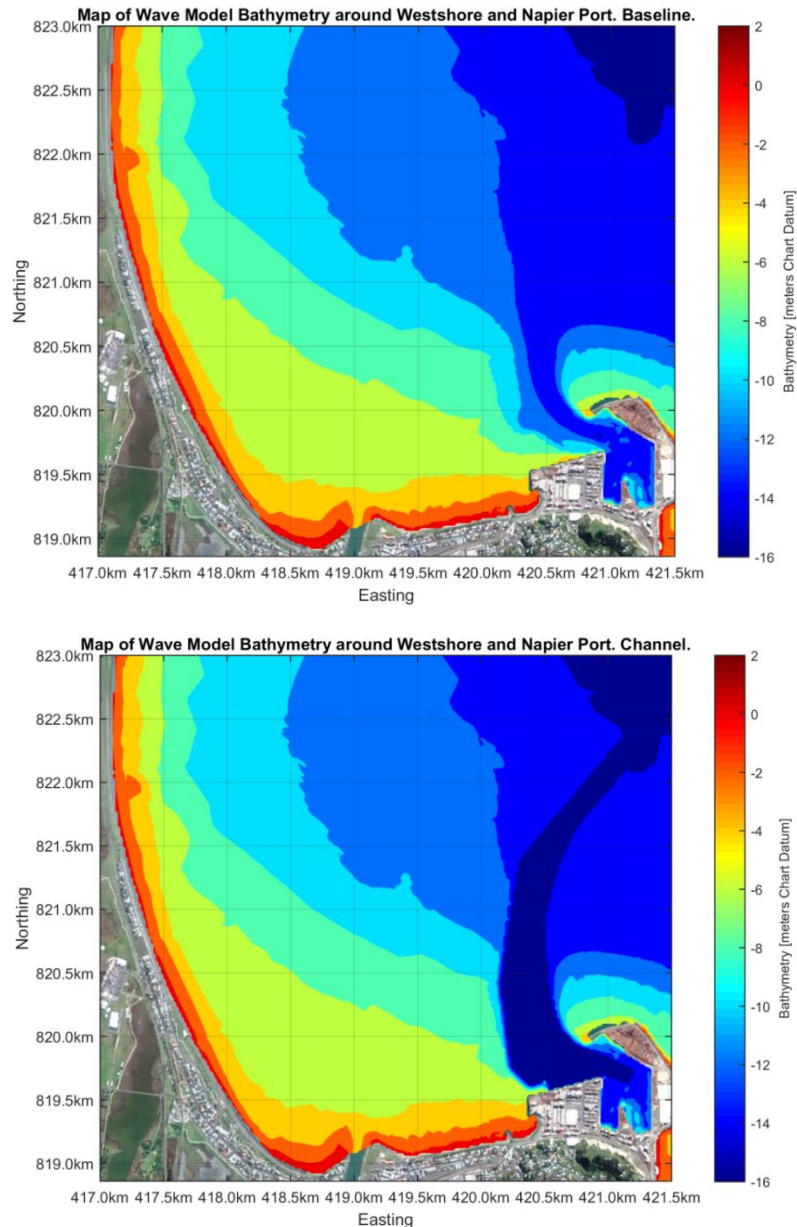


Figure 4-1: Upper panel: Detail of model bathymetry around Napier Port and Westshore, 'Baseline'. Lower panel: Detail of model bathymetry around Napier Port and Westshore, with proposed channel footprint dredged to depth of -14.5m Chart Datum. Bathymetric levels set at 2 metre intervals.



4.1.2 MIKE21 BW

Wave shoaling in very close proximity to the Port is determined by a combination of wave refraction and diffraction. In these regions a very fine description of the bathymetry is also required to adequately capture sharp gradients in wave energy.

MIKE 21 BW is capable of reproducing the combined effects of all important wave phenomena of interest in port, harbour and coastal engineering. These include Shoaling; Refraction; Diffraction; ; Wave breaking; Bottom friction; Partial reflection and transmission; Non-linear wave-wave interaction; Frequency spreading; and Directional spreading.

The 2DH module (two horizontal space co-ordinates) solves the enhanced Boussinesq equations by an implicit finite difference technique with variables defined on a space-staggered rectangular grid.

The Boussinesq wave model is applied to assess potential changes of surf breaks at Port Beach and East Pier due to channel deepening.

4.2 Wave Model Calibration and Validation

4.2.1 Calibration

Calibration of the wave model was undertaken using data collected at three inshore locations, using wave height at the calibration parameter. Wave data was collected between March and September 2016 using RBS Solo ® Pressure Transducers located in about 6m water depth. The sample frequency was 2Hz.

The time series data collected by NPL was analysed by Advisian to ascertain wave frequency spectra and integral wave parameters (H_{m0} , T_p , T_{m01}) every hour. A high-pass filter was applied to the raw time series prior to spectral analysis to remove components of the water level signal due to tide, surge and infragravity processes. Spectral parameters were calculated using a 20-minute time series, centred on the hour.

Two separate storm events ('Cal1' and 'Cal2') were selected for the purposes of model calibration Figure 4-2. Simulations were run using bottom friction, directional spreading and water levels as independent variables. Bulk error statistics were calculated for each location by amalgamating model results across both storms to give approximately 150 comparisons between simulated and observed data at each location. Graphs showing the error statistics are shown in Figure 4-3 to Figure 4-5.

The *Mean Absolute Error* (MAE) is a quantity used to measure how close the model results are to the measured data. A MAE of 0.1m means that the model is considered accurate to $\pm 0.1m$.

The *Bias* is a measure of whether the model tends, on average, to over-or under-predict the observed wave heights at a particular location. A positive bias means that the model tends to over-predict. A negative bias means that the model tends to under-predict.



The *Scatter Index* is a non-dimensional measure of whether the natural scatter in the comparison between model and data is comparable to the natural variation in the observations themselves. The Scatter Index is defined as the standard deviation of the difference between model and observations, normalised by the mean of the observations, and ideally should as small as possible.

The *Skill* of the model is another non-dimensional performance statistic. A Skill score of 1 indicates a perfect agreement between measured and simulated values. Scores equal to or less than 0 indicates that the model is completely unable to reproduce the observed wave data. Generally accepted qualifications of different skill scores are shown in Table 4-1.

Table 4-1: Skill Score qualifications (after Sutherland et al, 2004)

Range	Qualification
0.8 to 1.0	Excellent
0.6 to 0.8	Good
0.3 to 0.6	Reasonable
0 to 0.3	Poor
Less than 0	Unacceptable

The best calibration for bottom friction was achieved with JONSWAP friction of 0.06. This value is similar to that found to perform best at other locations with swell waves of similar height and periods, in similar water depths and seafloor composition.

The best calibration for wave directional spreading was achieved for a directional spreading parameter of $n = 10$. In general, the directional spreading factor for swell ranges from 8 to 100, with values of 8 to 20 being in the typical range.

Comparison of model error for water level in the range of Lowest Astronomical Tide (LAT) to Highest Astronomical Tide (HAT) found little sensitivity to water depth. All further simulations are undertaken at Mean Sea Level, which is 0.95m above Chart Datum.

The calibration error statistics are summarised in Table 4-2. The model reproduces wave heights at the calibration location to an accuracy (MAE) of better than $\pm 0.1\text{m}$, with a bias of less than or equal to 0.05m. The skill score of the model is close to or greater than 0.8, corresponding to 'excellent' accuracy.

Time series plots comparing the calibrated model against observed H_{m0} and T_p for the storm events at each of the three locations are shown in Figure 4-6 to Figure 4-8.

Table 4-2: Summary of calibration error statistics for calibrated wave model

Location	MAE (m)	Bias (m)	Scatter Index	Skill Score
Beacons	0.08	0.05	0.17	0.85
East Pier	0.06	0.03	0.20	0.78
Hardinge Road	0.04	-0.01	0.13	0.89

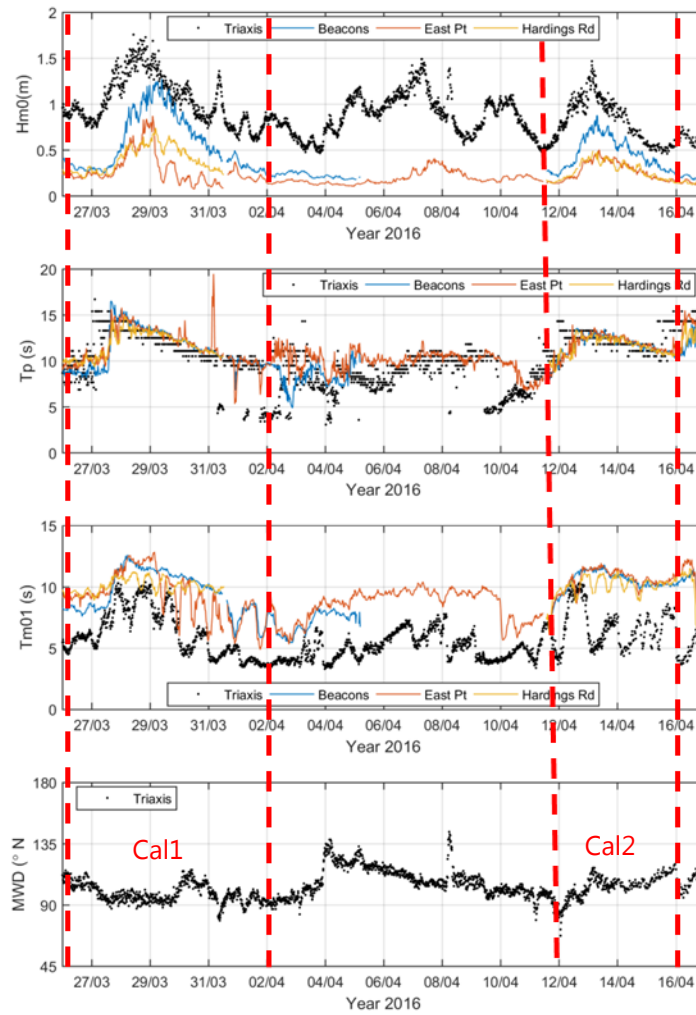


Figure 4-2: Storm events used for wave model calibration.

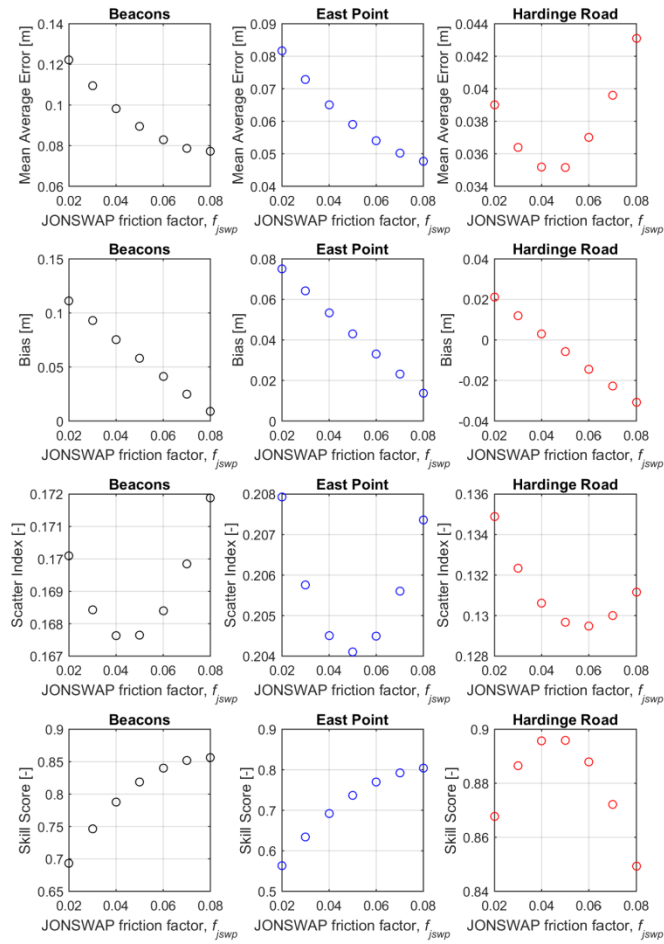


Figure 4-3: Wave model error statistics at the three calibration sites, considering bed friction as independent variable.

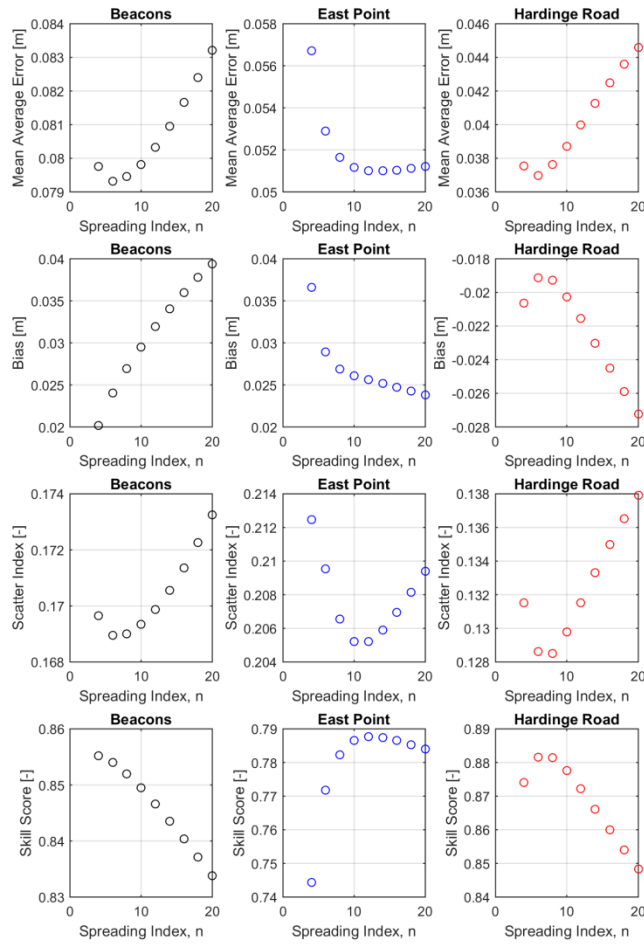


Figure 4-4: Wave model error statistics at the three calibration sites, considering wave directional spreading as independent variable.

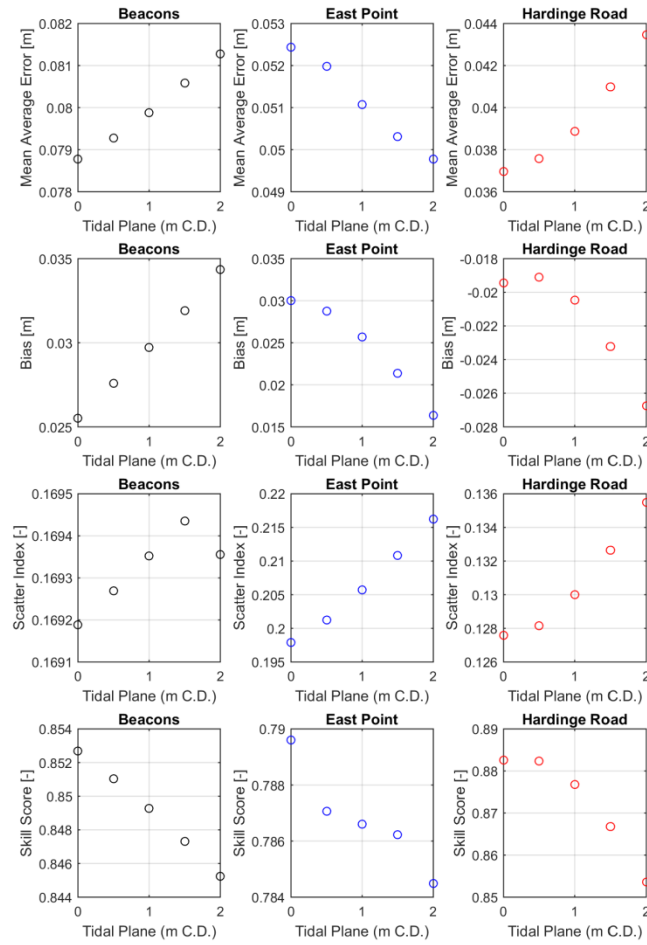


Figure 4-5: Wave model error statistics at the three calibration sites, considering tidal plane as independent variable.

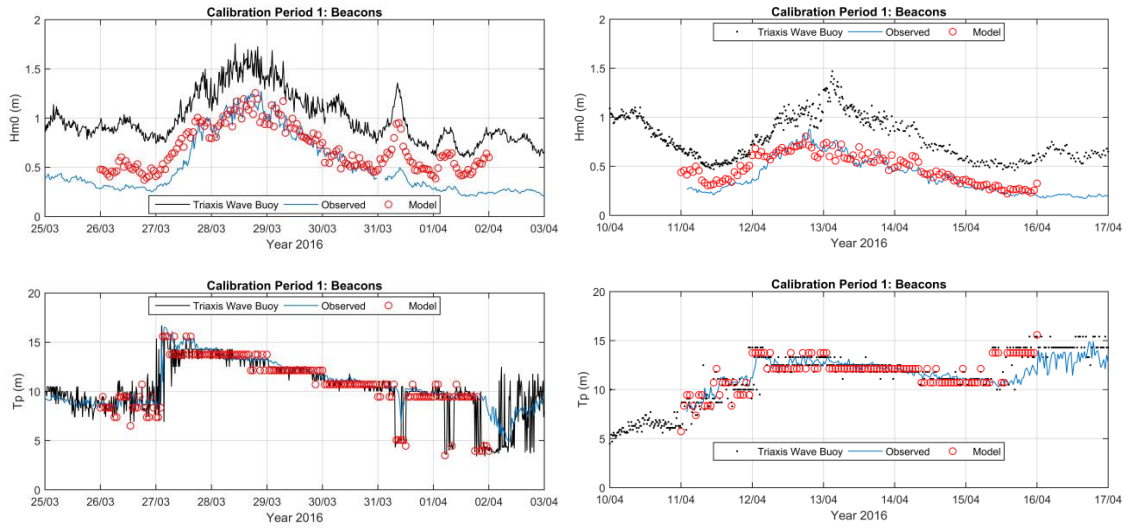


Figure 4-6: Comparison of calibrated wave model against storms 'Cal1' and 'Cal2'. Calibration site 'Beacons'.

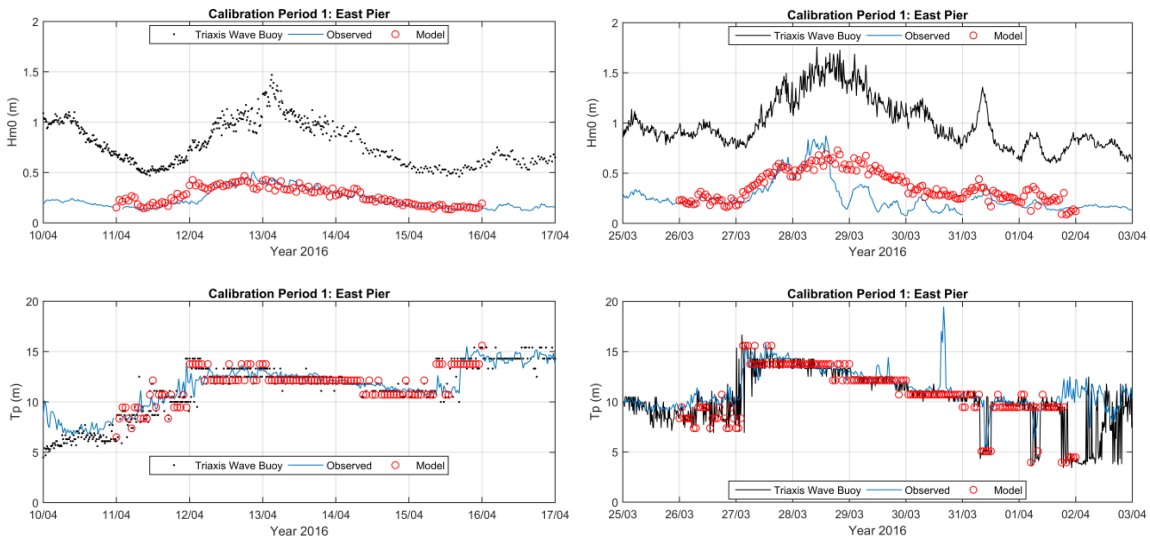


Figure 4-7: Comparison of calibrated wave model against storms 'Cal1' and 'Cal2'. Calibration site 'East Pier'.

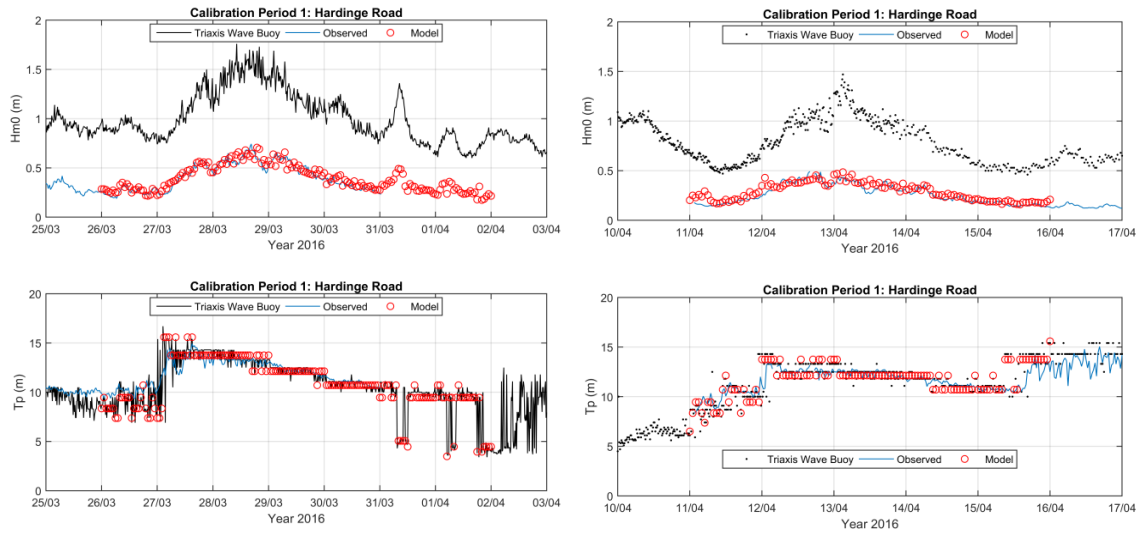


Figure 4-8: Comparison of calibrated wave model against storms 'Cal1' and 'Cal2'. Calibration site 'Hardinge Road'.

4.2.2 Validation

The capability of the calibrated wave model to reproduce observed wave height, period and direction is assessed for three further storm events. These are considered as an independent check of the model. Figure 4-9 validates the performance of the wave model at 'Beacons', 'East Pier' and 'Hardinge Road' for three large storm events occurring between May and July 2016. Figure 4-10 further validates the model for wave direction as measured by Triaxis waverider buoy at the 'Pilot Buoy' located a short distance west of the channel approaches.

The model MAE for wave height remains at better than $\pm 0.1\text{m}$. At the Pilot Buoy the MAE for wave period is better than ± 1 second, and MAE for wave direction better than ± 5 degrees.

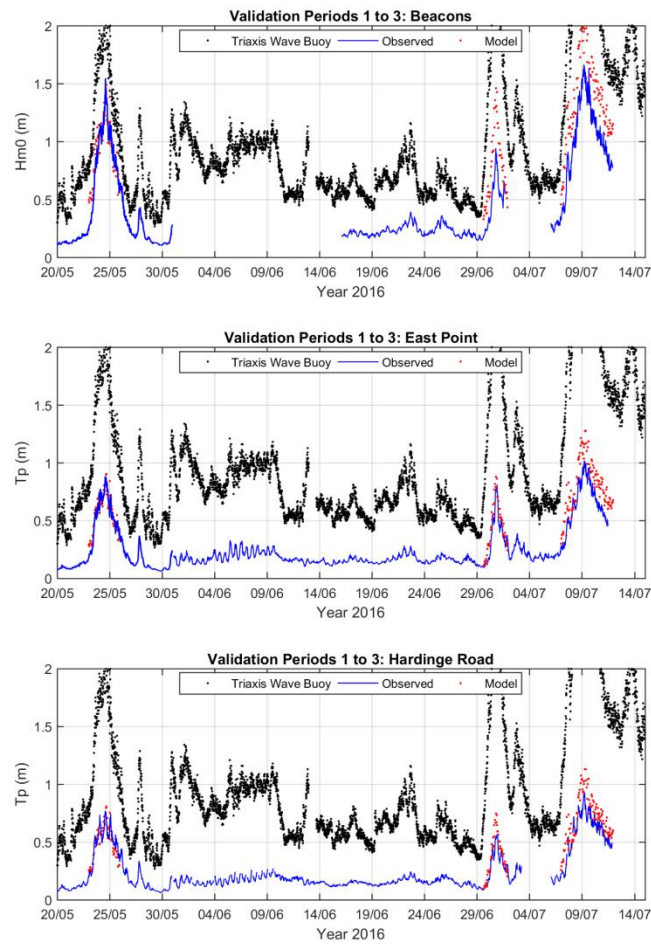


Figure 4-9: Validation of wave model at inshore locations 'Beacons', 'East Pier' and 'Hardinge Road' using parameters selected during calibration of wave model.

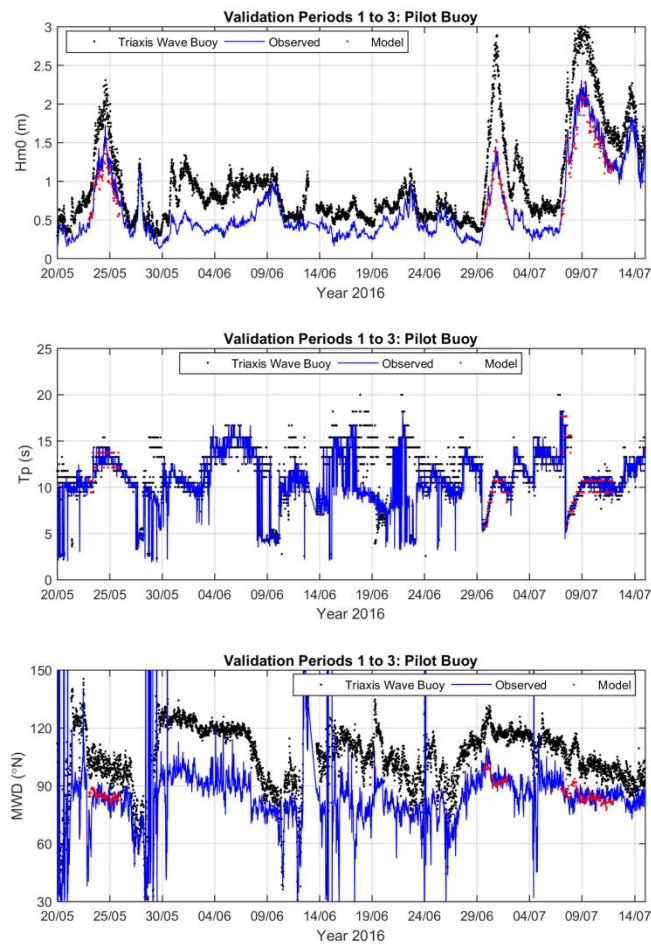


Figure 4-10: Validation of wave model for wave height, period and direction for at inshore location 'Pilot Buoy' (also referred to as 'Channel Approaches' in report text).



5 Wave Refraction

5.1 Introduction

The morphological behaviour of coastlines is dictated by changes to wave refraction. As beaches in general tend to be aligned in the direction of incident waves, any changes to wave direction will affect coastal morphology. Changes to wave height govern the speed at which this change will happen.

In areas where wave refraction is strongly two-dimensional, such as around navigation channels, the degree to which waves are refracted, focussed or scattered depends on the wave incidence angle and wave period. Therefore, a convenient method of visualising changes to the wave climate is to assess the 'energy-weighted mean wave condition'.

5.2 Method of Assessment

The method is applied to the wave climate measured at the Triaxis waverider buoy maintained by Port of Napier. The process is:

1. Classify the wave climate measured at the buoy to discrete combination intervals of mean wave direction, period and wave height.
2. Calculate the occurrence probability of each combination of [MWD, T_p , H_{m0}]. Weight the occurrence probability in accordance to the energy of each bin. That is, weight in accordance to the square of the wave height.
3. Apply each combination of [MWD, T_p , H_{m0}] as a boundary condition to the calibrated wave model. For this analysis, some 200 combinations of wave direction, period and height were simulated.
4. Obtain values of simulated wave parameters at each grid point over all wave classes, and multiply by the energy-weighted occurrence probability. Summing over all weighted wave conditions results in the mean 'energy weighted' wave height, period and direction.

The analysis is undertaken for 'baseline' and 'dredge channel' bathymetries. Subtracting the 'baseline' model results from the 'dredge channel' results give the change to wave height and direction.

The advantage of this method is that by weighting the importance of each wave condition by its contribution to the total wave energy, relatively rare waves (e.g. large storms) that infrequently occur but are of importance to sediment transport are not neglected. Similarly, the contribution from frequently occurring but small waves is not exaggerated.



5.3 Optimisation of Channel Footprint

A due-diligence process has been followed during this project to optimise the geometry of the dredge channel such that any impacts to wave refraction are minimised as much as possible. Design elements of the navigation channel dredge footprint that have been varied to optimise the final design include:

- Location of the 'dogleg' in the navigation channel as the approaches change from NE to N orientation.
- Impact of channel curvature between the dogleg and the swing basin, and diameter of swing basin.
- Angle of the swing basin as it transitions between the navigation channel and Wharf 6 berth pocket.

A total of seven alternative dredge footprint geometries were assessed before settling on a final design. For completeness the calculated change in energy weighted mean wave height and direction are shown in Figure 5-1 to Figure 5-3.

Impacts of the optimal design channel footprint are presented more fully in Section 5.4.

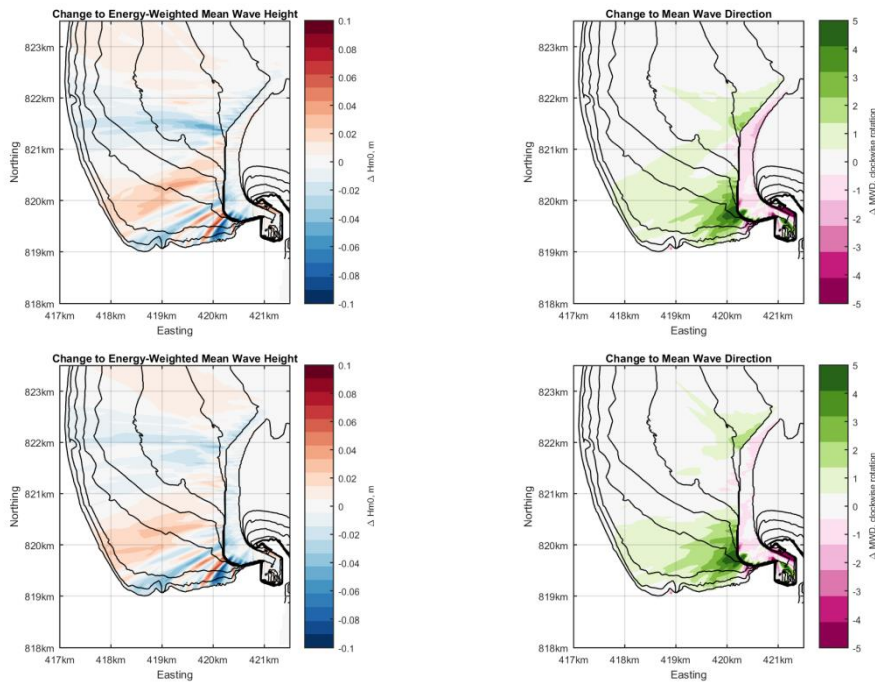


Figure 5-1: Analysis of channel geometry design on wave refraction patterns: Location of 'dogleg' on JOSCO channel approaches about 1km North of Port entrance.

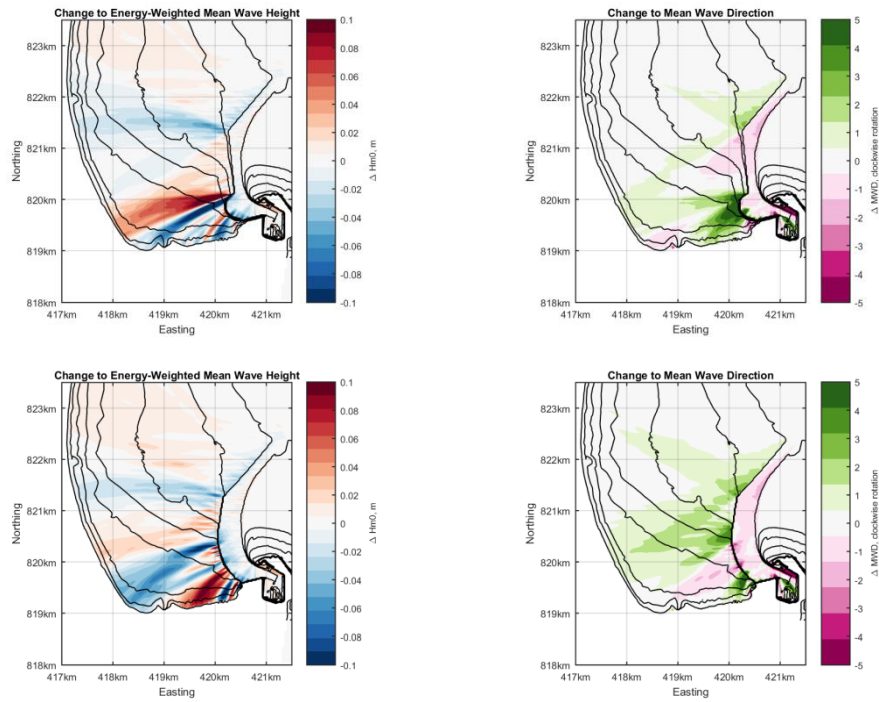


Figure 5-2: Analysis of channel geometry design on wave refraction patterns: Impact of turning basin and curvature of JOSCO channel approaches to port entrance.

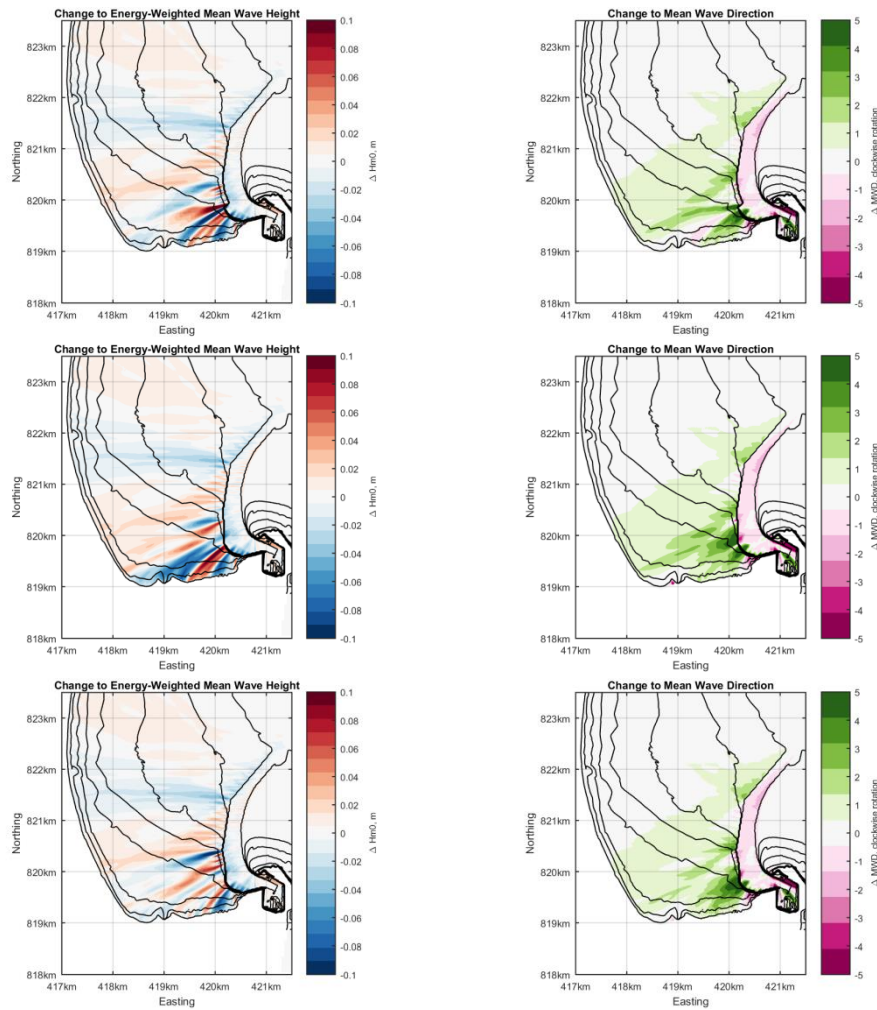


Figure 5-3: Analysis of channel geometry design on wave refraction patterns: Impact of fine detail of turning basin geometry on wave refraction patterns.



5.4 Impact of 'Final' Dredge Channel Design

5.4.1 Wave refraction patterns

Figure 5-4 shows the energy-weighted mean wave height and direction for 'baseline' and with the design footprint of the navigation channel dredged to a depth of -14.5m C.D. In general, minimal change is apparent in the vectors and the wave height. Some modification of the wave height and direction is evident along Hardinge Road due to strong refraction by the navigation channel approaches and swing basin. Wave focusing on this part of the shoreline will be strongly dependant on wave period and incidence angle seaward of the Port.

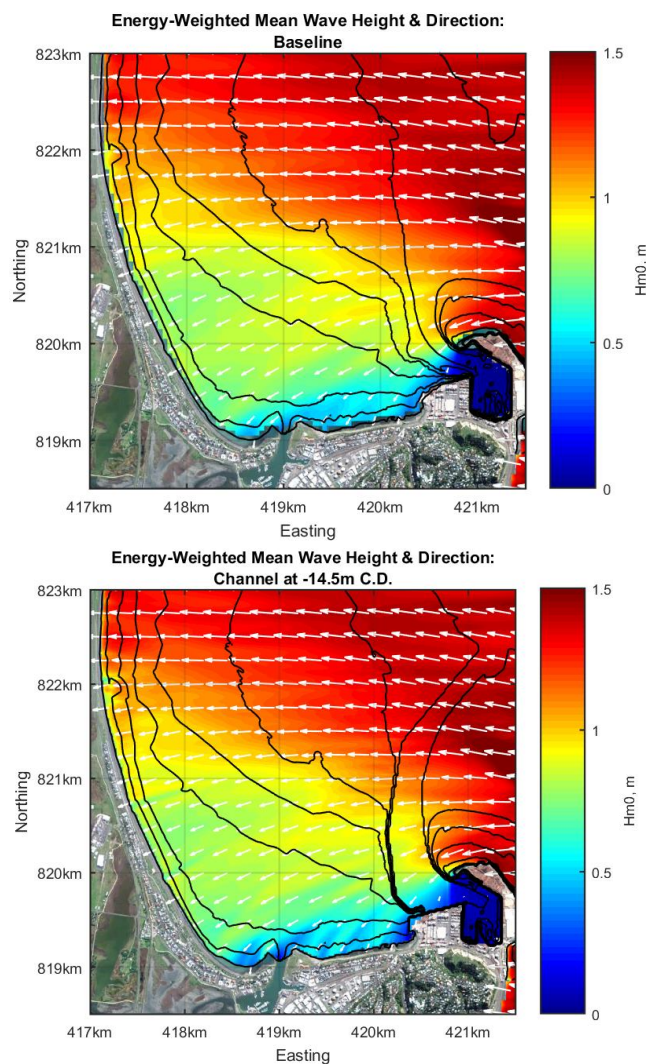


Figure 5-4: 'Energy weighted' patterns of wave refraction around Napier Port. Upper Panel: 'Baseline' conditions represent how waves refract today. Lower Panel: Simulated wave refraction patterns for optimal design of navigation channel and turning basin, dredged to depth of -14.5m C.D.



5.4.2 Changes to Energy Weighted Mean Wave Height and Direction

Plotting the change in energy weighted wave height and direction (Figure 5-5, Figure 5-6) reveals more clearly the impact of the navigation channel. Wave height and direction is strongly modified in the vicinity of the Port. The geometry of the swing basin scatters wave energy away from Port Beach and towards the entrance of Ahuriri Inlet. Wave directions are also strongly modified, with a *clockwise* rotation of between 1 and 4 degrees. The influence of channel dredging rapidly decreases to the west. Along Westshore wave angles are modified by less than 1 degree. Wave energy is reduced at the southern end of Westshore, and slightly increased at the northern end towards Bay View.

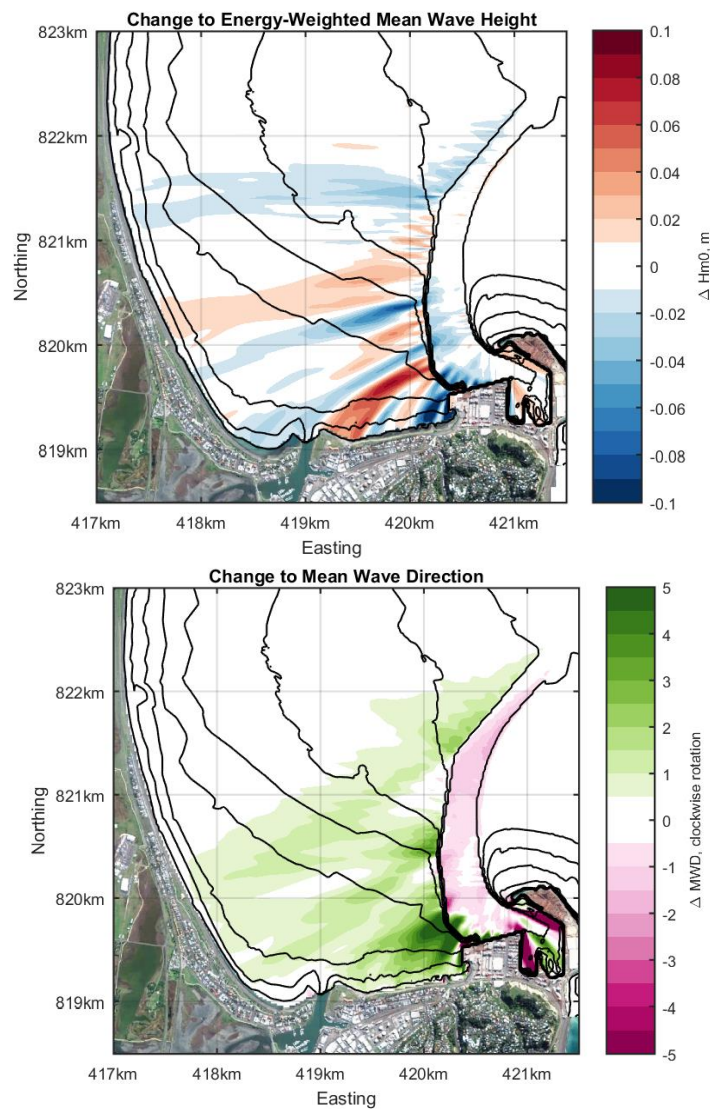


Figure 5-5: Changes in patterns of wave refraction around Napier Port due to deepening of navigation channel to -14.5m C.D. Upper Panel: Change in mean wave height. Lower Panel: Change in mean wave direction.

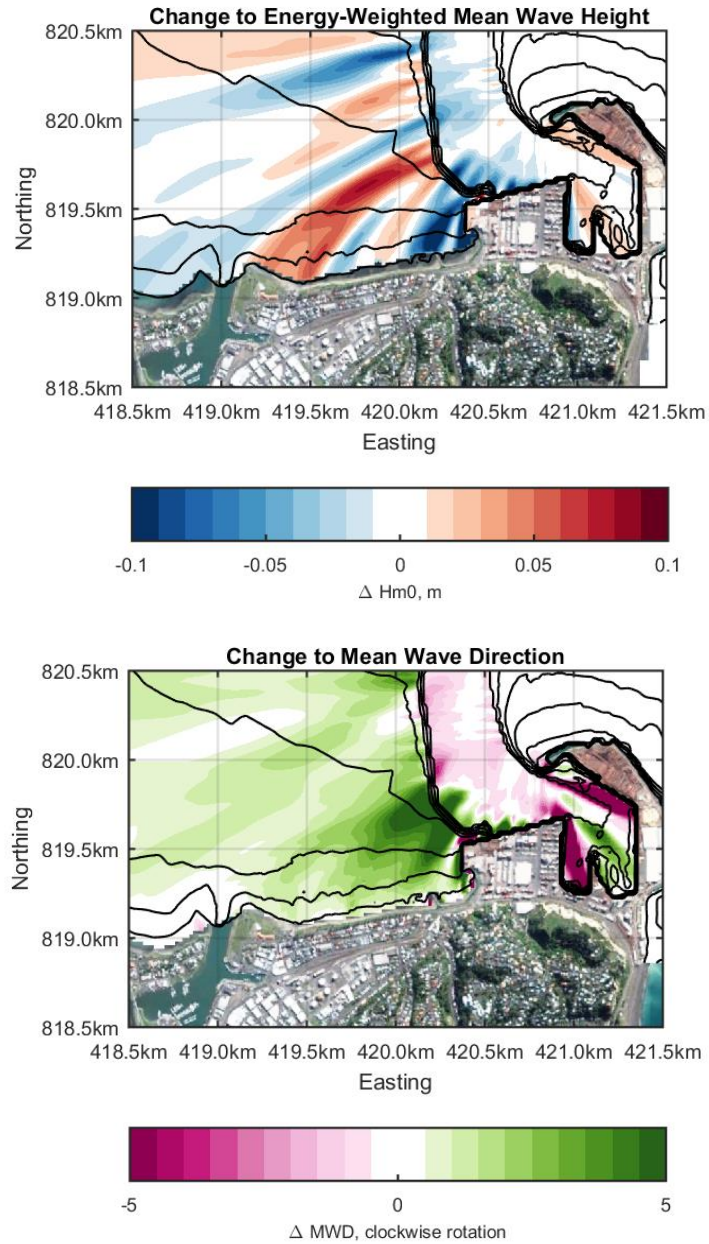


Figure 5-6: Detail of changes in wave refraction patterns between Port Beach and East Pier due to Channel Dredging to 14.5m C.D.



6 Impact of Channel on Surf Breaks

6.1 Analysis

The impact of channel dredging to the quality and size of surf breaks is assessed using a detailed Boussinesq simulation of a storm event measured in July 2016. This storm was selected due to the relatively large offshore wave height, and was widely observed to result in good surfing conditions along the surf breaks at Napier. The wave conditions measured at the Triaxis waverider buoy offshore of the port were $H_{m0} = 3.0\text{m}$, $T_p = 11\text{s}$ and $MWD = 90^\circ$. That is, at the peak of the storm the waves were approaching from due East. Simulations were conducted assuming a tidal plane of 0m C.D. (i.e. approximately MLWS), as this represents the situation where refraction will be strongest.

Simulations considered refraction, diffraction, nonlinear wave-wave interaction, wave asymmetry and skewness, and depth-induced wave breaking. The results are shown in Figure 6-1 to Figure 6-3. The simulation was run for a 45 minute warm-up time, followed by a 30 minute period over which statistics were gathered from simulated surface elevation, measured at a frequency of 2Hz.

Locally important surf breaks are present near to Port Beach (referred to as Hardinge Road in the NZ Surfing Guide) and to the west of Ahuriri Inlet (referred to in the NZ Surfing Guide as City Reef).

There are two additional small surf breaks located at 'The Gap' and 'Westshore', but these are not considered in the numerical models as the direction of the waves are only favourable for surfing from the north east and are not refracted by the navigation channel.

6.2 Results

6.2.1 Significant Wave Height

The *significant* wave height (H_{m0}) is a measure of the mean wave height in a group of waves as they approach the shore. Visually it corresponds approximately to the average height of the highest one-third of the waves occurring over, say, a 2 minute period. Therefore, changes to the significant wave height represent changes to the wave group as a whole as the waves are refracted by the navigation channel.

Figure 6-1 shows the surf break at Hardinge Road from east of the groyne to the west of the groyne. Minimal change is predicted to the *significant* wave height at the City Reef surf break. For an offshore wave of $H_{m0} = 3\text{m}$ approaching from the east, the inshore wave is predicted to *increase* by about 0.1m.

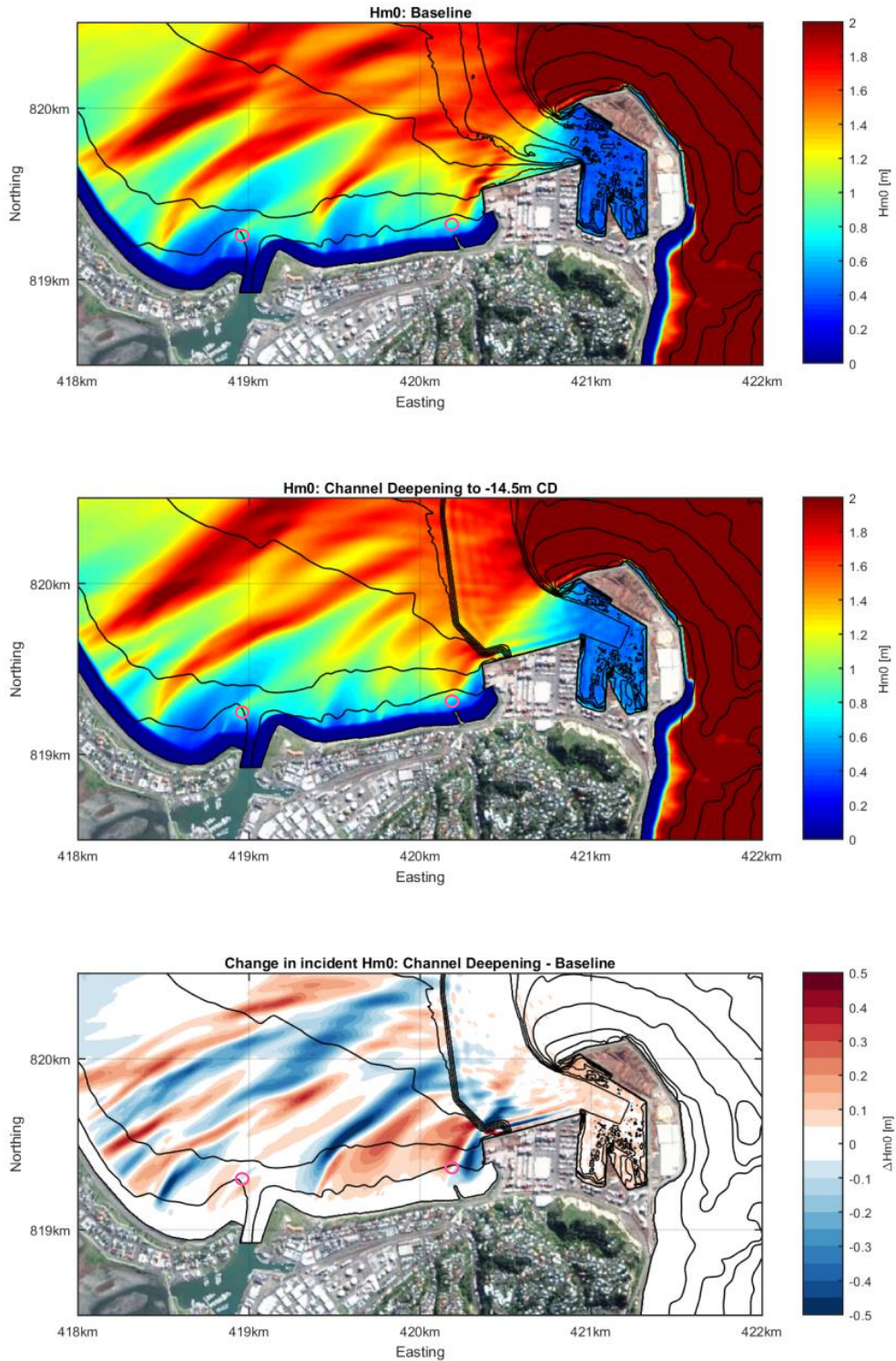


Figure 6-1: Changes in significant wave height for easterly storm occurring at Low Water. Offshore wave height 3.0m, Wave Period 11.0s , incidence angle 90° (due East). Circles show locations of surf breaks at Hardinge Road and City Reef.



6.2.2 Maximum Wave Height

The *maximum* wave height (H_{\max}) is the maximum wave height measured at a location over a defined period of time. In this assessment H_{\max} is the highest wave observed over a 30-minute period. Changes to H_{\max} give an indication of predicted changes to the most desirable waves to surf.

Simulated changes to H_{\max} (Figure 6-2) are similar to those for the *significant* wave height: The maximum wave height is predicted to reduce at Hardinge Road, and increase at City Reef. Because depth-induced wave shoaling affects the largest waves in a wave group to a greater extent than smaller waves, gains in H_{\max} at City Reef are larger than those expected for H_{m0} . For the storm wave considered, H_{\max} is predicted to *increase* by about 0.4m at City Reef and *decrease* by about 0.4m at Hardinge Road. However a short distance to the west of the existing surf break at Hardinge Road the H_{\max} is predicted to remain unchanged.

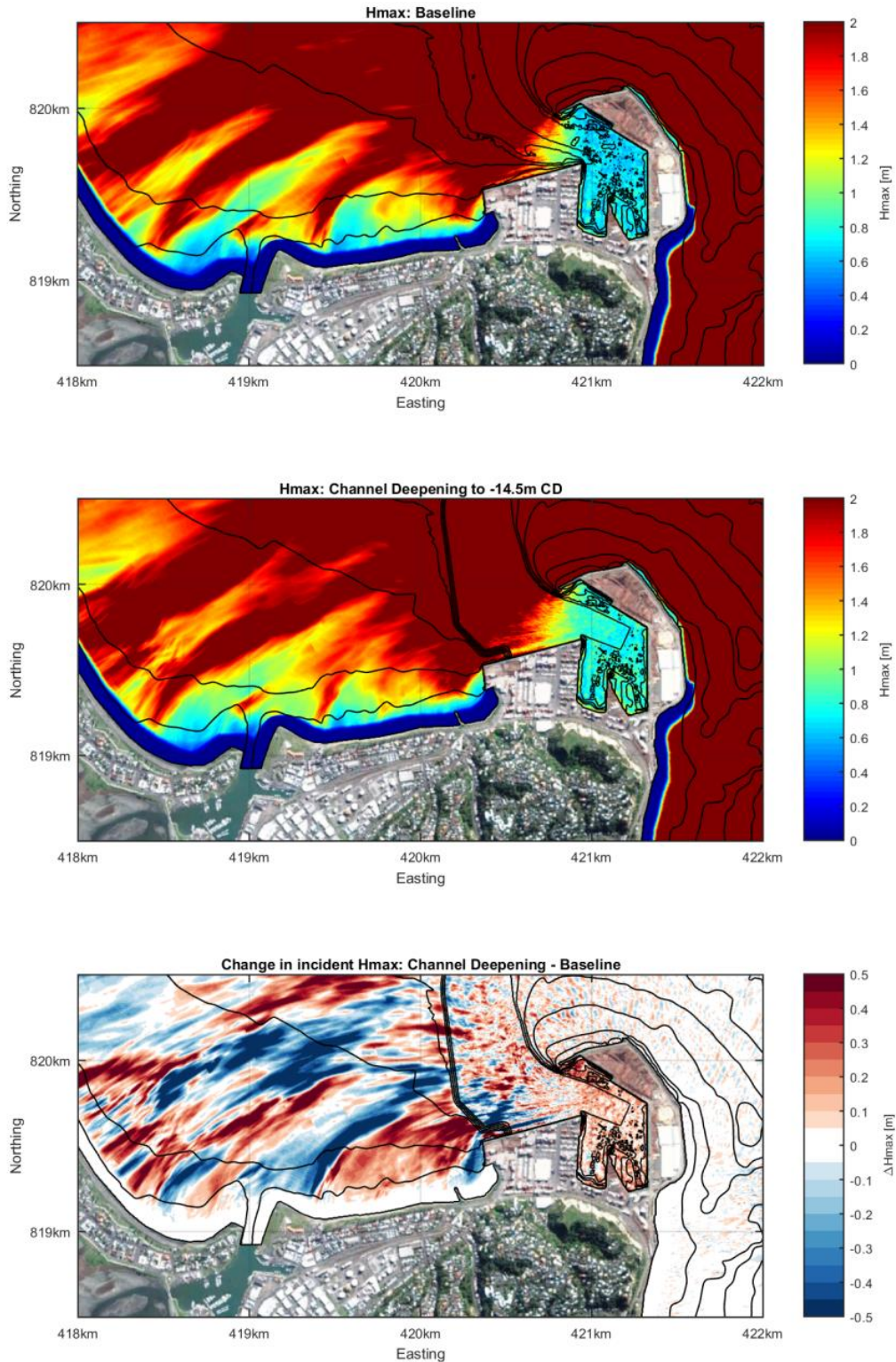


Figure 6-2 - Changes in maximum wave height for easterly storm occurring at Low Water. Offshore wave height 3.0m, Wave Period 11.0s , incidence angle 90° (due East).

6.2.3 Wave Crest Patterns

For the storm conditions and water level considered, wave crests are broadly predicted to remain unchanged at both the Hardinge Road and City Reef surf breaks. Swell crests will remain long and clean with good quality right-hander surf. Increase in H_{m0} and H_{max} along Hardinge Road under these easterly storm conditions suggests that the potential for riding waves from Napier Port to City Reef will be enhanced by wave scattering from the swing basin.

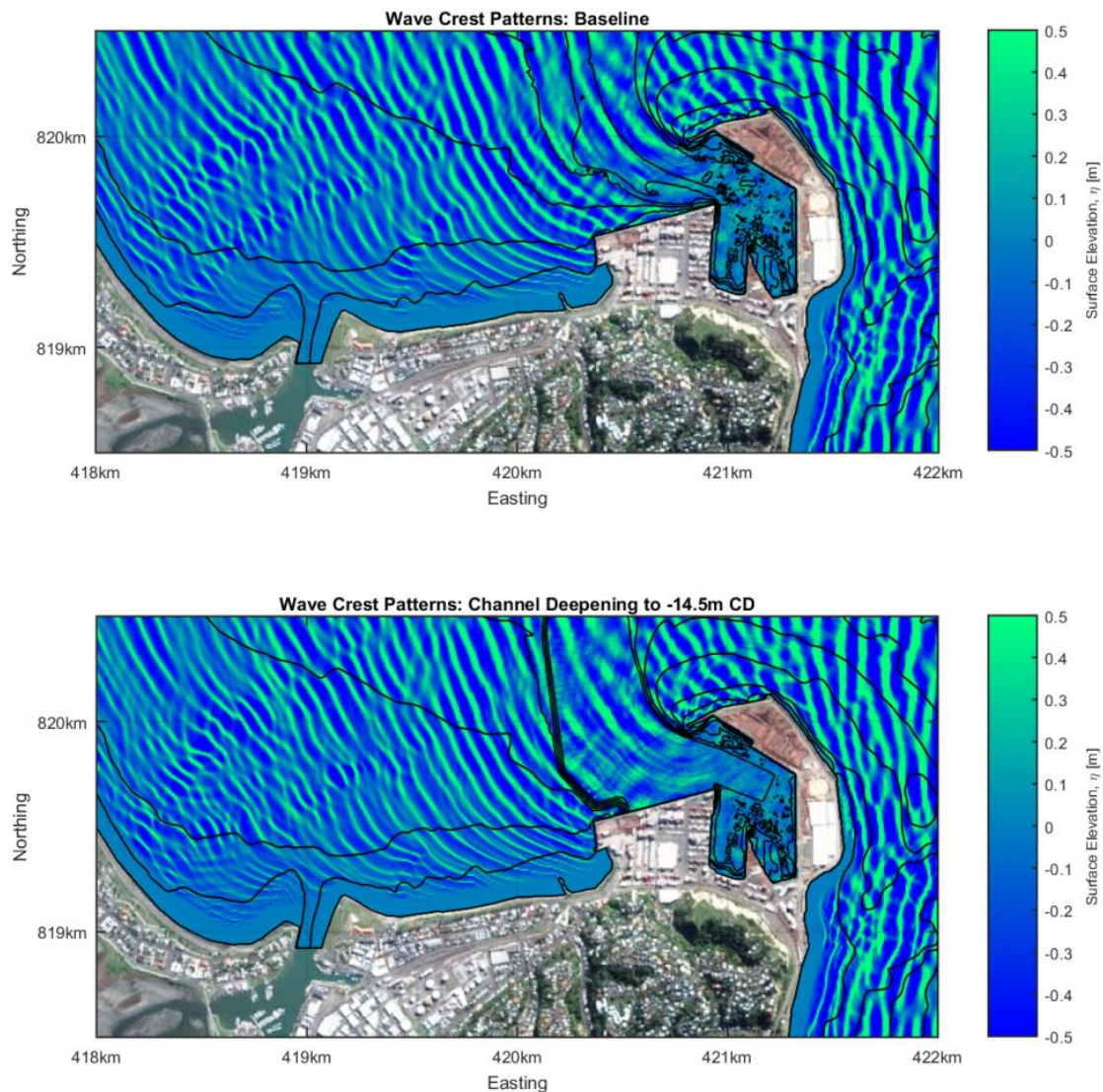


Figure 6-3: Wave crest patterns for 'baseline' and 'dredge channel' bathymetry. Easterly storm occurring at Low Water. Offshore wave height 3.0m, Wave Period 11.0s, incidence angle 90° (due East).



6.3 Detailed Assessment of Surfing Amenity

The impact of the proposed dredging on surfing amenity in the vicinity of Napier Port has been assessed with respect to existing conditions. Two surf breaks in the vicinity of Napier Port have been analysed in detail:

- Hardinge Road; and
- City Reef (including left-hand and right-hand surfing paths, and "inner" break).

Conditions at the two surf breaks were analysed in detail using the calibrated and validated SWAN spectral wave model described in Section 4. This model was used to derive a series of transformed wave conditions at two surf breaks at Hardinge Road and City Reef.

Offshore wave conditions corresponding to the range of measured wave heights, periods and directions from the offshore Triaxis Buoy as described in Section 3.4 were transformed to each of the two surf breaks shown in Figure 6-4, below.

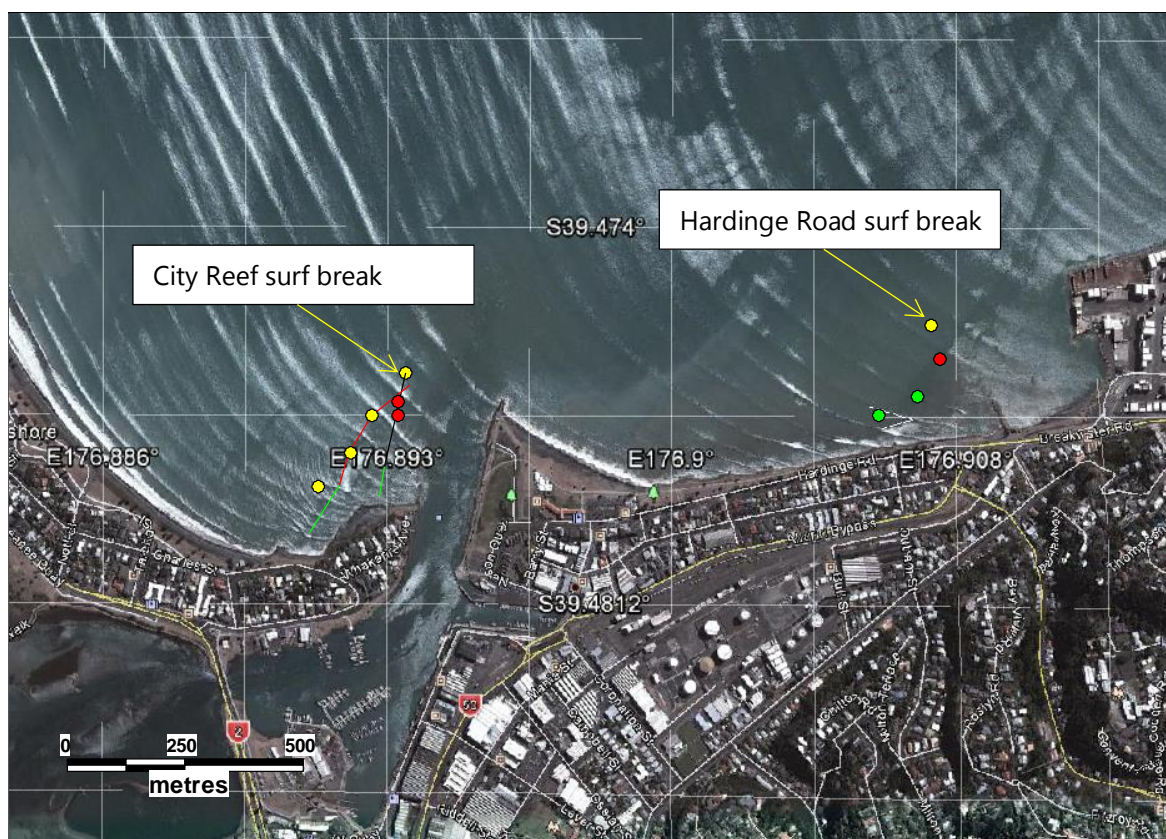


Figure 6-4: Location of surf breaks (aerial image from Google Earth, 28 Feb 2013). Dots represent discrete locations within the surf breaks where surfing amenity has been analysed.



The range of offshore wave directions, periods and significant wave heights run through the SWAN spectral wave model correspond to the measured wave parameters from the Triaxis buoy over the ten-year period from 2004 to 2014, and are shown in Table 6-1. The combination of wave period, direction and offshore wave height represents 280 discrete scenarios run through the model and transformed to equivalent inshore wave heights, directions and periods at the two surf breaks.

Table 6-1: Range of wave directions, periods and significant wave heights run through SWAN model

Offshore Mean Wave Direction (°)	Offshore peak wave period (s)	Offshore Significant wave height (m)
30, 60, 90, 120, 150	4, 6, 8, 10, 12, 14, 16	0.5, 1, 1.5, 2, 2.5, 3, 3.5, 4

The 280 scenarios were used to develop a look-up table of transformed spectral wave model results over the entire model domain, under existing and proposed (post-dredged) conditions. From this look-up table, the transformed local wave parameter time-series at 30 minute intervals for the full 10 year offshore data set was able to be derived at discrete locations in the model domain, corresponding to various sections within the two surf breaks.

The discrete locations at which 10 year wave time-series were derived included:

- Hardinge Road surf break, 2 m depth contour;
- Hardinge Road surf break, 1 m depth contour;
- City Reef, take-off point (2 m depth contour)
- City Reef, left-hand break (1 m depth contour)
- City Reef, "inner" left-hand break (1 m depth contour)
- City Reef, "inner" left-hand break (0.5 m depth contour)
- City Reef, right-hand break (1 m depth contour)
- City Reef, right-hand break (0.5 m depth contour)

6.4 Quantification of surfing amenity

Lewis *et al* (2015) described various methods for quantifying the surfing amenity. Mead (2003) described the recreational surfing amenity through a series of descriptive parameters including the wave peel angle, breaker intensity and breaking wave height.

6.4.1 Wave Peel Angle

The *peel angle* is defined "as the angle between the crest of an unbroken wave and the trail of the broken wave (white water). Larger peel angles (70° - 90°) suit beginners, with smaller peel angles (30° - 50°) more suited to advanced surfers and associated with faster surfer velocities. Peel angles



less than about 25° mean that a large section of the wave breaks simultaneously and cannot be surfed (this is known in surfing parlance as a “close-out”).

Often the peel angle can be determined by aerial photography on a given date. For the two surf breaks at Hardinge Road and City Reef, a time-series of peel angle has been determined by extracting the wave approach angle from the model results at the discrete locations within the surf breaks, assuming that the trail of the broken water is parallel to the bottom bathymetry contours at the breaking location.

The methodology for determining the peel angle is illustrated in Figure 6-5.



Figure 6-5: Peel angle at Hardinge Road and wave approach angles from SWAN model calculated using method of Mead (2001), note white water is parallel to the bed contours (aerial photo Google Earth 28 Feb 2013)

6.4.2 Breaking Intensity

When waves approach shallow water or an underwater feature such as a reef, the waves shoal and steepen until the wave becomes unstable and breaks. The breaking wave height, H_b , is defined as the height between the wave crest and wave trough at the point at which the wave is about to break. Breaking waves can be classified as spilling, plunging, collapsing or surging, depending on the wave steepness. The biggest influence on the shape of the waves is induced from changes in



bathymetry, with undersea slope governing the breaker type (Lewis *et al*, 2015). Breaker type is described by the wave steepness parameter, or *Iribarren number*, given by:

$$\xi_b = \frac{\beta}{\sqrt{\frac{H_b}{L_\infty}}}$$

where ξ_b = Iribarren number
 β = bottom slope
 H_b = breaking wave height
 L_∞ = deepwater wavelength.

Four main breaker types are described by CERC (1984) based on the Iribarren number:

- Spilling Breaker ($\xi_b < 0.4$)
- Plunging Breaker ($0.4 < \xi_b < 2.0$)
- Surging or Collapsing Breaker ($\xi_b > 2.0$).

Waves suitable for surfing tend to break in the spilling or plunging range. Spilling breakers break gradually and are characterised by white water at the crest. Plunging waves curl over at the crest with a plunging forward of the mass of water at the crest. The base of surging breakers surge up the beach before the crest is able to plunge forward, whereas collapsing breakers tend to break over the lower half of the wave.

Characteristics of the four main types of breaking waves are illustrated in Figure 6-6.



	
<p style="text-align: center;">Spilling Breaker</p> <ul style="list-style-type: none"> • Bubbles and turbulent water spill down front face of wave. • The upper 25% of the front face may become vertical before breaking • Iribarren Number: <p style="text-align: center;">$\xi_b < 0.4$</p>	<p style="text-align: center;">Plunging Breaker</p> <ul style="list-style-type: none"> • Crest curls over a large air pocket. • Smooth splash-up usually follows • Iribarren Number range: <p style="text-align: center;">$0.4 < \xi_b < 2.0$</p>
<p style="text-align: center;"></p> <p style="text-align: center;">Surging Breaker</p> <ul style="list-style-type: none"> • Wave slides up beach with little or no bubble production. • Water surface remains almost plane except where ripples may be produced on the beach face during runback • Iribarren Number: <p style="text-align: center;">$\xi_b > 2.0$</p>	<p style="text-align: center;"></p> <p style="text-align: center;">Collapsing Breaker</p> <ul style="list-style-type: none"> • Breaking occurs over lower half of wave. • Minimal air pocket • Usually no splash-up. Bubbles, foam present • Iribarren Number: <p style="text-align: center;">$\xi_b > 2.0$</p>

Figure 6-6: Breaker types characterised by Iribarren number (after Lewis *et al.* 2015)

6.4.3 Methods for describing surfing amenity

Walker (1974) developed a classification of surfer ability based on peel angle and wave height. This classification is illustrated in the form of a nomogram in Figure 6-7, with various classifications of surfer ability depending on breaker height, peel angle and surfer velocity.

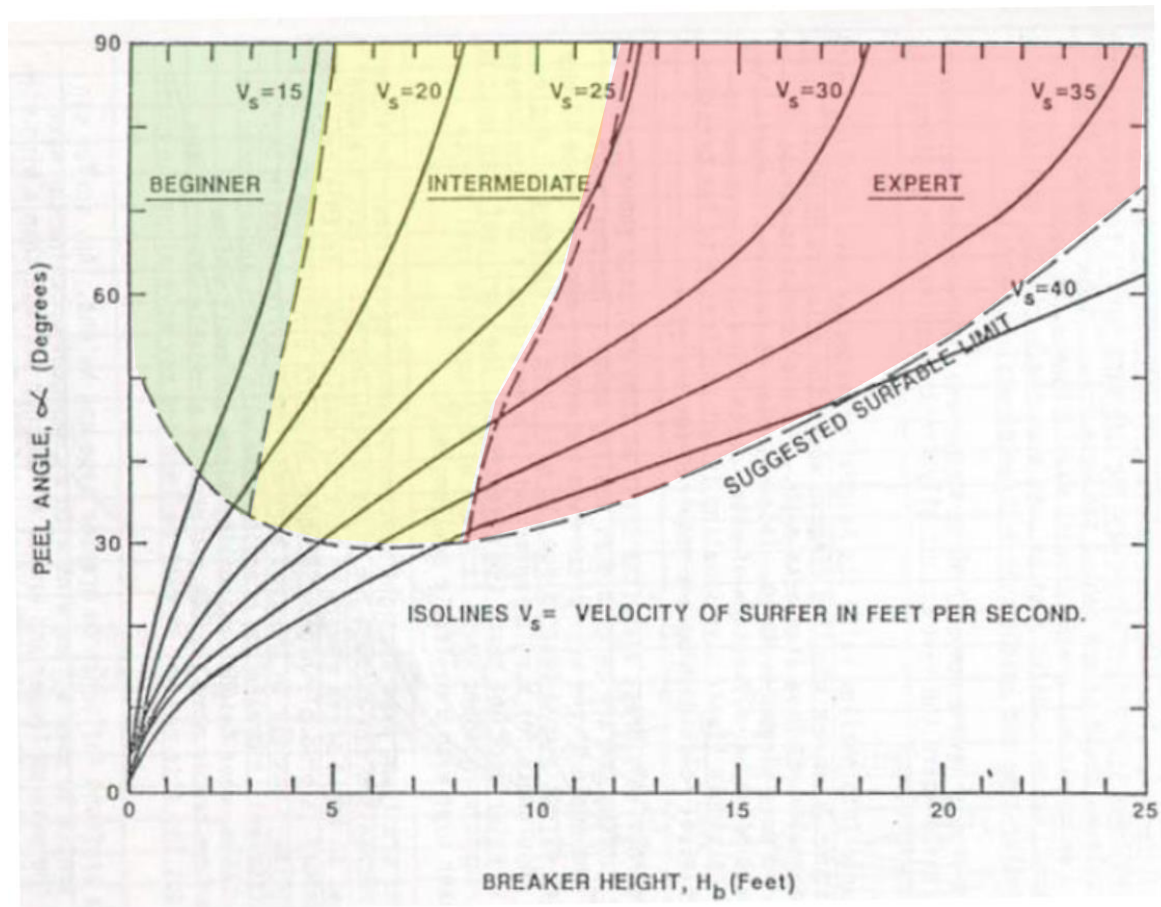


Figure 6-7: Classification of surfing skill based on peel angle and wave height (Walker, 1974)

Hutt *et al.* (2001) attempted to update this relationship based on advancements in surfboard design and the discovery of more challenging surfing locations. Hutt *et al.* (2001) developed a nomogram to describe surfer skill in terms of peel angle and wave height (Figure 6-8), with nine regions defined in Table 6-2.

The characteristics of each of the two surf breaks have been studied using the results of the wave transformation analysis covering the entire length of wave record and plotting the wave height vs. peel angle at each of the discrete locations along the ride path within the two surf breaks.

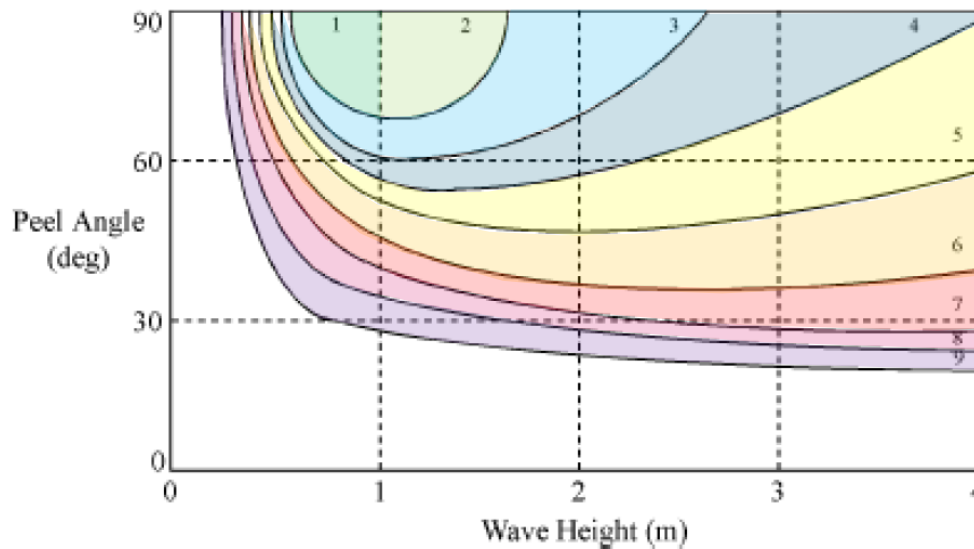


Figure 6-8: Nomogram describing surfing skill in terms of peel angle and breaker height (Hutt et al. 2001)

Table 6-2: Description of regions in nomogram in Figure 6-8 (Hutt et al. 2001)

ID	Surfer Rating	Peel Angle limit (°)	Min./Max. wave height (m)
1	Beginner surfers not yet able to ride the face of the wave and simply moves forward as the wave advances	90	0.7 / 1.0
2	Learner surfers able to successfully ride laterally along the crest of a wave	70	0.65 / 1.5
3	Surfers that have developed the skill to generate speed by “pumping” on the face of the wave	60	0.6 / 2.5
4	Surfers beginning to initiate and execute standard surfing manoeuvres on occasion	55	0.55 / 4.0
5	Surfers beginning to initiate and execute standard surfing manoeuvres consecutively on a single wave	50	0.5 / >4.0
6	Surfers able to execute standard manoeuvres consecutively. Executes advanced manoeuvres on occasion.	40	0.45 / >4.0
7	Top amateur surfers able to consecutively execute advanced manoeuvres	29	0.4 / >4.0
8	Professional surfers able to consecutively execute advanced manoeuvres	27	0.35 / >4.0
9	Top 44 surfers able to consecutively execute advanced manoeuvres	Not reached	0.3 / >4.0
10	Surfers in the future	Not reached	0.3/ >4.0



6.5 City Reef

The City Reef wave break is located immediately west of the Ahuriri harbour entrance at the southern end of Westshore Beach. The surf break is characterised by Rangatira Reef, which covers an area approximately 55,000 m² between the western training mole at Ahuriri inlet and the concrete cube groyne at the southern end of Westshore Beach (Hawke's Bay Regional Council, 2014). It is reported that the reef break offers good left and right-handed surf breaks, with "surfable" conditions reported 14% of the time and "good" surfing conditions 3% of the time (Hawke's Bay Regional Council, 2014).

The location of the break is shown in Figure 6-9. MetOcean Solutions Ltd. (2009) undertook a study of the break, recording surf tracks through the use of GPS, as part of a study into the effects of a breakwater that was proposed for the area. The GPS study identified the location of the left-hand and right-hand surf breaks, plotted in relation to the bathymetry (Figure 6-10 and Figure 6-11).

In addition to the left-hand and right-hand breaks, an "inner" break, predominantly used by surfers with kayaks and longboards, has been identified in Hawke's Bay Regional Council (2014).

Locations at which existing and post-dredge spectral wave model time-series were extracted are indicated in Figure 6-9.



Figure 6-9: Location of left-hand and right-hand surf breaks at City Reef, with discrete locations for surfing amenity analysis plotted, and indicative modelled wave approach vectors

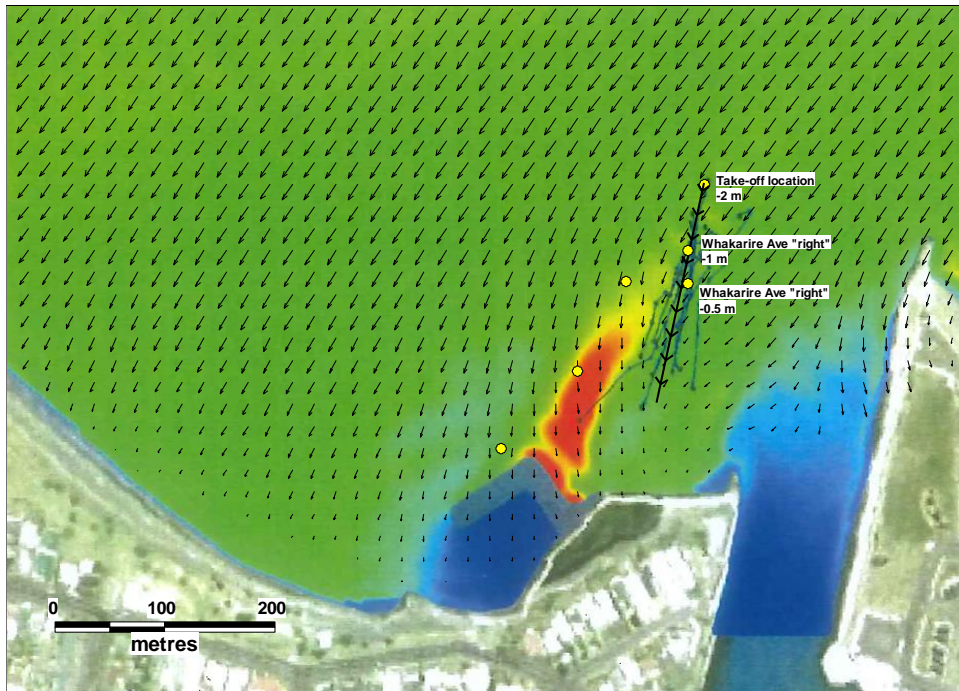


Figure 6-10: GPS tracks indicating right-hand surfing path (after MetOcean Solutions, 2009), with red representing wave focussing and blue representing wave sheltering

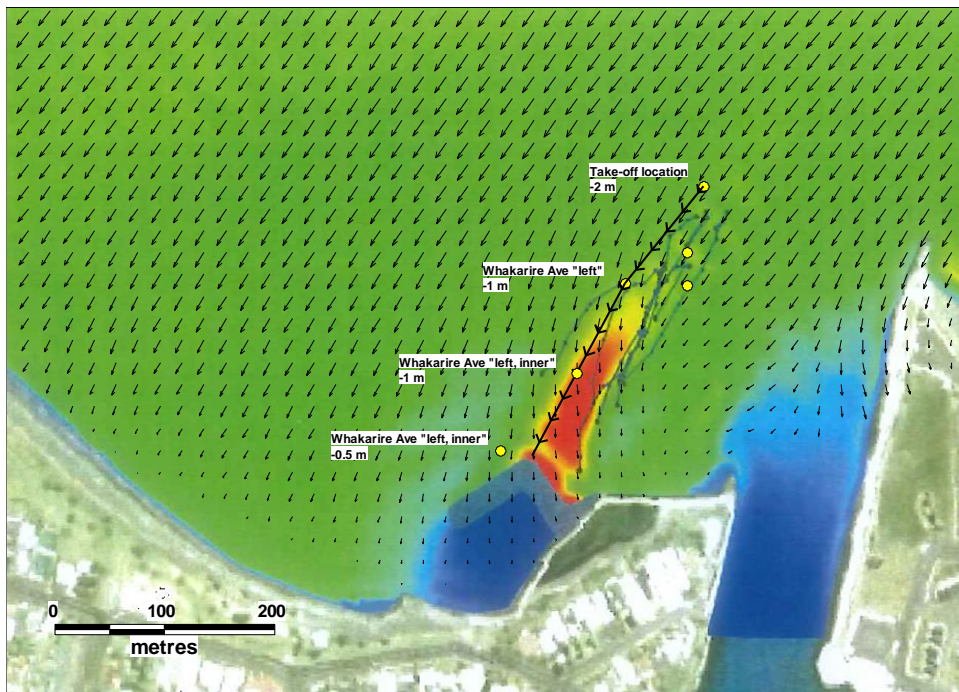


Figure 6-11: GPS tracks indicating left-hand surfing path (after MetOcean Solutions, 2009), with red representing wave focussing and blue representing wave sheltering



6.5.1 Surfing Amenity – take-off location

The full transformed wave time-series (between 2004 and 2014) at the City Reef take-off location was analysed to obtain statistics of wave conditions and breaker type, to ascertain the percentage of time that waves would be considered “surfable”, both under existing conditions and post-dredging conditions.

Waves were considered “surfable” if they met the following criteria:

- Wave period > 6 s
- $H_{m0} > 0.3$ m (the lower limit for surfable waves as per Hutt 2001, Table 6-2)

In addition, the wave steepness parameter (Iribarren number) under existing and post-dredging conditions was calculated for the entire time-series, to ascertain whether the character of the breakers (spilling or plunging) would be changed as a result of the proposed dredging. The results of this analysis are provided in Figure 6-12. It can be seen that of the waves that met the surfability criteria, waves were considered “spilling” breakers 84% of the time and “plunging” breakers 16% of the time under existing conditions. This ratio is expected to be virtually unchanged following the dredging, with 83% of waves predicted to be “spilling” and 17% “plunging”.

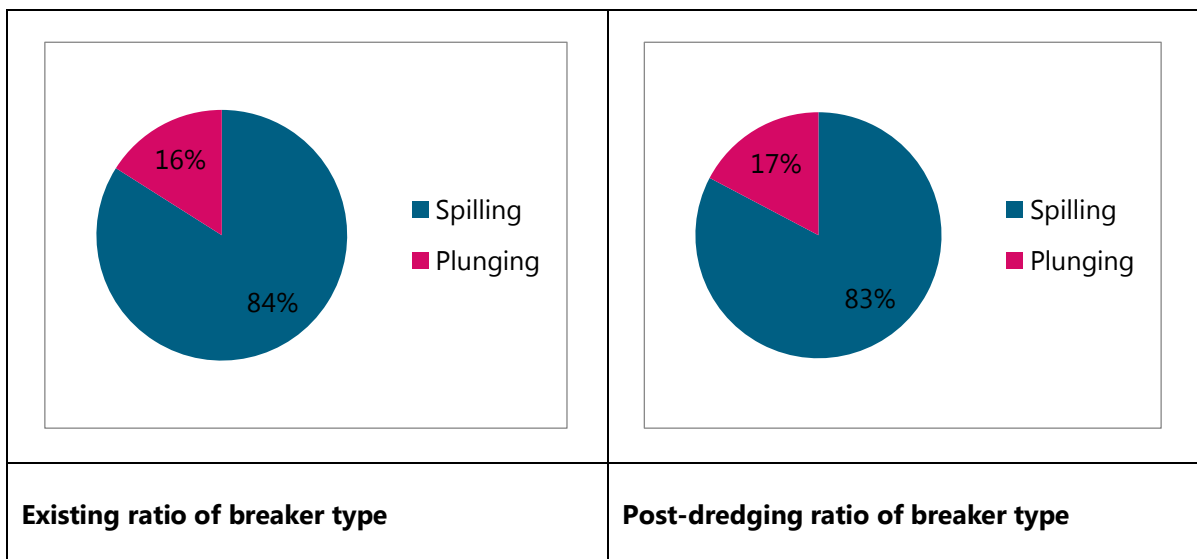


Figure 6-12: Predicted changes to breaking type, pre and post-dredging, at City Reef take-off location

Changes to surfing amenity at the take-off location as a result of the dredging were considered also using the nomograms of Walker (1974) and Hutt *et al.* (2001). These changes are illustrated in Figure 6-13. It can be seen that for the majority of the time, peel angles at the site are between 50° and 70° and that conditions generally suit beginners or intermediate surfers. It can be seen from these figures that there would be very little change to the wave height or peel angle at this site and consequently very little change to the surfing amenity.

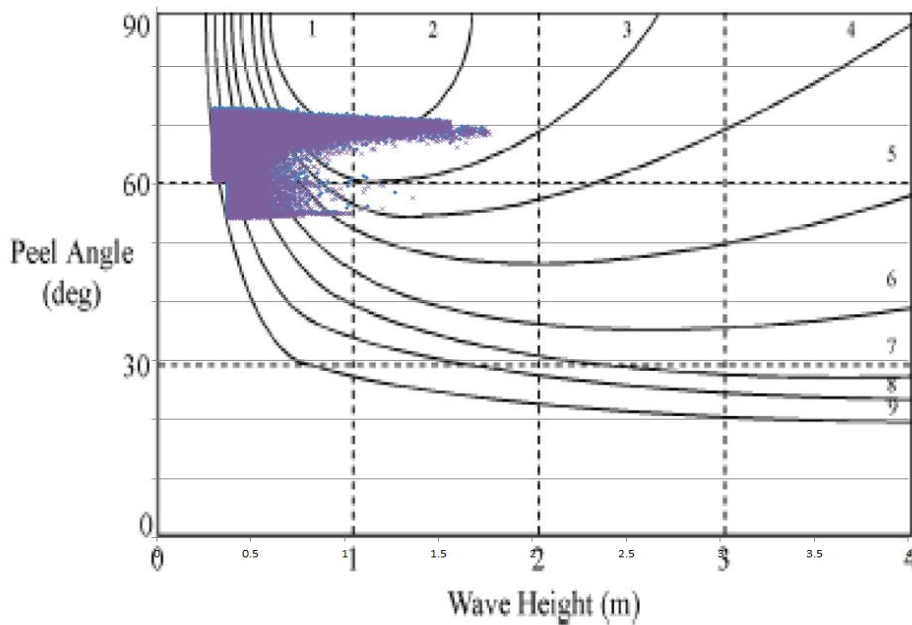
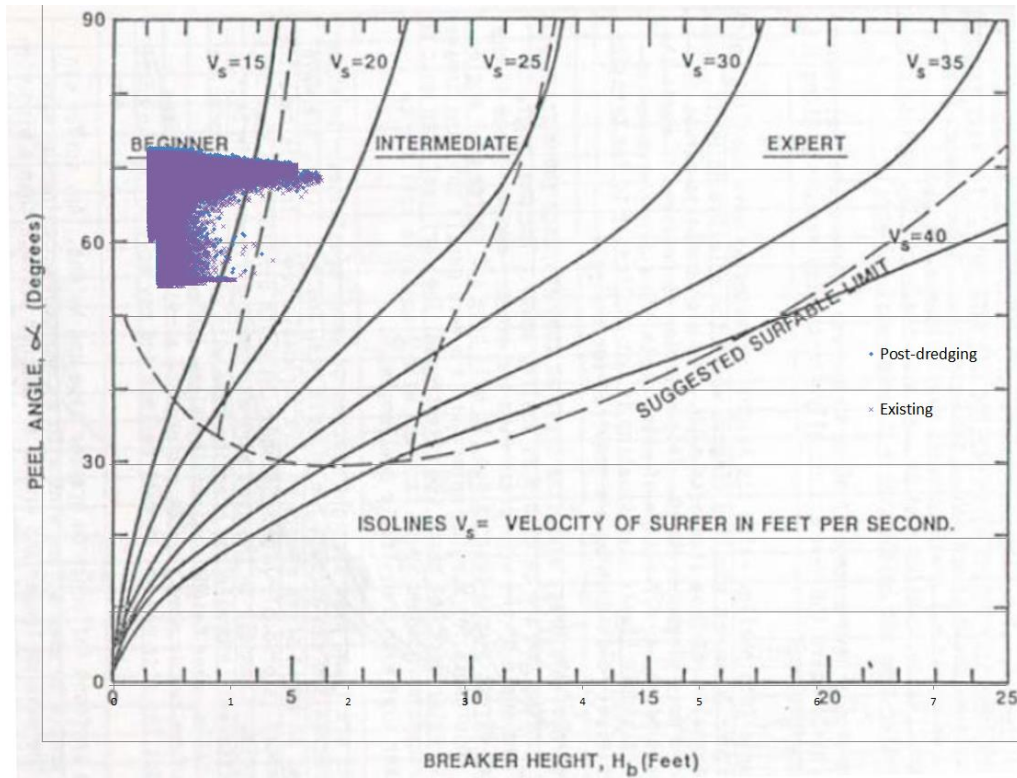


Figure 6-13: Surfing Amenity analysis using Walker (1974) nomogram (top) and Hutt *et al.* 2001 (bottom), City Reef take-off location. Purple = existing, Blue = post-dredging.



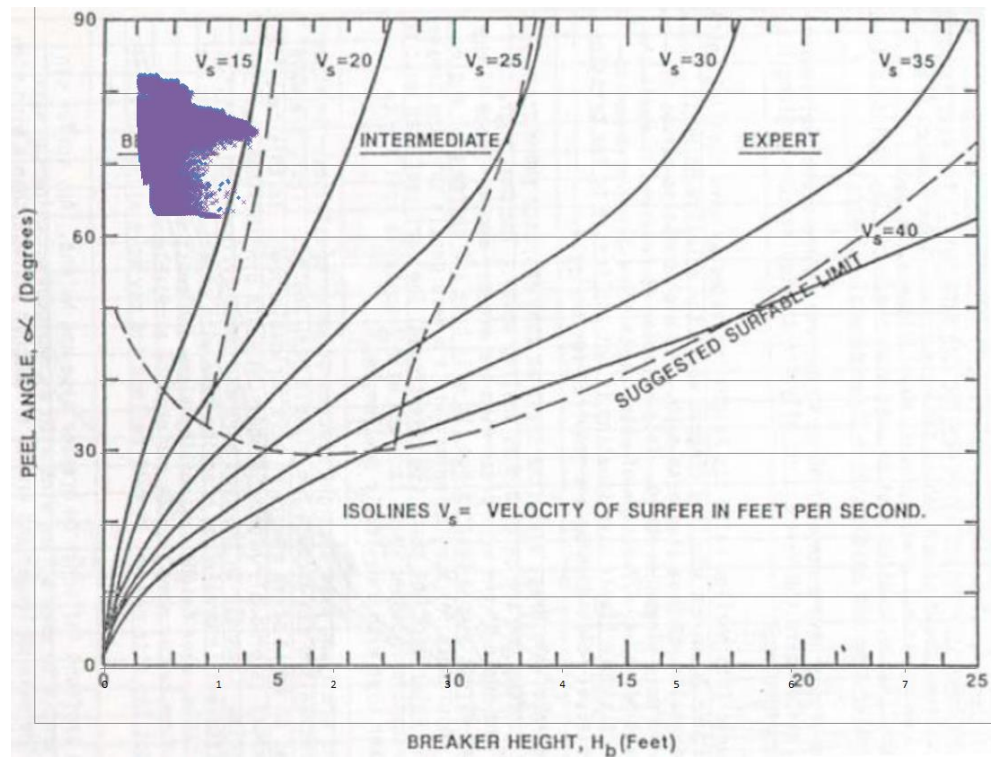
6.5.2 City Reef – Left-hand break

The left-hand break locations illustrated in Figure 6-9 were analysed for surfing amenity in accordance with the same criteria applied for the take-off location. The change in breaker type as a result of the dredging was assessed, with the results presented in Table 6-3. It can be seen that there is very little change in the breaker type as a result of the dredging, with a slight increase in the proportion of waves that are plunging breakers compared with spilling breakers.

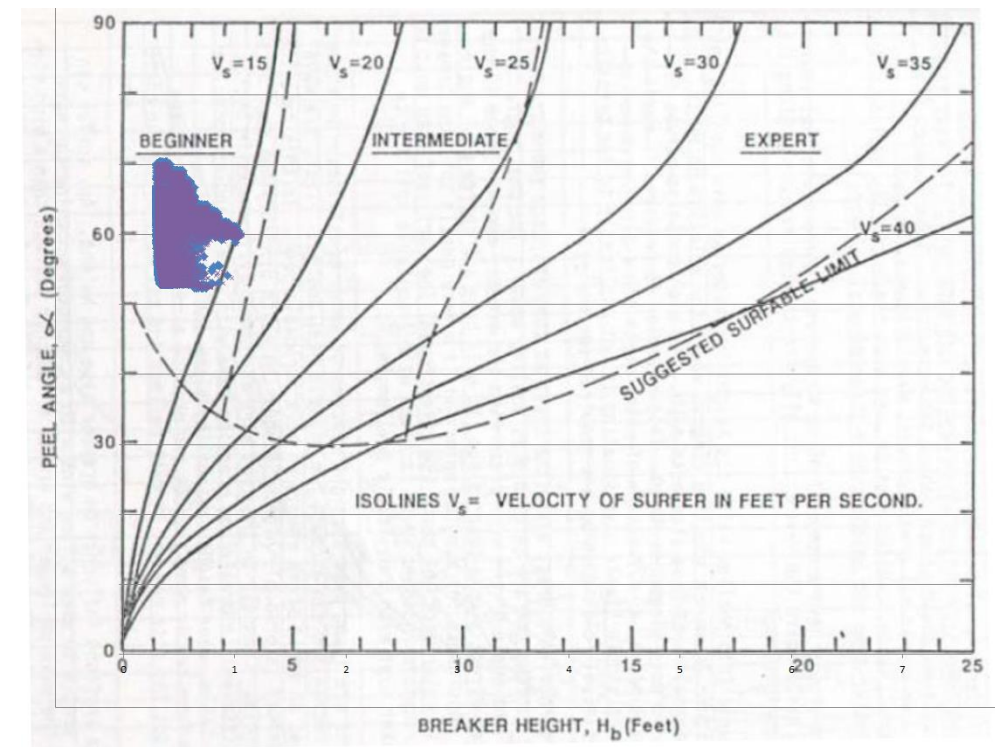
Table 6-3: Existing and post-dredging breaker types, City Reef left-hand break

Location	Pre-dredging	Post-dredging
City Reef left (-1 m contour)	88% "Spilling", 12% "Plunging"	86% "Spilling", 14% "Plunging"
City Reef left inner (-1 m contour)	81% "Spilling", 19% "Plunging"	79% "Spilling", 21% "Plunging"
City Reef left inner (-0.5 m contour)	55% "Spilling", 45% "Plunging"	53% "Spilling", 47% "Plunging"

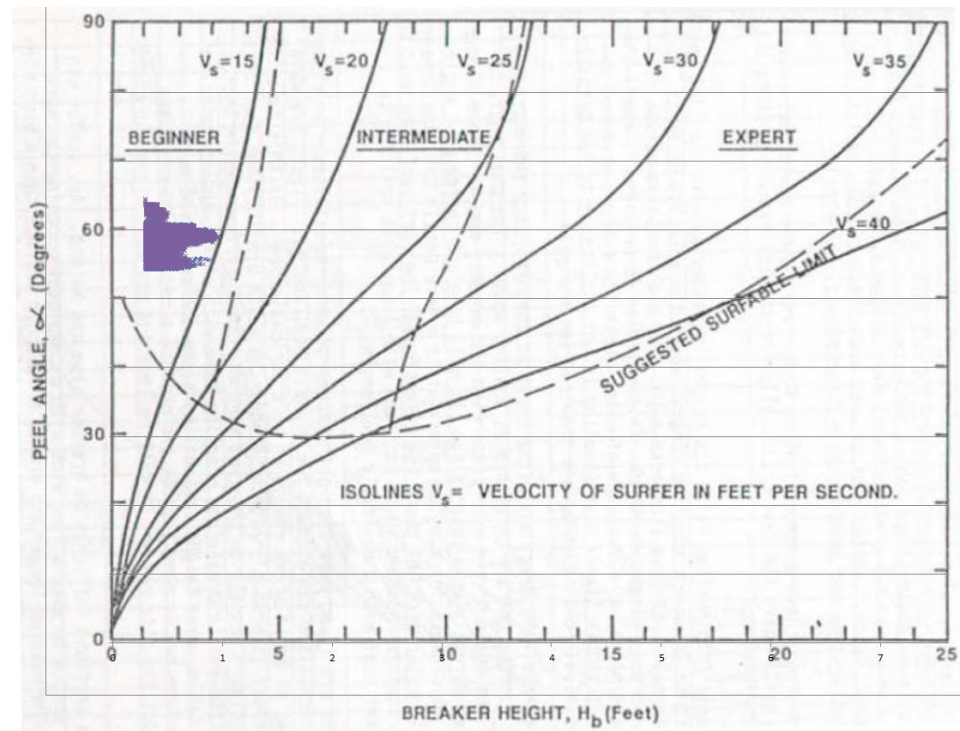
Figure 6-14 illustrates the surfing amenity classification for the City Reef "left" and "left-inner" surf breaks according to the method of Walker (1974), and Figure 6-15 illustrates the surfing amenity according to Hutt *et al.* (2001). It can be seen that the peel angle is between 60° and 75° and the maximum breaking wave height is around 1 – 1.5 m (depending on the local depth), indicating that the left "inner" surf break is suitable for beginners. The figures show that the peel angle and hence the surf amenity classification does not change significantly as a result of the dredging for the City Reef left-hand and left-hand inner breaks.



City Reef "left" (-1m contour)



City Reef "left inner" (-1m contour)



City Reef "left inner" (-0.5 m contour)

Figure 6-14: Walker (1974) surf amenity classification, City Reef (left and left inner breaks). Purple = existing, blue = post-dredging.

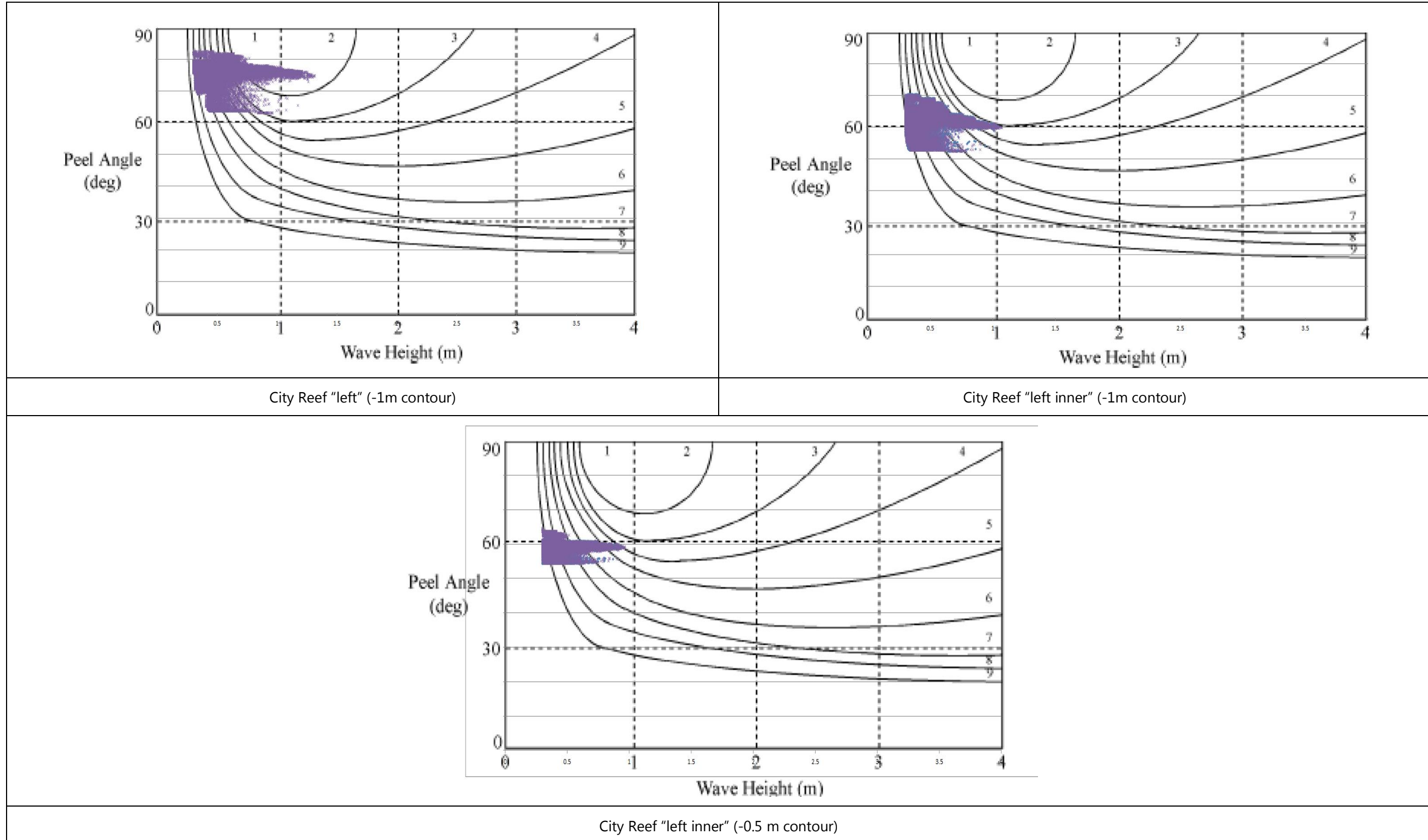


Figure 6-15: Surfing amenity assessment using method of Hutt *et al*, (2001), City Reef (left and left inner breaks). Purple = existing, blue = post-dredging



6.5.3 City Reef – Right-hand break

The right-hand break locations illustrated in Figure 6-9 were analysed for surfing amenity in accordance with the same criteria applied for the left-hand break. The change in breaker type as a result of the dredging was assessed, with the results presented in Table 6-4. It can be seen that there is very little change in the breaker type as a result of the dredging, with a slight increase in the proportion of waves that are plunging breakers compared with spilling breakers.

Table 6-4: Existing and post-dredging breaker types, City Reef right-hand break

Location	Pre-dredging	Post-dredging
City Reef right (-1 m contour)	90% "Spilling", 10% "Plunging"	89% "Spilling", 11% "Plunging"
City Reef right inner (-0.5 m contour)	90% "Spilling", 10% "Plunging"	88% "Spilling", 12% "Plunging"

Figure 6-16 illustrates the surfing amenity classification for the City Reef "right" surf breaks according to the method of Walker (1974), and Figure 6-17 illustrates the surfing amenity according to Hutt *et al.* (2001). It can be seen that the peel angle is between 50° and 70° and the maximum breaking wave height is around 1 – 1.5 m (depending on the local depth), indicating that the right-hand surf break is suitable for beginners and occasionally may be suitable for intermediate skilled surfers. The figures show that the peel angle and hence the surf amenity classification does not change significantly as a result of the dredging for the City Reef right-hand break.

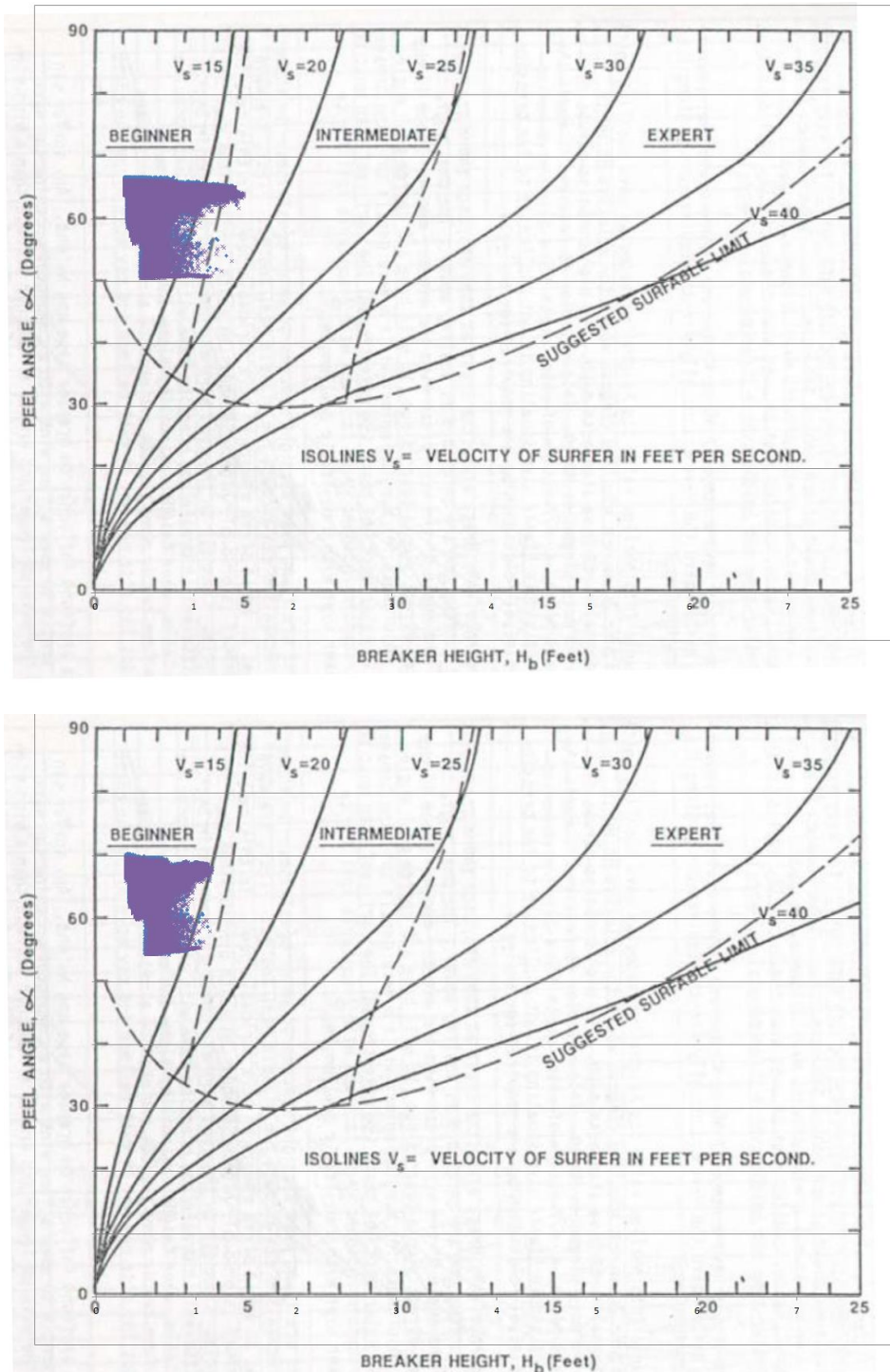


Figure 6-16: Walker (1974) surfing amenity assessment for City Reef (right-hand) break. Top: -1m contour, bottom: -0.5 m contour. Purple = existing, blue = post dredging

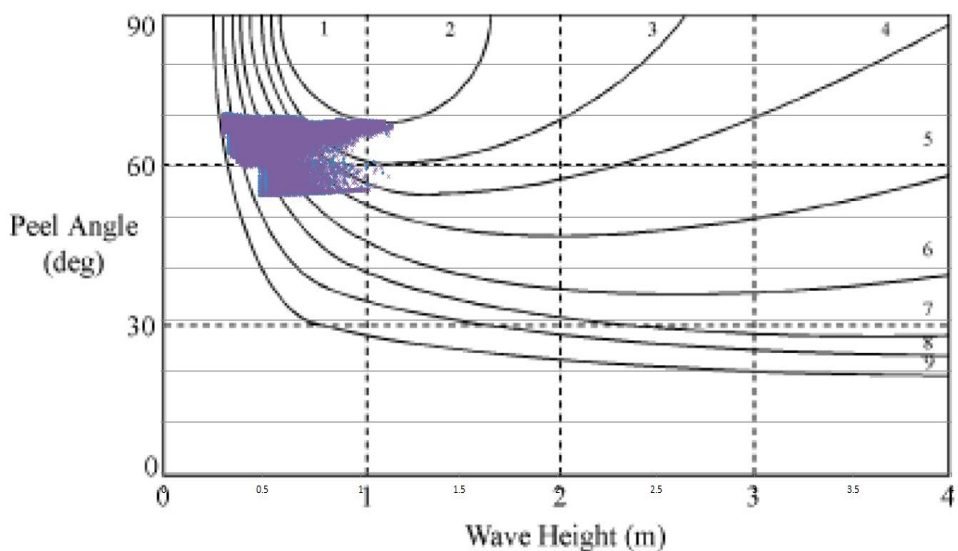
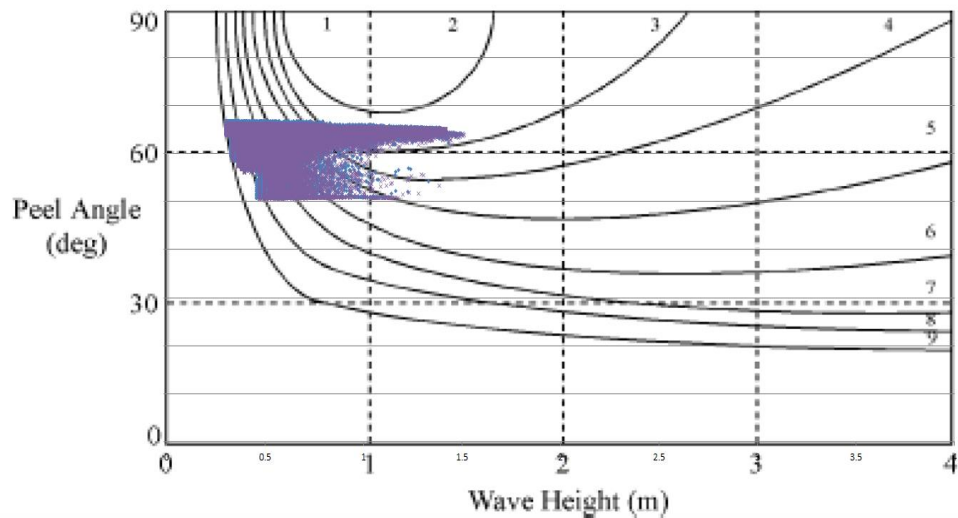


Figure 6-17: Hutt *et al.* (2001) surfing amenity assessment for City Reef (right-hand) break. Top: -1m contour, bottom: -0.5 m contour. Purple = existing, blue = post dredging

6.6 Hardinge Road

The surf break at Hardinge Road, which extends west of the groyne at Battery Road, is also used for surfing. This area is a beach break characterised by a uniform foreshore slope, with swell waves from the east and south sectors refracting around the Port of Napier and providing a long ride length with relatively large peel angles under the right conditions. Existing and post-dredging wave conditions were transformed through the spectral wave model for the offshore time-series



recorded between 2004 and 2014 at the Triaxis wave buoy. Locations at which existing and post-dredge spectral wave model time-series were extracted for the purpose of undertaking a surfing amenity assessment are indicated in Figure 6-18.



Figure 6-18: Hardinge Road surf break with discrete locations for surfing amenity analysis plotted, and indicative modelled wave approach vectors

6.6.1 Surfing Amenity Assessment

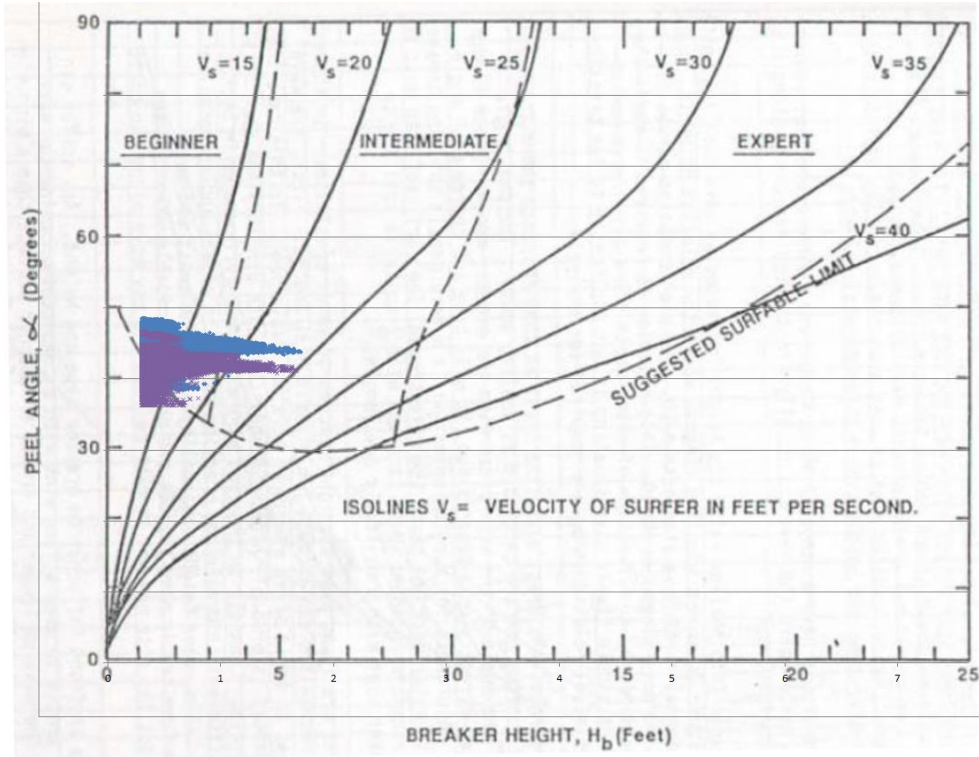
The left-hand break locations illustrated in Figure 6-18 were analysed for surfing amenity in accordance with the same criteria applied for the break at Hardinge Road. The change in breaker type as a result of the dredging was assessed, with the results presented in Table 6-5. It can be seen that there is very little change in the breaker type as a result of the dredging, with a similar proportion of waves that are plunging breakers compared with spilling breakers under existing and post-dredging conditions.



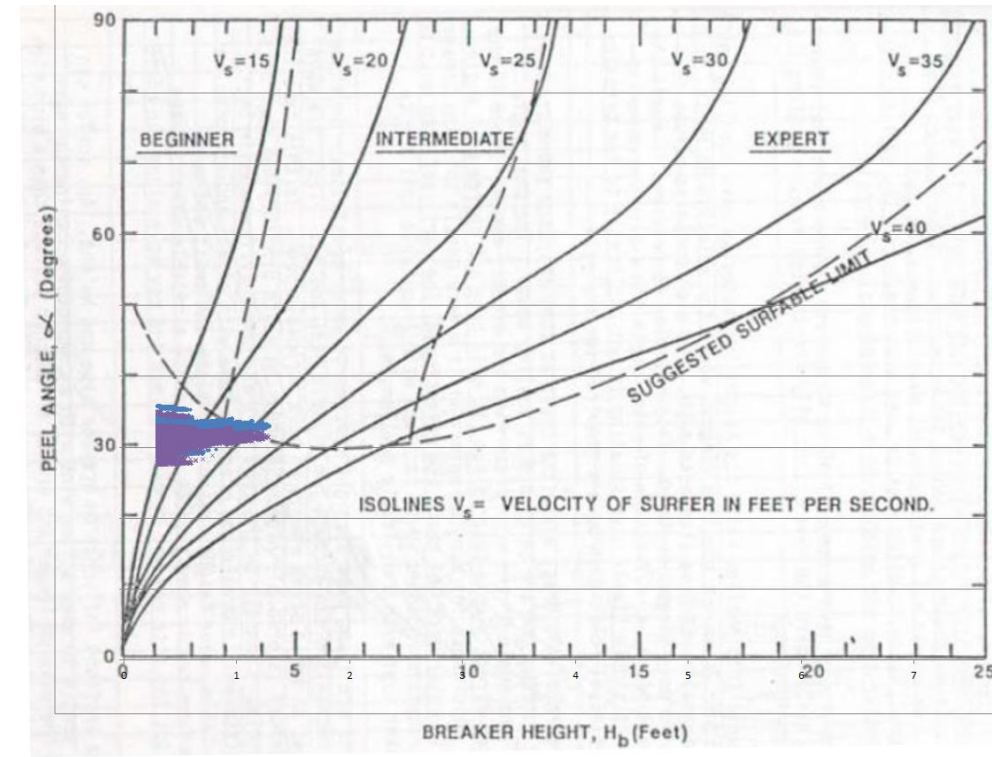
Table 6-5: Existing and post-dredging breaker types, Hardinge Road break

Location	Pre-dredging	Post-dredging
Hardinge Road (-2 m contour)	79% "Spilling", 21% "Plunging"	77% "Spilling", 23% "Plunging"
Hardinge Road (-1 m contour)	76% "Spilling", 24% "Plunging"	76% "Spilling", 24% "Plunging"
Hardinge Road (-0.5 m contour)	71% "Spilling", 29% "Plunging"	72% "Spilling", 28% "Plunging"

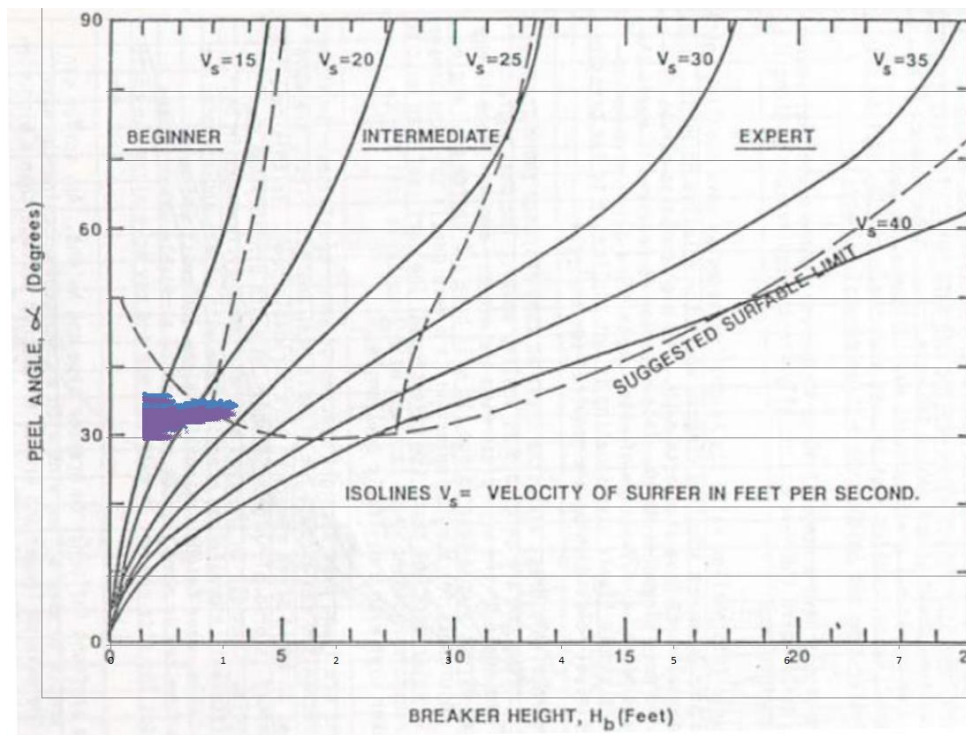
Figure 6-19 illustrates the surfing amenity classification for the Hardinge Road surf break according to the method of Walker (1974), and Figure 6-20 illustrates the surfing amenity according to Hutt *et al.* (2001). It can be seen that the peel angle is between 30° and 50° and the maximum breaking wave height is around 1 – 1.5 m (depending on the local depth), indicating that this break is suitable for somewhat more advanced and intermediate surfers than the break at City Reef. The figures show that the peel angle increases slightly following the dredging, consistent with a predicted 2° clockwise rotation of the mean approach wave angle at Hardinge Road. From these results, the surf amenity classification does not change significantly as a result of the dredging for the Hardinge Road break, with the surfing amenity improving slightly (i.e. there is a greater proportion of waves at the break following the dredging which plot within the areas on the Hutt *et al.* (2001) and Walker (1974) nomograms indicating that the waves are suitable for surfing).



Hardinge Road (-2m contour)



Hardinge Road (-1m contour)



Hardinge Road (-0.5 m contour)

Figure 6-19: Walker (1974) surf amenity classification, Hardinge Road break. Purple = existing, blue = post-dredging.

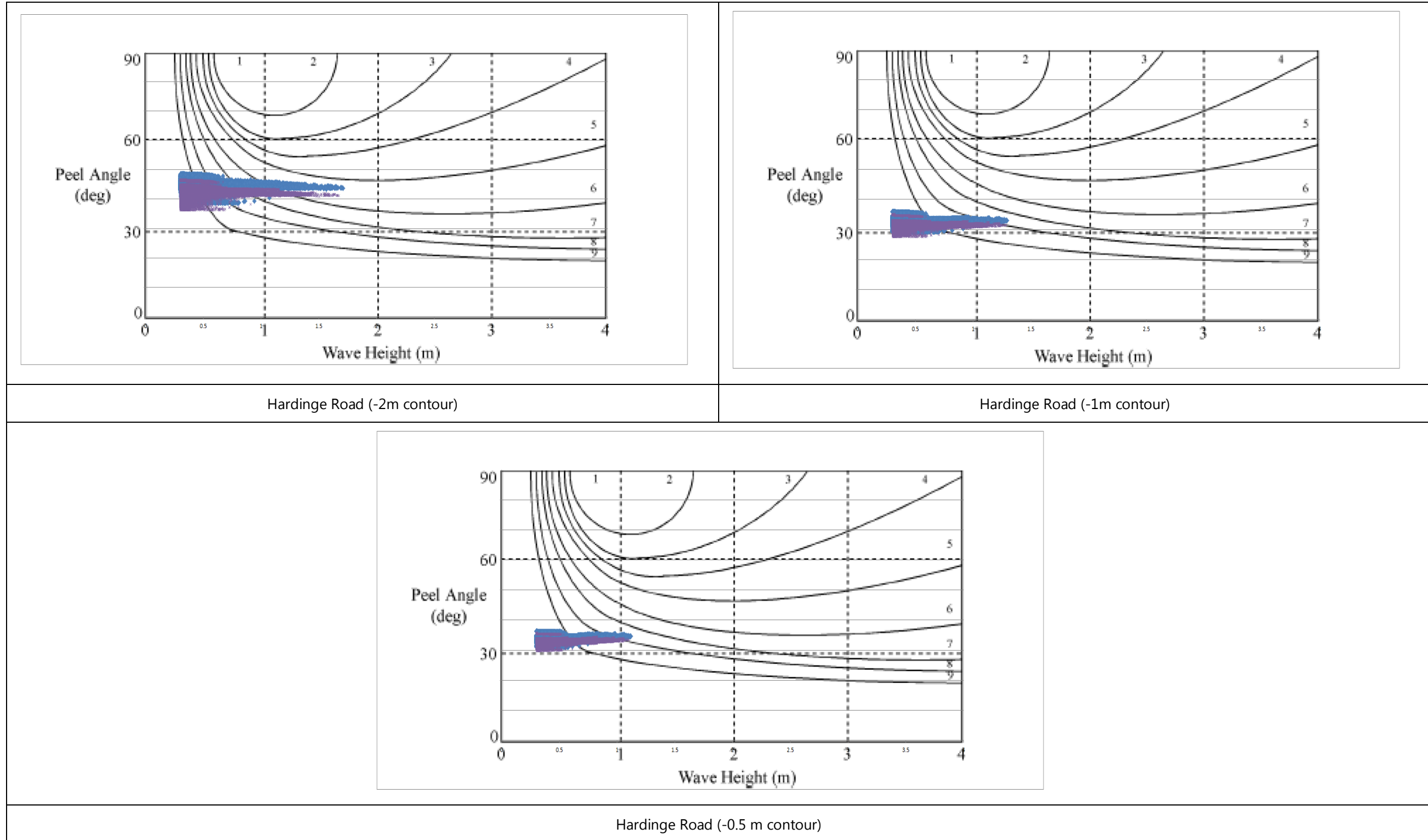


Figure 6-20: Surfing amenity assessment using method of Hutt *et al.*, (2001), Hardinge Road break. Purple = existing, blue = post-dredging



6.7 Summary

The impact of the proposed dredging on surfing amenity in the vicinity of Napier Port has been assessed in terms of peel angle, wave height and wave breaker type in accordance with the methods described by Mead (2003), and Lewis *et al* (2015). The two surf breaks analysed in detail include City Reef (including left-hand and right-hand surfing paths, and "inner" break) and Hardinge Road.

It was found that there would be minimal change to the surfing amenity at City Reef as a result of the proposed dredging, with very little change in peel angle and only a slight increase in the proportion of plunging breakers when compared with spilling breakers.

At Hardinge Road, there would be a slight increase in the peel angle, caused by a clockwise rotation in the approach direction of the waves. This slight increase would result in very little change in surfing amenity, with a slightly higher proportion of waves being assessed as surfable following the dredging, due to the predicted increase in peel angle.



7 Impact of Channel on Shoreline Change

7.1 Introduction

The potential for shoreline change between Napier Port and Esk River is assessed by comparing relative change to the 'energy weighted' incident wave height and direction, close to the surf zone.

7.2 Analysis

The analysis employed may be summarised as follows:

- Propagate inshore a series of wave events corresponding to different combinations of wave height, period and direction, as described in Section 5.2. Combine and sum in accordance with their occurrence probability at the wave model boundary, and sum over all events to derive the 'energy weighted mean wave condition'.
- Extract the results at discrete locations along the -2m C.D. contour, taken as depth which most reasonably represents the wave breaker zone. Figure 7-1 shows positions along which information was extracted from the wave models.
- Compare the results for 'baseline' and 'design channel depth' to calculate the *relative change* in wave height and direction at each of the locations.

7.3 Relative Change in Wave Height and Incidence Angle

Transport of beach sediment is driven by wave energy incident upon the shore. Storm waves tend to drive sediment transport in the *cross-shore* dimension, removing sediment from the upper beach to build a bar system below low water. During calm periods this bar gradually moves onshore by gentle wave action, whereupon it welds back on to the beach profile.

Over timescales longer than about a year, these processes tend to cancel out. Instead, changes in shoreline position are driven by sediment supply and *longshore* transport. Longshore transport potential is a function of wave height and incidence angle at the point of breaking, relative to shore-normal. Waves approaching from a greater angle relative to shore-normal cause greater transport in the alongshore dimension. For a given wave incidence angle, larger waves are able to move more beach material than smaller waves.

Generally, if a beach is constrained between two headlands and subject to constant wave action approaching from an angle from shore normal, material will be removed from the 'up-drift' portion and transported to the 'down-drift' headland, whereupon it will be deposited. Over time this causes the shoreline to 'rotate' towards an equilibrium alignment where shore-normal is exactly aligned with the oncoming waves, and the net longshore transport reduces to zero. For the shore between Napier Port and Esk River, there are effectively two compartments, separated by Ahuriri Inlet. The Hardinge Rd compartment (east of Ahuriri Inlet) is close to closed as far as beach



sediment, with some leakage to the west, and some input from offshore. Westshore is not in equilibrium as it is eroding, and has a southern “headland” (represented by the groyne at Whakarire Avenue) and two sediment supplies (beach nourishment gravels and Esk River). There is some degree of “rotational alignment” of the shoreline towards equilibrium, but this is constrained in the lee of the Whakarire Avenue headland, where the shore is normal to the northeasterly wave and deposition is occurring in the nearshore (as shown by the bathymetry in Figure 7-1).

Table 7-1 shows the calculated *change* in energy weighted mean wave direction for discrete locations between Napier Port and Esk River. Changes in incident wave direction would typically indicate that the beach will tend to evolve to a new alignment, assuming that sufficient mobile sediment is available to allow shoreline change. For example, with reference to Table 7-1, while the change in energy weighted mean wave direction may be highest for the Hardinge Road compartment, there is very little mobile sediment available at this compartment (due to the presence of rock rubble and boulder protection) to allow the beach to evolve to a different alignment.

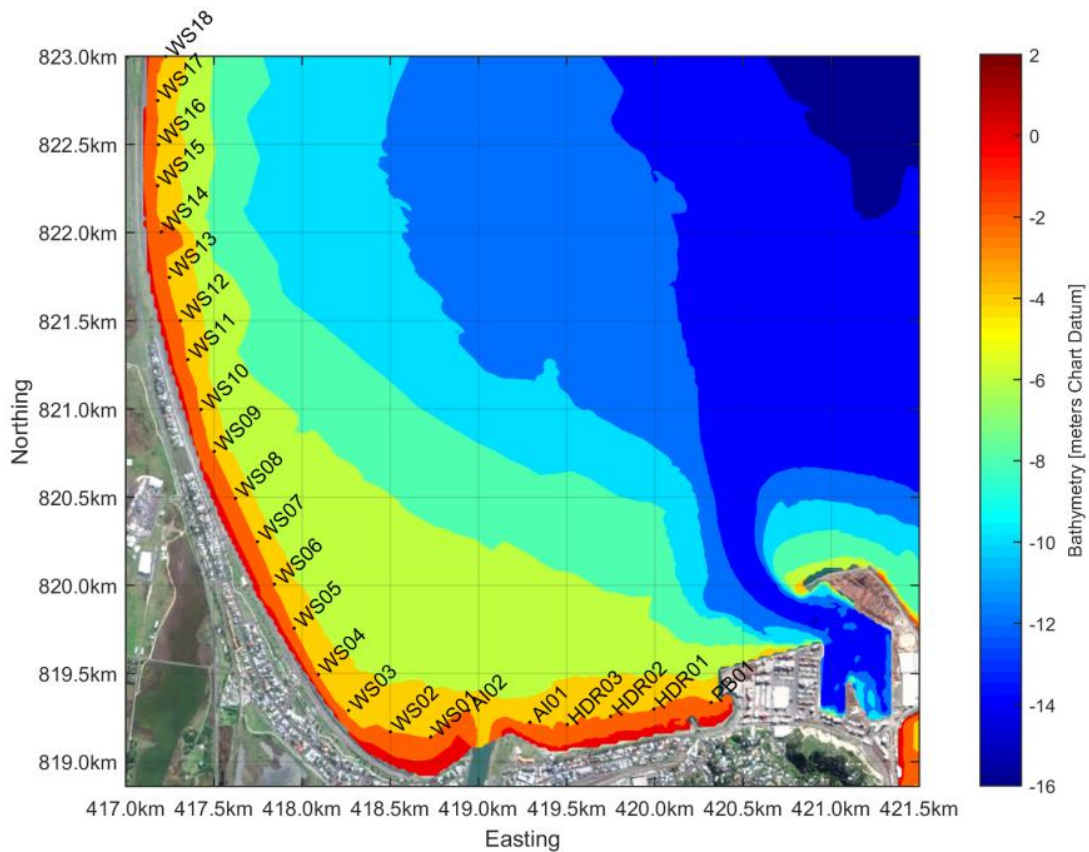


Figure 7-1: Locations of inshore wave points between Napier Port and Esk River, along the -2m C.D. contour.



Table 7-1: Changes in energy weighted mean wave height and direction at the 2m C.D. contour for various discrete locations between Napier Port and Westshore.

Frontage	Location	Change in Mean Wave Height (m)	Change in Mean Wave Direction (degrees clockwise)
Port Beach	PB01	-0.05	2.2
Hardinge Road	HDR01	0.01	2.0
	HDR02	-0.03	2.0
	HDR03	0.06	0.7
Ahuriri Inlet	AI01	0.04	1.0
	AI02	-0.02	0.3
Westshore	WS01	-0.02	0.3
	WS02	-0.02	0.3
	WS03	0.01	0.6
	WS04	0.00	0.5
	WS05	-0.01	0.4
	WS06	0.01	0.7
	WS07	0.02	0.5
	WS08	0.01	0.3
	WS09	0.00	0.2
	WS10	-0.01	0.1
Bay View	WS11	-0.01	0.0
	WS12	-0.01	0.0
	WS13	0.00	0.0
	WS14	0.00	0.1
	WS15	0.00	0.0
	WS16	0.00	0.1
	WS17	0.00	0.1
	WS18	0.00	0.1

The changes to the different frontages may be summarised as follows:

- A change in mean wave direction of about 2 degrees, but an overall reduction in wave energy incident to Port Beach.
- Localised wave focussing along Hardinge Road, combined with a tendency for littoral transport to become more westerly (or less easterly) along the shore. The existence of boulder and rock rubble protection along this section of shoreline means that changes in the incident wave climate will not alter the shoreline position.
- A slight increase in wave height at the eastern mole of Ahuriri, combined with a change in wave direction by about one degree. This is likely to manifest as a very slight clockwise rotation of the beach, but requires that incident wave energy is sufficient to drive morphological change.



- Small or negligible changes to wave energy arriving at Westshore, and a slight clockwise rotation in the equilibrium shoreline angle of less than one degree. This corresponds to an 'opening out' of the beach planform alignment (i.e. an increase in the radius of beach curvature) that is already occurring naturally. It should be noted that the relative change in incident wave angle is less than that expected to occur due to natural variability in the wave climate between different seasons and years.
- No change in wave height or direction to the beach north of Napier Airport, and The Gap.



8 Wave-driven Sub-Littoral Sediment Transport

Simulations of changes to sub-littoral sediment transport patterns are undertaken using Delft3D, which is a coupled wave-current-sediment transport model. A brief description of the model is given in Section 4.

Simulation of sediment transport around Napier Port is undertaken with a grid resolution of 20m. The 3D flow mode includes wave-driven currents from wave setup, dissipation, breaking and rips, undertow and dynamic feedback between waves and currents. Sand transport is calculated using the TRANSPORT2004 sediment transport algorithm, which represents the state-of-the-art in knowledge of non-cohesive sediment transport processes.

Note that the simulations presented in this section provide maps of sediment transport potential due to multiple wave conditions. Sediment transport potential does not necessarily equate to actual sediment transport, as sediment particles of an appropriate size must be available to be transported. Therefore, although quantities of sediment transport are calculated and shown in the results, these values are used for comparison between the existing and post-dredging situations rather than to determine actual sediment transport rates.

8.1 Spatial Distribution of Marine Sands around Napier

A description of marine sands around Napier is provided in Section 3.2. Data from Mead et al (2001) and grab samples collected by NPL for the purposes of this coastal assessment have been combined (Figure 8-1) and used as a spatial map of sediment grain size within the sediment transport model.

Particle Grain Size analysis of sediments taken in similar water depths (marked GS1 to GS4 in Figure 8-1) suggest that sediments around Westshore and the Port breakwater have a very similar distribution of particle diameters, comprising predominantly fine sand.

8.2 Selection of 'Morphological Waves'

The calculation of annual-average potential sediment transport makes use of the 'morphological wave' concept. This is similar in method to that used for assessing the energy weighted mean wave height in Section 5:

First, the wave climate is divided into discrete intervals of Mean Wave Direction. For the purposes of this analysis, a bin interval of 20° was used.

Next, each wave direction bin is further sub-divided to $H_{m0} = 1m$ intervals. The centroid 'energy-weighted' H_{m0} , MWD and associated T_p is calculated for each [MWD, H_{m0}] class.



Finally, the probability of occurrence of each morphological wave is calculated from the contribution of that [MWD, Hm0] class to the total wave record.

Figure 8-2 shows the wave conditions selected for calculating sediment transport patterns. The method captures contribution from frequently occurring 'mean' wave conditions and less frequently occurring but important 'storm' wave conditions.

Simulating the magnitude and direction of sediment transport due to each morphological wave condition, and then summing across the associated energy-weighted probabilities of occurrence gives the annual average sediment transport field.

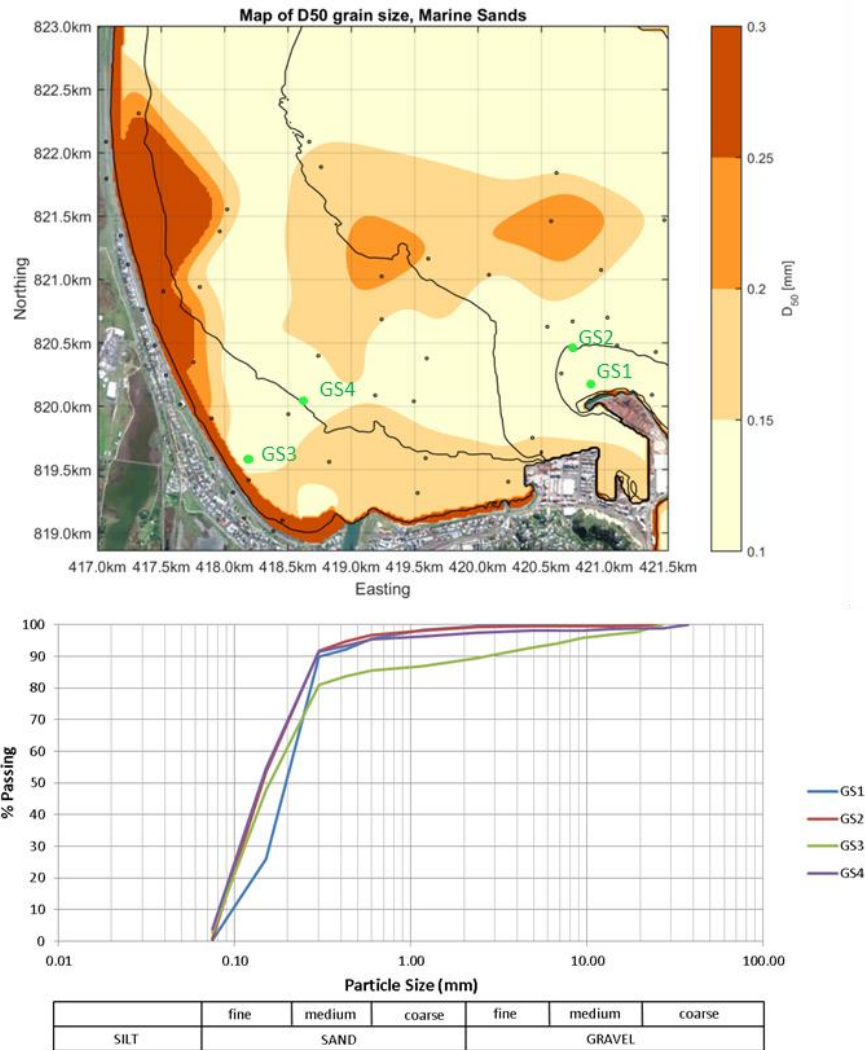


Figure 8-1: Upper panel: Spatial distribution of sand sizes in sub-littoral zone at Napier (black dots represent grab sample positions). Lower panel: Particle Size Distribution of grab samples taken adjacent to the Port breakwater (samples GS1 and GS2) and Westshore (GS3 and GS4).

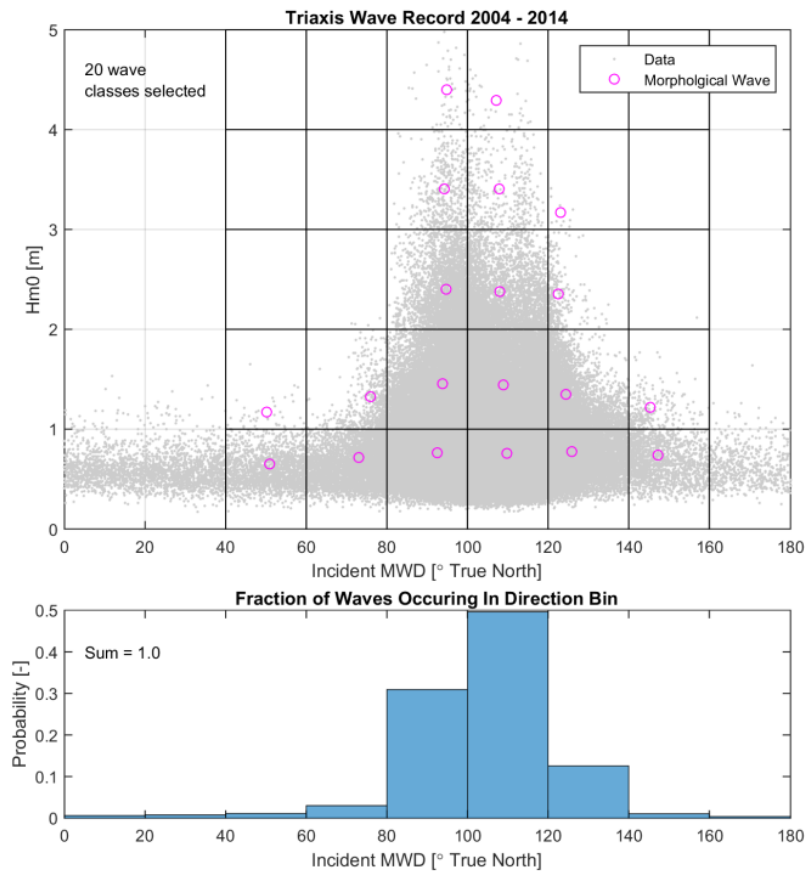


Figure 8-2: Selected morphological waves for sand transport around Napier Port.

8.3 Results

Annual average sediment transport patterns for 'baseline' and 'channel deepening' are shown in Figure 8-3. The difference in the magnitude of sediment transport potential is shown in Figure 8-4. Areas where sediment transport is predicted to increase will tend towards erosion. Areas where sediment transport is predicted to decrease will tend towards sediment deposition.

The sediment transport model is validated in a very broad-brush manner by comparing predicted sediment movement at the edge of the navigation channel with historical dredge records kept by Napier Port.

Analysis of maintenance dredging records suggest that on average some 37,000 m³/yr of material are removed by the Port, mostly comprising the berth areas, fairway, turning basin and channel adjacent to the breakwater. The sediment transport model predicts, for 'baseline' conditions, that potentially 70,000 m³/yr of sediment bypasses the breakwater tip to ingress to the channel and turning basin. That is, model prediction is in the range of the observed values.



Figure 8-3 shows areas of relatively high sediment mobility at the Port breakwater and seaward of the Bay View frontage. This is due to the relatively high levels of wave exposure, particularly from the dominant SSE swells from which the majority of the storm waves approach.

High sediment mobility is also predicted seaward of Westshore. Although relatively sheltered from incident swell wave activity, the flatter slope of the sea floor causes wave breaking over a wider area, enhancing the ability of the waves to suspend and transport sediment.

Comparative analysis of sediment transport magnitudes in Figure 8-4 suggests the following general conclusions can be drawn:

- Measured along the -4m CD contour, sediment mobility is predicted to increase by roughly 10% at the northern end of Westshore and decrease by approximately 10% at the southern end of Westshore.
- Sediment mobility immediately offshore of the East Pier Beach is predicted increase, commensurate to the increased exposure to wave activity.
- Sediment mobility immediately offshore of Hardinge Road and Port Beach is predicted to decrease.

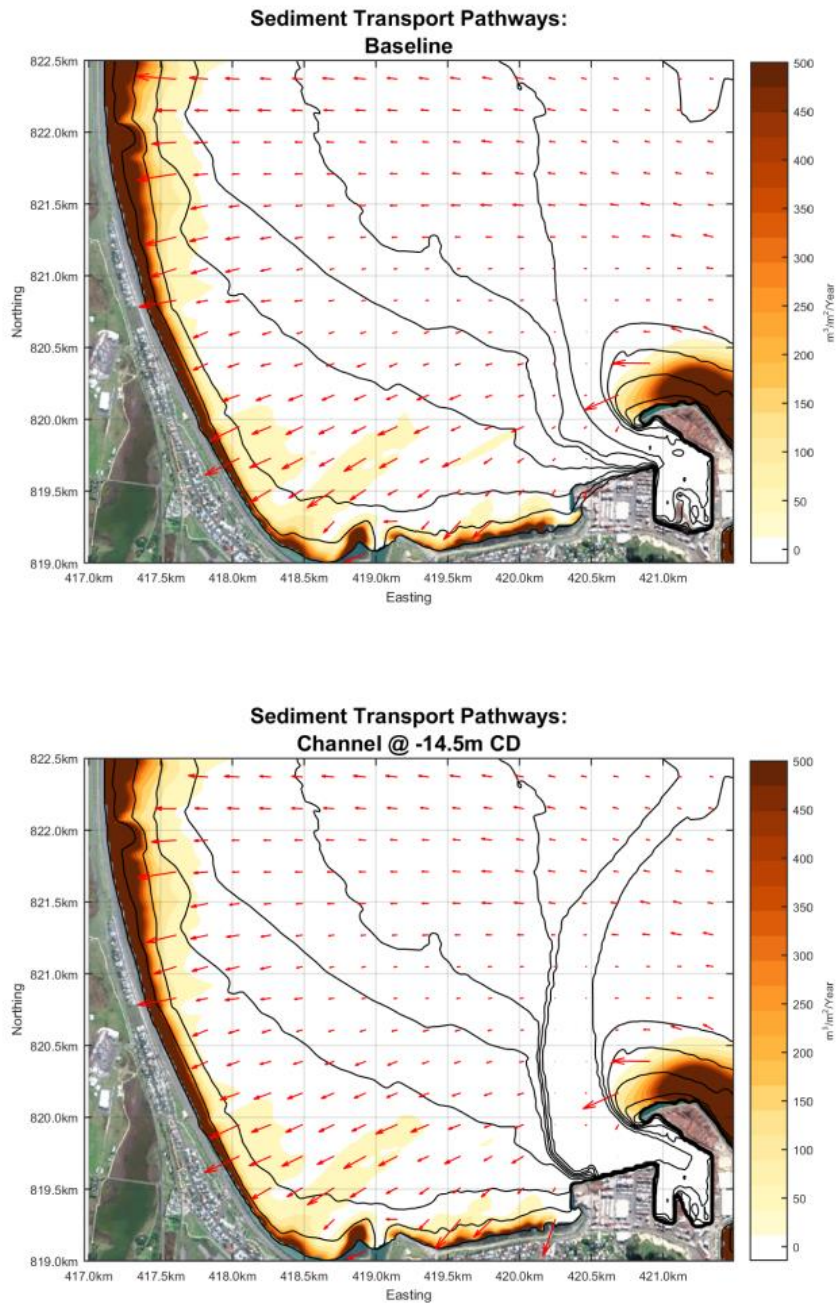


Figure 8-3: Annual-average sediment transport magnitude and vectors in the region of Napier Port. Volumes are m^3/yr .

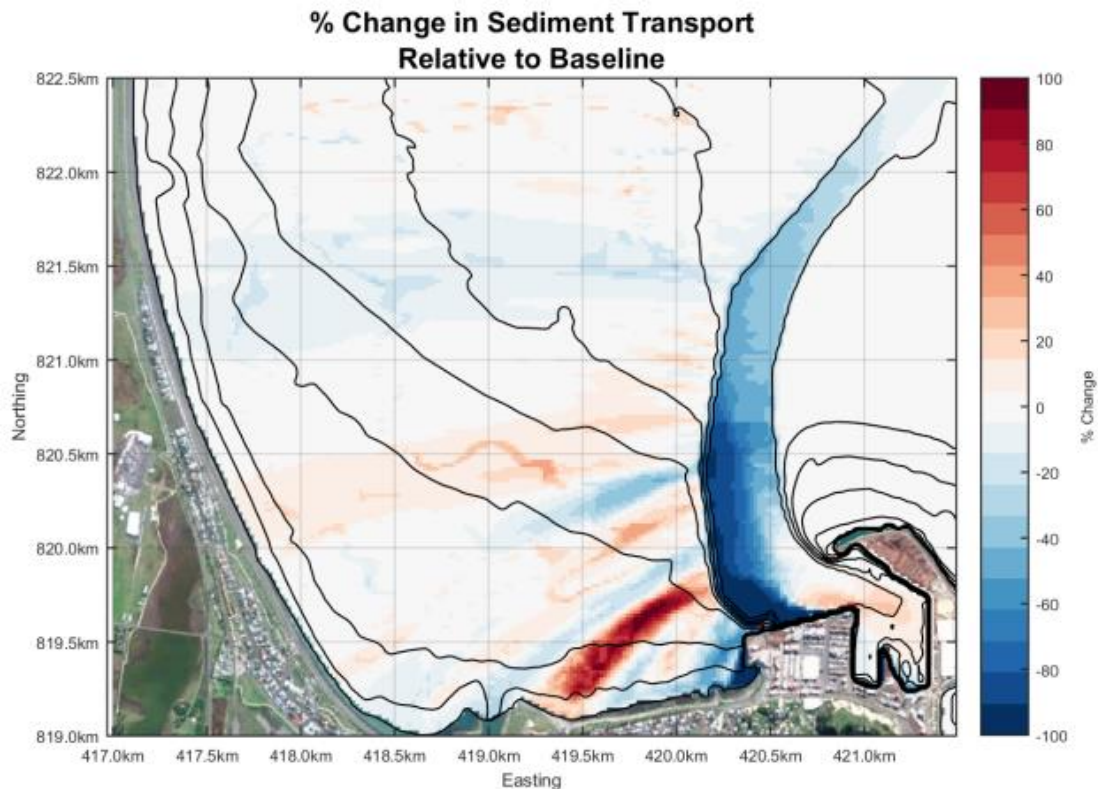


Figure 8-4: Predicted change in sub-littoral transport of fine sands in the region of Napier Port. Relative change in sediment transport compared to baseline, expressed in percent.

8.4 Interpretation of Numerical Model Results

In sediment transport modelling, usually it is considered that a good result shows predicted rates of transport to be generally in the right order of magnitude and going in the correct direction. The difficulties remaining with simulating sediment transport means usually that a high degree of interpretation of the results is required in the light of conceptual understanding of processes occurring at the site.

The predominant processes at work in transporting fine sandy material at Napier are as follows:

- Local generation of sand and silts via mechanical abrasion of gravel by wave action
- Removal of fine sediments to deeper water by storm waves
- Movement and transport of sediment by swell waves
- Gradual transport of sediment suspended by wave action in the direction of any current that exists in the overlying water column.

Therefore, the direction in which sediment is moved is a balance between current processes and wave processes and the direction of the ambient current in relation to the direction in which waves are traveling.

8.4.1 Conceptual Model of Sand Movement at Napier

8.4.1.1 Wave sorting of natural sand

The movement and suspension of natural sand occurs when the local bed shear velocity (due to waves and currents) exceeds the fall velocity of the sediment (Van Rijn, 1993). In shallow water, which is the case for all swell waves at Napier the onshore orbital motion under the crest (is stronger than that under the trough, which is directed offshore (Figure 8-5). As coarser sediment requires a higher bed shear velocity, coarse sediment is moved onshore whilst finer sediment, which can be suspended by a much smaller shear velocity, is winnowed offshore. In deeper water of calmer wave activity the direction of transport is onshore.

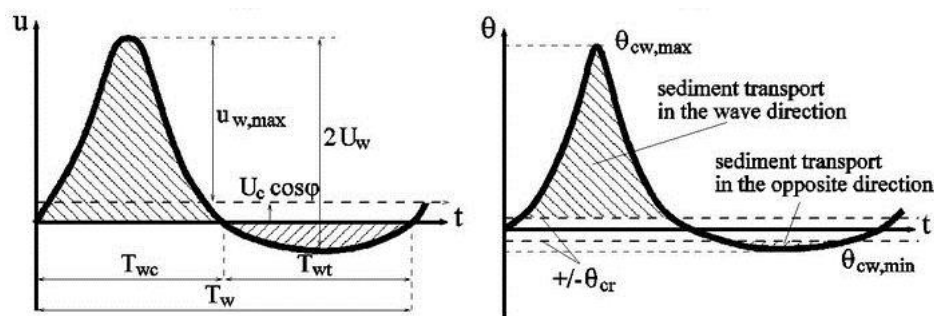


Figure 8-5: Conceptual mechanism of onshore vs offshore sediment transport, showing wave-orbital asymmetry under shoaling waves. U and θ defined as positive in the onshore direction.

8.4.1.2 Transport under Waves and Currents

Engineering formulae (TRANSPoor2004; Van Rijn 2007) suggest sediment will be available for transport when local wave height exceeds approximately 1.0m and depth-average current exceeds about 10cm/s. Analysis of ADCP observations at Beacons and Channel Approaches suggest this occurs 8 – 10% of time in 5 to 15m water depth.

At these times sediment will follow wind-driven current pathways, i.e. the predominant direction of currents between Westshore and the port navigation channel present when the wind flow is from NW, W and SW as shown in Figure 3-8. The slow speed of these currents means that the magnitude of sediment suspended will not change from that predicted by the model, but the direction will change.

The effectiveness of currents in transporting finer sediments selectively is indicated in Figure 8-6, which shows the relationship between sediment grain size and fall velocity for fine and medium



sands as encountered at Napier. The fall velocity for sand of 0.1mm size is roughly one third that for diameter of 0.3mm, and roughly one half of that for a diameter of 0.2mm. For a given suspension height and current speed, suspended sediments of 0.1mm diameter will travel twice as far as those of 0.2mm, and three times further than those of 0.3mm.

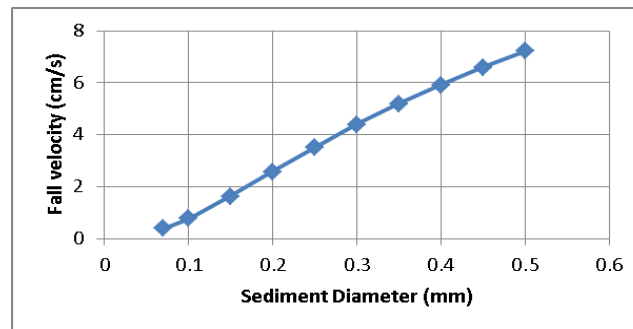


Figure 8-6: Relationship between sediment grain diameter and fall velocity in typical coastal waters. After Van Rijn, 2007.

As current speeds decrease relative to wave height, sediment will instead start to move as a composite of wave direction (due to suspension by orbital motion) and residual current. In very nearshore (or in very calm winds), movement is controlled purely by wave action via strong orbital motion and wave-driven currents (i.e. wind-driven currents are no longer important).

Analysis of the wind and wave record at Napier found no correlation between wave activity and wind strength or direction. Under these circumstances it is most appropriate to calculate the sediment transport magnitude under wave activity, and assign an 'annual mean direction' based on an analysis of the ambient currents.

These processes are summarised in to a conceptual model of sand transport between Napier Port and Westshore, shown in Figure 8-7.

Advisian (2017^b) presents additional analysis and simulation of sediment transport under the influence of both waves and currents, for multiple sediment fractions. Figure 8-8 and Figure 8-9 show 'mean annual' sediment transport pathways for 'fine' sand (up to 125 μm ; representing approximately 70% of seabed sediments) and 'medium' sand (300 μm or greater; representing approximately 2% of seabed sediments), respectively.

The results confirm the interpretation of mean transport pathways suggested in Figure 8-7. That is, fine sands are more easily transported by near-surface currents in the water column and hence are, over time, preferentially transported in the direction of the prevailing current directed eastward and southward around Napier Port. Coarser sediment instead tends to move onshore under wave action – as suggested by the sediment transport vectors around Westshore, where the direction of transport for coarser sediment is primarily to the north.

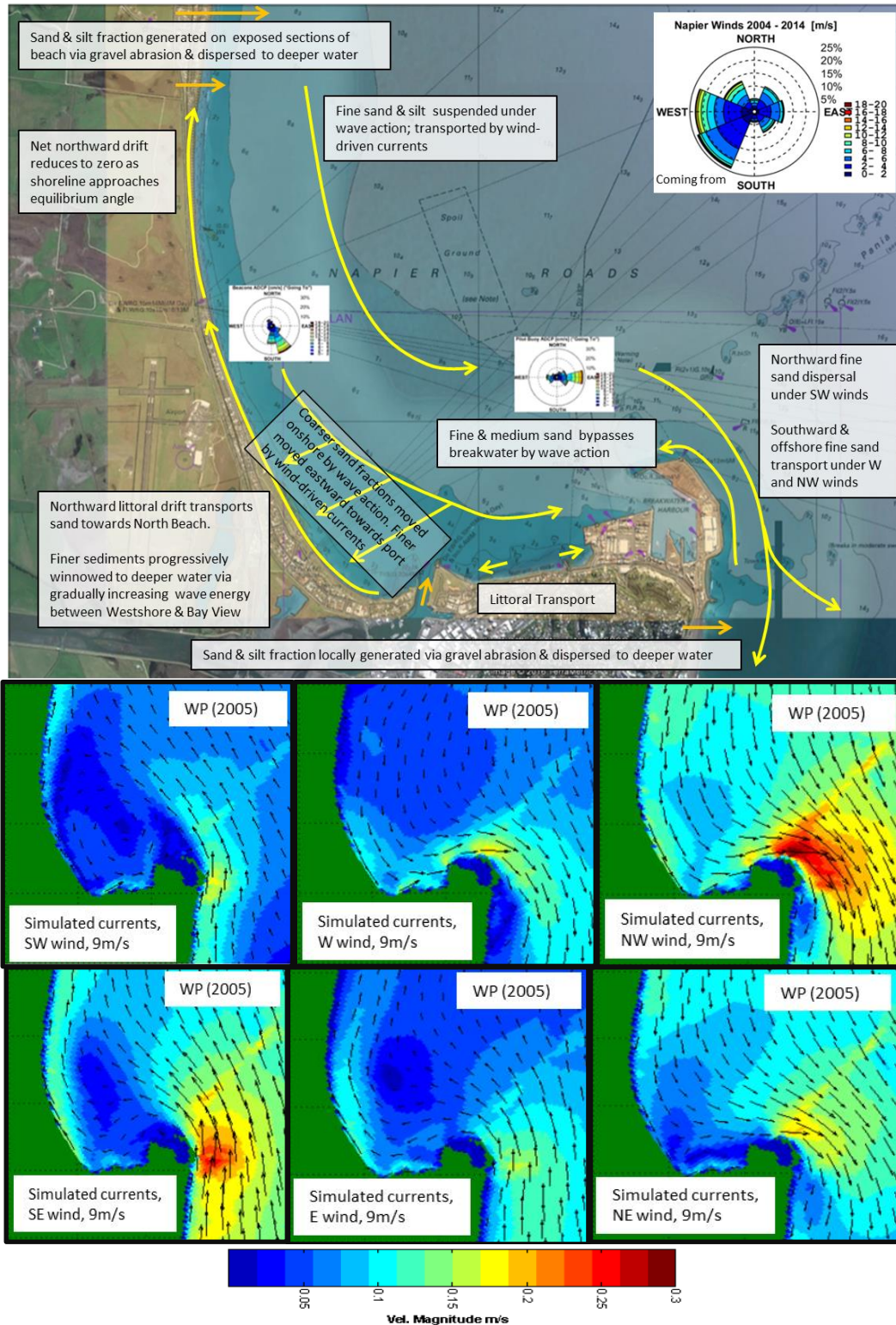


Figure 8-7: Interpretation of annual mean sediment transport pathways around Napier Port (upper panel) on basis of wind-driven currents (lower panel) and known wave refraction patterns (Section 5).



The potential influence of deepening the navigation channel on sediment transport magnitudes and pathways can therefore be estimated by consideration of Figure 8-4, which shows that the magnitude of sediment transport potential will increase slightly in some areas and decrease in others, the most affected region being immediately west of the channel between the swing basin and Ahuriri Inlet. The direction of mean annual transport will be unaffected by the presence of a deeper channel, and hence the sediment transport pathways shown in Figure 8-8 and Figure 8-9 would not be expected to change.

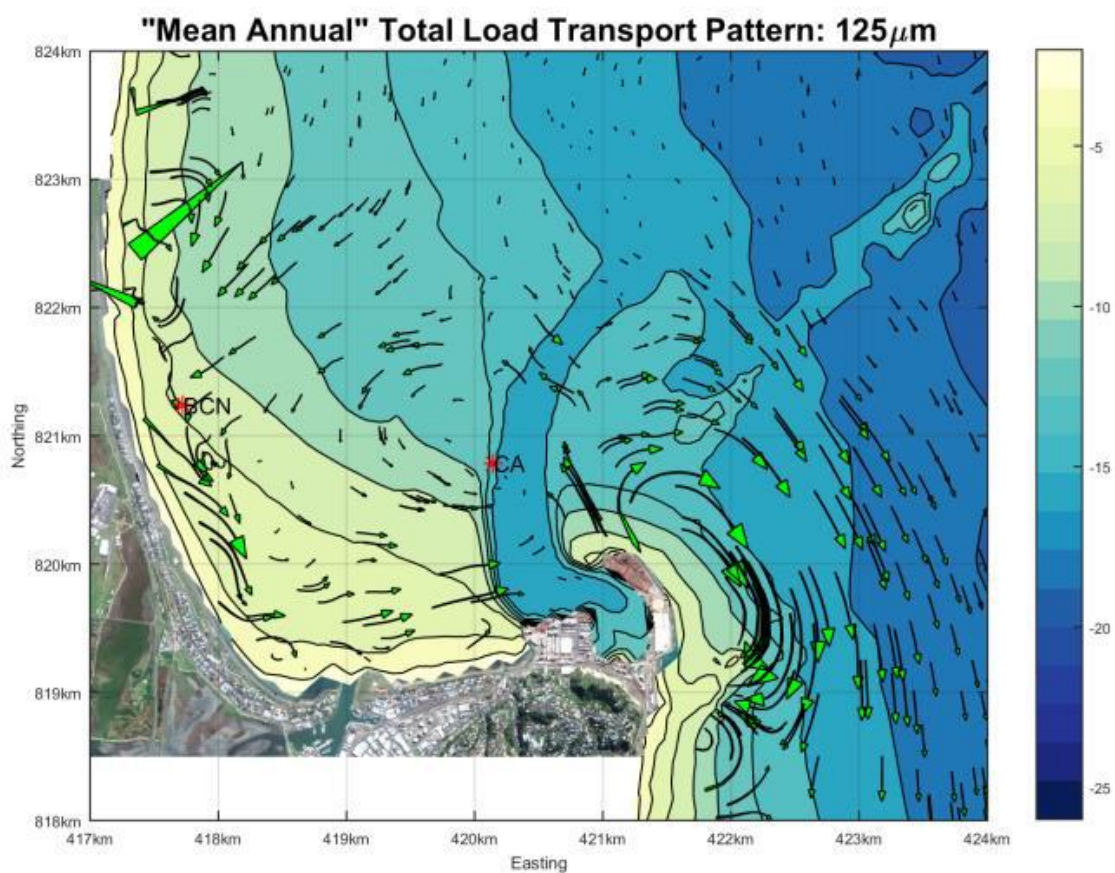


Figure 8-8: Mean Annual average sediment transport pathways for sediment diameter of approximately 125 µm. 'BCN' and 'CA' correspond to positions of 'Beacons' and 'Channel Approaches' ADCP units, respectively, deployed to validate the 3D numerical model. From Advisian (2017^b).

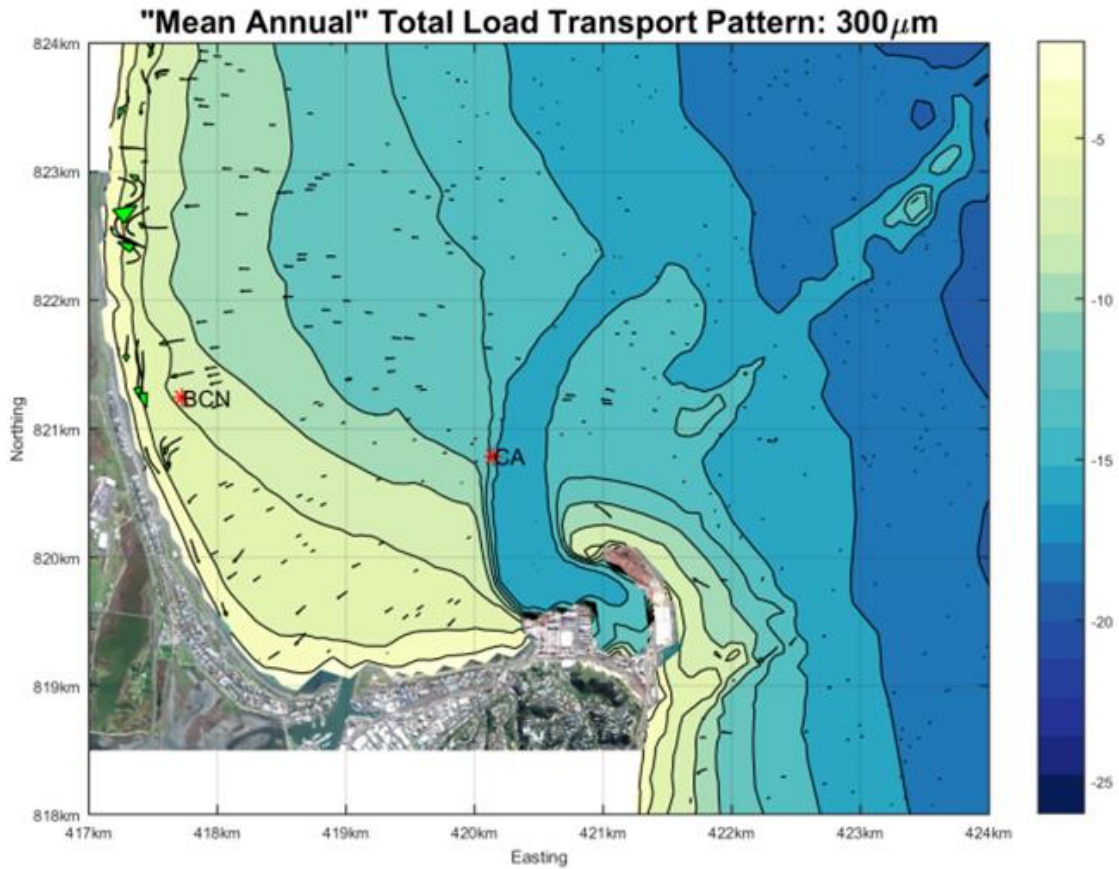


Figure 8-9: Mean annual average sediment transport pathways for sediment diameter of approximately 300 μ m. 'BCN' and 'CA' correspond to positions of 'Beacons' and 'Channel Approaches' ADCP units, respectively, deployed to validate the 3D numerical model. From Advisian (2017^b).



9 Conclusions and Recommendations

9.1 Wave Refraction

Wave and sediment transport modelling of pre- and post-dredge bathymetries indicates that the proposed dredging will have only minor impacts on the wave climate to the beaches to the west of the Port as follows:

- A reduction in wave height and 2° clockwise rotation of the wave climate direction at Port Beach.
- A clockwise rotation in incident wave angles along Hardinge Road. The change to wave height is variable along the frontage, and will depend upon the specific combination of wave period and wave angle incident at the Port. In general, the wave height is predicted to decrease.
- Mean wave energy is predicted to increase slightly on the eastern breakwater of Ahuriri Inlet but decrease slightly on the western side.
- Impacts to the mean wave height between the southern boundary of Westshore Beach and the Esk River are negligible. A slight decrease is predicted at the southern boundary of Westshore. The mean wave direction is predicted to rotate by less than one degree clockwise along the length of Westshore frontage.

9.2 Surf Breaks

A simple comparative analysis of wave shoaling and refraction patterns for a large storm event suggests that the impacts to surf breaks will be variable:

- The occurrence and height of surfable waves is likely to very slightly increase at the City Reef surf break.
- Dredging the channel will have minimal impact on wave crest patterns at both Hardinge Road and City Reef surf breaks.

A detailed assessment of surfing amenity was undertaken in terms of peel angle, wave height and wave breaker type in accordance with the methods described by Mead (2003), and Lewis *et al* (2015). The two surf breaks analysed in detail include City Reef (including left-hand and right-hand surfing paths, and "inner" break) and Hardinge Road.

It was found that there would be minimal change to the surfing amenity at City Reef as a result of the proposed dredging, with very little change in peel angle and only a slight increase in the proportion of plunging breakers when compared with spilling breakers.



At Hardinge Road, there would be a slight increase in the peel angle, caused by a clockwise rotation in the approach direction of the waves. This slight increase would result in very little change in surfing amenity, with a slightly higher proportion of waves being assessed as surfable following the dredging, due to the predicted increase in peel angle.

9.3 Sediment Movement and Shoreline Change

Comparative sediment transport calculations based on the wave modelling results and the review of previous studies has been used to evaluate the impact of proposed dredging on the shoreline:

- Potential changes in littoral drift, inferred by changes to wave refraction patterns and hence incident wave height and incidence angle within the surf zone, is well within the range of natural variability known to occur through fluctuations in wave climate and sediment supply.
- Wave angles at Ahuriri Inlet are predicted to rotate clockwise by less than 1 degree, suggesting that the beach fronting the east harbour mole will rotate slightly in response to become more easterly facing. This rotation can only be realised if there is sufficient wave energy on the beach to drive morphological change.
- Along Hardinge Road littoral drift potential will become more westerly. At the western boundary of Hardinge Road this will increase sediment transport potential towards the beach fronting the east mole of Ahuriri inlet. At the east boundary of Hardinge road this will reduce the tendency for sediment to be transported eastward towards Port Beach.
- The change in wave climate at Port Beach will cause the beach to rotate clockwise by approximately 2 degrees, becoming more northerly in its orientation. The predicted decrease in wave energy suggests that there is little potential for beach erosion due to changes in wave climate. Rotation of the beach will manifest as erosion on the eastern boundary by the Port, and accretion on the western boundary by the rock groyne.

Overall, the predicted impacts of the proposed dredging on the beaches west of the Port are small or negligible..

9.4 Recommendations

Further monitoring of the beach and nearshore areas of Port Beach and Ahuriri Inlet and should be undertaken in line with the following recommendations:

- Beach profile surveys to be undertaken at regular 6 monthly intervals (or more frequently), at least 1 year before commencement of the dredge project, and continue until at least one year after the final dredging depth and configuration is achieved.



- Beach profiles should be monitored for trends and changes in beach volume.
- Beach plan alignment should be monitored for trends and changes in shoreline alignment and direction.
- Such data should be interpreted by an appropriate expert and reported to Hawke's Bay Regional Council.



10 References

Advisian (2017^a): Port of Napier Proposed Wharf and Dredging Project: Dredge Plume Modelling. Report to Napier Port Ltd, June 2017.

Advisian (2017^b): Port of Napier Proposed Wharf and Dredging Project: Post-Disposal Fate of Dredged Sediments. Report to Napier Port Ltd, May 2017.

BECA (2016). 6 Wharf Development – Geotechnical Factual Report. Prepared for Napier Port Ltd. 29th February.

Campbell, M.D.N. (1975). Story of Napier 1874–1974 (Footprints along the Shore). Napier, New Zealand: Napier City Council, 252p.

Cawthron (2005): Assessment of Effects on Benthic Ecology for a Proposed No.6 Berth Development at the Port of Napier (Draft). Unpublished report prepared for the Napier Port Ltd. Cawthron Report No. 977

CERC (1984), Shore Protection Manual

Coggins, J.H.J., Parsons, S., and Schiel, D. (2015). An Assessment of the Ocean Wave Climate of New Zealand as Represented in Kidson's Synoptic Types. *International Journal of Climatology*. 36(6), pp2481 – 2496.

Davis, J.L. (1964). A morphogenic approach to world shorelines. *Zeitschrift für Geomorphologie*, v. 8, pp 127 – 142.

De Lang (1996). Storm surges on the New Zealand Coast. *Tephra*, vol 15(1), pp 24-31.

Francis, R.I.C.C., (1985): An alternative water circulation pattern for Hawke Bay. *NZ Journal of Marine and Freshwater Research* 19: 399-404.

Gibb, J. (1996). Coastal Hazard Zone assessment for the Napier City Coastline between the Ahuriri Entrance and Esk River Mouth. Unpublished report to Napier City Council, C.R. 96/2 April 1996. 80pp.

Gibb, J. (2003). Review of the Westshore Nourishment Scheme – Napier City. Report to Napier City Council, C.R.2002/6.

Gorman, R.M.; Bryan, K.R., and Laing, A.K., (2003). A wave hindcast for the New Zealand region— deep water wave climate. *New Zealand Journal of Marine and Freshwater Research*, 37, 589–611.

Hawke Bay Regional Council (2014). Hawke Bay – New Zealand Global Climate Change and Barrier Beach Responses. HBRC Report No. AM 14-02, March 2014.



Hawke Bay Regional Council (2013). Assessment of Resource Consent Application, Whakarire Avenue, Napier, consent numbers CL130253R, CL130254M, CL130255M, CL130257C, CL130258O, CL1302589D.

Hutt, J.A.; Black, K.P., and Mead, S.T., (2001). Classification of surf breaks in relation to surfing skill. *Journal of Coastal Research*, Special Issue No. 29, pp. 66–81.

Jennings, R., Shulmeister, J., 2002. A field based classification scheme for gravel beaches. *Marine Geology* 186, 211–228.

Kirk, R.M., 1980. Mixed sand and gravel beaches: morphology processes and sediments. *Progress in Physical Geography* 4, 189–210.

Kirk, R.M. and Single, M.B. (1999). Coastal Change at Napier with special reference to erosion at Westshore: A review of Causative factors. Report to Napier Port Ltd., March 1999

Komar, P.D. (2005). Hawkes Bay, New Zealand: Environmental Change, Shoreline Erosion and Management Issues. Report for the Hawke Bay Regional Council. November 2005.

Komar, P.D. (2010). Shoreline Evolution and Management of Hawke Bay, New Zealand: Tectonics, Coastal Processes, and Human Impacts. *Journal of Coastal Research*: Volume 26, Issue 1: pp. 143 – 156.

Komar, P.D. and Harris, E. (2014). Hawke Bay, New Zealand: Global Climate Change and Barrier Beach Responses. Report to the Hawke Bay Regional Council. Report No. AM 14-02.

Lewis, J., S. Hunt, T. Evans (2015). Quantification of Surfing Amenity for Beach Value and Management. Proceedings NSW Coastal Conference, 2015.

Marshall, P. (1933). Effects of the earthquake on the coastline near Napier. *New Zealand Journal of Science and Technology*, 15, 79–92.

Mead, S. 2003 Keynote address: Surfing Science, Proceedings of the 3rd International Surfing Reef Symposium, Raglan, New Zealand, June 22-25, 2003. p1-36

Mead, S., Black, K., McComb, P. (2001). Westshore Coastal Process Investigation: A study to Determine the Coastal Processes in the Bay at Westshore and Provide a Long-Term Solution to Erosion Problems. ASR Ltd, 2001.

MetOcean Solutions (2009). Technical Note P0010-03, Wave Reflections from the proposed breakwater, 21/07/09

Ocel (2004): Geotechnical Report on the Proposed Reclamation to the West of the Port behind the Proposed No. 6 Berth. Unpublished report prepared for the Napier Port Ltd.

Single, M.B. (1985). Post-Earthquake Beach Response, Napier, New Zealand, Christchurch, New Zealand: University of Canterbury, Master's thesis, 150p.



Single, M.B. (2017). Port of Napier proposed wharf and dredging project: Physical coastal environment. Report prepared for Port of Napier Ltd.

Smith, R.K. (1968). South Hawke Bay Beaches: Sediments and Morphology. Christchurch, New Zealand: University of Canterbury, Master's thesis.

Smith, R.K. (1993). Westshore Beach Erosion Review. Report to Napier City Council, Hamilton, New Zealand: National Institute of Water and Atmospheric Research, Consultancy Report NAP004, 17p.

Sutherland, J. and Peet, A.H. and Soulsby, R.L. (2004). Evaluating the performance of morphological models. *Coastal Engineering*, 51 (8-9). 917-939.

Van der Meer, J.W. and K.W. Pilarczyk (1988), Rock slopes and gravel beaches under wave attack. *Delft Hydraul. Commun.* 396 (1988), pp. 1-152.

Van Rijn, L.C. (1993), (2012). Principles of sediment transport in rivers, estuaries and coastal seas. Aqua Publications, Amsterdam, The Netherlands (WWW.AQUAPUBLICATIONS.NL)

Van Rijn, L.C., (2007). Unified view of sediment transport by currents and waves, I: Initiation of motion, bed roughness, and bed-load transport. *Journal of Hydraulic Engineering*, 133(6), p 649-667.

Walker, J.R., (1974). Recreational Surfing Parameters. Honolulu, Hawaii: University of Hawaii, Department of Ocean Engineering, LOOK Laboratory Technical Report 30, 311p.

Water Quality Centre (1989): Dredge Spoil Disposal Offshore from the Port of Napier. Unpublished report prepared for the Napier Port Ltd.

WorleyParsons (2002): Port of Napier: Shoreline Effects of Stage 1 and Ultimate Development: 28 November 2002 report to the Port of Napier, Worley Infrastructure Pty Ltd, Perth, Australia

WorleyParsons (2005): Port of Napier No. 6 Berth Development Study. Dredging Effects Study. Report 302/00384/a48, September 2005.

WorleyParsons (2011). Proposed Dredging – Port of Napier. Shoreline Effects Study. Report 301010-00974 – CS-REP-0002, September 2011.



Advisian

WorleyParsons Group

Appendix A: Glossary





Glossary

The following meanings are attached to terms that may be used within this report:

Accretion	The accumulation of (beach) sediment, deposited by natural fluid flow processes.
Algorithm(s)	Formula or combination of formulae used for calculations.
Alongshore	Parallel to and near the shoreline; same as longshore.
Amphibolis	A type of seagrass that forms meadows on calcareous sands. The interweaving roots and leaves consolidate the substrate of the ocean floor, protecting it from erosion by currents and wave action.
Astronomical tide	The tidal levels and character which would result from gravitational effects, e.g. of the Earth, Sun and Moon, without any atmospheric influences.
Backshore	(1) The upper part of the active beach above the normal reach of the tides (high water), but affected by large waves occurring during a high tide. (2) The accretion or erosion zone, located landward of ordinary high tide, which is wetted normally only by storm tides.
Bank	See Shoal
Bar	An offshore ridge or mound of sand, gravel, or other unconsolidated material which is submerged (at least at high tide), especially at the mouth of a river or estuary, or lying parallel to and a short distance from, the beach.
Bathymetry	The measurement of depths of water in oceans, seas and lakes; also the information derived from such measurements.
Bay	A recess or inlet in the shore of a sea or lake between two capes or headlands, not as large as a gulf but larger than a cove. See also <i>bight, embayment</i> .
Beach	The zone of unconsolidated material that extends landward from the low water line to the place where there is marked change in material or physiographic form, or to the line of permanent vegetation. The seaward limit of a beach – unless otherwise specified – is the mean low water line. A beach includes foreshore and backshore.
Beach erosion	The carrying away of beach materials by wave action, tidal currents, littoral currents or wind.
Beach face	The section of the beach normally exposed to the action of wave uprush. The foreshore of the beach.

Beach profile	A cross-section taken perpendicular to a given beach contour; the profile may include the face of a dune or sea wall, extend over the backshore, across the foreshore and seaward underwater into the nearshore zone.
Beach width	The horizontal dimension of the beach measured normal to the shoreline.
Beach nourishment	The process of placing sand from elsewhere onto an eroding shoreline to create a new beach or to widen an existing beach. Beach nourishment manages erosion by replacing sand lost and providing new sand to continue to feed the sand losing process.
Bed	The bottom of a watercourse, or any body of water.
Berm	On a beach: a nearly horizontal plateau on the beach face or backshore, formed by the deposition of beach material by wave action or by means of a mechanical plant as part of a beach recharge scheme.
Boussinesq	Boussinesq, J was a French mathematician and physicist who made significant contributions to the theory of hydrodynamics, specifically wave action. Boussinesq-type equations are used in computer models for the simulation of water waves in shallow seas and harbours. This type of modelling is considered to give the best representation of wave transformation that is possible at present.
Breaker zone	The zone within which waves approaching the coastline commence breaking, typically in water depths of between 5 m and 10 m on the open coast but in shallower waters within bays.
Breaking depth	The still-water depth at the point where the wave breaks.
Breakwater	Offshore structure aligned parallel to the shore, sometimes shore-connected, that provides protection to the shore from waves.
Calcarenite	A type of limestone that is composed predominantly of sand-size carbonate grains of, typically, corals, shells, fragments of older limestones and dolomites, other carbonate grains, or some combination of these. Calcarenite is the carbonate equivalent of sandstone.
CD	Chart Datum – usually the lowest tide level and a reference level for nautical charts used for navigation.
Chart datum	The plane or level to which soundings, tidal levels or water depths are referenced, usually low water datum.
Climate change	Refers to any long-term trend in changes to mean sea level, wave height, wind speed, etc.

Coastal currents	Currents that flow usually parallel to the shore and constituting a relatively uniform drift in the deeper water adjacent to the surf zone. These currents may be tidal, transient, wind-driven or associated with oceanic currents.
Coastal processes	Collective term covering the action of natural forces, such as winds, waves and tides, on the shoreline and the nearshore seabed.
Coastal zone	The land-sea-air interface zone around continents and islands extending from the landward edge of a barrier beach or shoreline of coastal bay to the Continental Shelf.
Coastline	The line where terrestrial processes give way to marine processes, tidal currents, wind waves, etc.
Common Distributables	Project costs that are not associated with any specific direct account. These may include such things as the field office, office supplies, temporary construction, utilities, etc., which, usually, are borne by the owner
Configuration dredging	A process of shaping the seabed in such a way as to modify the wave transformation process to change wave direction and/or height.
Continental Shelf	The underwater landmass that extends seaward from a continent, resulting in an area of relatively shallow water, generally less than 200 m deep, lying between the shoreline and the deep ocean. Much of the Continental Shelf was exposed during the ice ages.
Contingency	In estimating cost, an allowance for uncertainty as to the precise content of all items in the estimate, how work will be performed, what work conditions will be like when the project is executed and so on (the known-unknowns).
Current	Ocean currents can be classified in a number of different ways. Some important types include the following: <ul style="list-style-type: none"> - Periodic - due to the effect of the tides; such currents may be rotating rather than having a simple back and forth motion. The currents accompanying tides are known as tidal currents - Temporary - due to seasonal winds - Permanent or ocean - constitute a part of the general ocean circulation. The term drift current is often applied to a slow broad movement of the oceanic water - Nearshore - caused principally by waves breaking along a shore. Also, coastal currents that run parallel to the coast.
Datum	Any position or element in relation to which others are determined, as datum point, datum line, datum plane.

Deep water	In regard to waves, where depth is greater than one-half the wave length. Deep-water conditions are said to exist when the surf waves are not affected by conditions on the bottom.
Depth of closure (DoC)	For a given or characteristic time interval, the depth on a beach profile seaward of which there is no significant change in bottom elevation and no significant net sediment transport between the nearshore and the offshore during storms and ensuing calm weather.
Design Allowance	An allowance in a cost estimate for the growth of costs as more detail of the project evolves through design
Design storm	Coastal protection structures will often be designed to withstand wave attack by an extreme design storm. The severity of the storm (i.e., return period) is chosen in view of the acceptable level of risk of damage or failure. A design storm consists of a design wave condition, a design water level and a duration.
Down-drift	The direction of predominant movement of littoral drift.
Dredging	Excavation or displacement of the bottom or shoreline of a water body. Dredging can be accomplished with mechanical or hydraulic machines. Most is done to maintain channel depths or berths for navigational purposes; other dredging is for shellfish harvesting or for cleanup of polluted sediments. It can be used also to win sand to nourish beaches.
Dunes	Accumulations of windblown sand on the backshore, usually in the form of small hills or ridges, stabilised by vegetation or control structures.
Ebb tide	A falling tide or that portion of the tidal cycle between high water and the following low water.
Ebb tide (current)	The tidal current generated by a falling tide and associated with the waters within an estuary or bay being directed seaward.
Elevation	The distance of a point above a specified surface of constant potential; the distance is measured along the direction of gravity between the point and the surface.
Embayed	Formed into a bay or bays; as an embayed shore.
Embayment	(1) An indentation in a shoreline forming an open bay. (2) The formation of a bay.

EPCM	Engineering, Procurement and Construction Management - a contracting arrangement in which the owner selects a contractor to provide "management services" for the whole project on behalf of the owner. The EPCM contractor coordinates all design, procurement and construction work and ensures that the whole project is completed as required and in time. The EPCM contractor may or may not undertake actual site work.
Erosion	(1) Wearing away of the land by natural forces. On a beach, the carrying away of beach material by wave action, tidal currents or by deflation. (2) The wearing away of land by the action of natural forces.
Escarpment	A more or less continuous line of cliffs or steep slopes facing in one general direction which are caused by erosion or faulting, also called scarp.
Event	An occurrence meeting specified conditions, e.g. damage, a threshold wave height or a threshold water level.
Fetch	The length of unobstructed open sea surface across which the wind can generate waves (generating area).
Flood tide	A rising tide or that portion of the tidal cycle between low water and the following high water.
Flood tide (current)	The tidal current generated by a rising tide and associated with the flow of waters directed towards an estuary or bay from the ocean.
Foreshore	In general terms, the beach between mean higher high water and mean lower low water.
Geology	The science which treats of the origin, history and structure of the Earth, as recorded in rocks; together with the forces and processes now operating to modify rocks.
Geomorphology	That branch of physical geography which deals with the form of the Earth, the general configuration of its surface, the distribution of the land, water, etc.
Groyne (groin in the United States)	A rigid hydraulic structure built from the shore that interrupts the movement of littoral drift.
Hardpan	Firm sub-soil of clay, etc., hard unbroken ground.
High water (HW)	Maximum height reached by a rising tide. The height may be solely due to the periodic tidal forces or it may have superimposed upon it the effects of prevailing meteorological conditions. Also called the high tide.

Inshore	(1) The region where waves are transformed by their interaction with the sea bed. (2) In beach terminology, the zone of variable width extending from the low water line through the breaker zone.
Inshore current	Any current inside the surf zone.
Intertidal	The zone between the high and low water marks.
Isobath	A line on a plan that defines points of equal depth.
Lee shore	A nautical term applied usually to wind effects where a lee shore is downwind of a vessel; that is, the wind is blowing towards it over the vessel. In this context it refers to the shore on the side of a breakwater that is sheltered from wave effects.
Leeward	The direction toward which the prevailing wind is blowing; the direction toward which waves are travelling.
Littoral	(1) Of, or pertaining to, a shore, especially a seashore. (2) Living on, or occurring on, the shore.
Littoral currents	A current running parallel to the beach and generally caused by waves striking the shore at an angle.
Littoral drift	The mud, sand, or gravel material moved parallel to the shoreline in the nearshore zone by waves and currents.
Longshore	Parallel and close to the coastline.
Longshore transport rate	Rate of transport of sedimentary material parallel to the shore. Usually expressed in cubic meters per year.
Low water (LW)	The minimum height reached by each falling tide. Also called low tide.
Mean high water (MHW)	The average elevation of all high waters recorded at a particular point or station over a considerable period of time, usually 19 years.
Mean high water springs (MHWS)	The average height of the high water occurring at the time of spring tides.
Mean low water (MLW)	The average height of the low waters over a 19-year period. For shorter periods of observation, corrections are applied to eliminate known variations and reduce the result to the equivalent of a mean 19-year value.
Mean low water springs (MLWS)	The average height of the low waters occurring at the time of the spring tides.
Mean sea level	The average height of the surface of the sea for all stages of the tide over a 19-year period, usually determined from hourly height readings (see <i>sea level datums</i>).
Morphology	River/estuary/lake/seabed form and its change with time.

Neap tide	A tide around the first or third quarters of the moon when there is least difference between high and low waters.
Nearshore	In beach terminology an indefinite zone extending seaward from the shoreline well beyond the breaker zone.
Nearshore circulation	The ocean circulation pattern composed of the nearshore currents and the coastal currents.
Nearshore current	The current system caused by wave action in and near the breaker zone and which consists of four parts: the shoreward mass transport of water; longshore currents; rip currents; and the longshore movement of the expanding heads of rip currents.
NPL	Napier Port Limited
Nourishment	See Beach nourishment.
Offshore	In beach terminology, the comparatively flat zone of variable width, extending from the shoreface to the edge of the Continental Shelf.
Offshore breakwater	A breakwater built towards the seaward limit of the littoral zone, parallel (or nearly parallel) to the shore.
Offshore currents	(1) Currents outside the surf zone. (2) Any current flowing away from the shore.
Offshore wind	A wind blowing seaward from the land in the coastal area.
Onshore wind	A wind blowing landward from the sea.
Outflanking	erosion behind or around the inner end of a Groyne or bulkhead, usually causing failure of the structure.
Photogrammetry	The science of deducing the physical dimensions of objects from measurements on images (usually photographs) of the objects.
Progradation	The seaward movement of a coastline when sediment input exceeds the rate of erosion.
Prograde	Coastline advance towards the sea as a result of the accumulation of waterborne sediment.
Recession	A net landward movement of the shoreline over a specified time.
Reflected wave	That part of an incident wave that is returned (reflected) seaward when a wave impinges on a beach, seawall or other reflecting surface. Waves may be reflected off deep channels by the process of wave refraction.
Reflection	The process by which the energy of the wave is returned seaward or in a partially opposing direction to which it is travelling. Waves may be reflected off deep channels by the process of wave refraction.

Refraction	The process by which the direction of a wave moving in shallow water at an angle to the bottom contours is changed. The part of the wave moving shoreward in shallower water travels more slowly than that portion in deeper water, causing the wave to turn or bend to become parallel to the isobaths. Refraction also can cause waves to “reflect” off a deeper channel.
Return period	Average period of time between occurrences of a given event.
RSA	Rapid Sediment Analysis – settling tube analysis equilibrating the fall velocities of the sands to their grain diameters as carried out at the University of Auckland.
Salient	A bulge of sand projecting from the shore in the lee of an offshore breakwater.
Sand	An unconsolidated (geologically) mixture of inorganic soil (that may include disintegrated shells and coral) consisting of small but easily distinguishable grains, usually and mainly quartz, ranging in size from about 0.062 mm to 2.000 mm.
Sand dune	A mound formed of sand that extends usually along the shore at the back of a beach.
Sand wave	A seabed feature in sand comprising a long undulating form generated by strong currents and reflecting sand transport.
Sea	Refers to short-crested waves generated locally by the wind. Within Port Phillip Bay their periods range from 1 s to 5 s.
Sea level rise	The long-term trend in mean sea level.
Seawall	A structure separating land and water areas primarily to prevent erosion and other damage by wave action.
Sediment	Loose, fragments of rocks, minerals or organic material which are transported from their source for varying distances and deposited by air, wind, ice and water. Other sediments are precipitated from the overlying water or form chemically, in place. Sediment includes all the unconsolidated materials on the sea floor.
Shoal	(1) (noun) A detached relatively shallow area of sand or mud the depths over which may be a danger to surface navigation. Can also be termed a bank. (2) (verb) As pertaining to waves becoming shallow gradually.
Shore	That strip of ground bordering any body of water which is alternately exposed, or covered by tides and/or waves. A shore of unconsolidated material is usually called a beach.
Shoreface	The narrow zone seaward from the low tide shoreline permanently covered by water, over which the beach sands and GRAVELS actively oscillate with changing wave conditions.

Shoreline	The intersection of a specified plane of water with the shore.
Shoreline protection structure	A structure on the shore or nearshore, such as a groyne, revetment or seawall, constructed typically of rock, concrete or sandbags, and designed to protect the shore from recession.
Significant wave	A statistical term relating to the average of the one-third highest waves of a given wave group and defined by the average of their heights and periods.
Significant wave height	Average height of the highest one-third of the waves for a stated interval of time.
Silt	Sediment particles with a grain size between 0.004 mm and 0.062 mm, i.e., coarser than clay particles but finer than sand.
Spectral wave model	A computer program that schematises wind wave spectra in all directions and frequencies and computes their evolution and transformation in coastal regions with shallow water and ambient current.
Spring tide	A tide that occurs at or near the time of new or full moon and which rises highest and falls lowest from the mean sea level (MSL).
Storm surge	A rise or piling-up of water against shore, produced by strong winds blowing onshore. A storm surge is most severe when it occurs in conjunction with a high tide.
Subaerial beach	That part of the beach which is not covered by water (i.e., where users sit and sunbake, etc.).
Surf zone	The nearshore zone along which the waves become breakers as they approach the shore.
Survey, hydrographic	A survey that has as its principal purpose the determination of geometric and dynamic characteristics of bodies of water.
Survey, photogrammetric	A survey in which monuments are placed at points that have been determined photogrammetrically.
Survey, topographic	A survey which has, for its major purpose, the determination of the configuration (relief) of the surface of the land and the location of natural and artificial objects thereon.
Swell	Waves that have travelled a long distance from their generating area and have been sorted out by travel into long waves of the same approximate period. Swell wave periods range from 6 s to 25 s.
Tide	The periodic rising and falling of the water that results from gravitational attraction of the moon and sun acting upon the rotating earth. Although the accompanying horizontal movement of the water resulting from the same cause is also sometimes called the tide, it is preferable to designate the latter as tidal current, reserving the name tide for the vertical movement.

Tidal Current	The flow of water induced by the rise and fall of the tide.
Tombolo	A deposition landform in which an island is attached to the mainland by a narrow sand spit or bar.
Topographic map	A map on which elevations are shown by means of contour lines.
Topography	The form of the features of the actual surface of the Earth in a particular region considered collectively.
Vector	In this context, an arrow on a plan delineating the speed and direction of tidal flow or the transport of sediment as derived from modelling.
Vibrocoring	A technique for collecting core samples of underwater sediments. The core tube is driven into sediment by the force of gravity, enhanced by vibration energy.
Wave	(1) An oscillatory movement in a body of water manifested by an alternate rise and fall of the surface. (2) A disturbance of the surface of a liquid body, as the ocean, in the form of a ridge, swell or hump.
Wave climate	The range of wave conditions and their occurrence, as shown by height, period, direction, etc., at a place as measured over periods of years.
Wave direction	The direction from which waves are travelling.
Wave generation	Growth of wave height and period by wind action.
Wave height coefficient	The ratio between the height of a wave in a nearshore area to its height in deep water
Wave propagation	The development of water waves from wind action.
Wave transformation	The process of wave transmission through shallow waters and tidal currents.
Wind current	A current created by the action of the wind.